THE CATHOLIC UNIVERSITY OF AMERICA

Robot-Assisted Hand Movement Therapy after Stroke

A DISSERTATION

Submitted to the Faculty of the

Department of Biomedical Engineering

School of Engineering

Of The Catholic University of America

In Partial Fulfillment of the Requirements

For the Degree

Doctor of Philosophy

By

Christopher N. Schabowsky

Washington, D.C.

2010

Robot-Assisted Hand Movement Therapy after Stroke

Christopher N. Schabowsky, Ph.D.

Director: Peter S. Lum, Ph.D.

After therapy intervention, the majority of stroke survivors are left with a poorly functioning hemiparetic hand. Rehabilitation robotics has shown great promise in providing patients with intensive activity-based therapy leading to functional gains. Because of its crucial role in performing activities of daily living, attention to hand therapy has recently increased.

This thesis introduces a newly developed Hand Exoskeleton Rehabilitation Robot (HEXORR). This device has been designed to provide full range of motion (ROM) for all of the hand's digits. The thumb actuator allows for variable thumb plane of motion to incorporate different degrees of extension/flexion and abduction/adduction. Compensation algorithms have been developed to improve the exoskeleton's backdrivability by counteracting gravity, stiction and kinetic friction. A force assistance mode has also been designed to provide extension assistance based on each individual's needs. A pilot study was conducted to investigate the device's ability to allow physiologically accurate hand movements throughout the full ROM. The study also tested the efficacy of the force assistance mode with the goal of increasing stroke

subjects' active ROM while still requiring active extension movements. The initial stages of a clinical trial providing hand therapy to stroke patients are also discussed.

For 12 of the hand digits' 15 joints, there were no significant ROM differences between active extension movements performed inside and outside of HEXORR. For the 1st and 3rd digits, the slopes of joint-pair extension trajectories were no different inside and outside of the device. Stroke subjects were capable of performing hand movements inside of the exoskeleton and the force assistance mode was successful in increasing active ROM by 43% and 22% for the fingers and thumb, respectively. For both subjects, finger and thumb active ROM increased after the conclusion of therapy using HEXORR.

Our pilot study shows that this device is capable of moving the hand's digits through the entire ROM with physiologically accurate trajectories. Stroke subjects received the device intervention well and were able to actively extend and flex their digits inside of HEXORR. Our active-assisted condition was successful in increasing the subjects' ROM while generally promoting active participation.

This dissertation by Christopher N. Schabowsky fulfills the dissertation requirement for the doctoral degree in Biomedical Engineering approved by Peter S. Lum, Ph.D., as Director, and by John A. Judge, Ph.D., and Baohong Yuan, Ph.D. as Readers.

_____

Peter S. Lum, Ph.D., Director

_____

John A. Judge, Ph.D., Reader

_____

Baohong Yuan, Ph.D., Reader

DEDICATION

This work is dedicated to Sasha Zeedyk. Thank you for everything, I love you.

Acknowledgements

I would like to express appreciation to my mentor, Dr. Peter Lum, for all of his guidance and support and, most importantly, his patience throughout the term of my studies. His assistance and guidance was pivotal in the development of this work.

I would also like to thank both Rex and Ashley Lewis of Turnkey Automation, Inc for manufacturing HEXORR. Their professionalism and craftsmanship is unmatched.

Table of Contents

List of Figures

Figure 8.2 Display of different stages of the Isometric Squeeze-Release Game including **A** finger (blue) and thumb (black) cursors in the initial positions outside of the horizontal channel (green), **B** cursors moved into the channel by fingers and thumb flexion torques, and **C** relaxation of the flexors and extension torques to successfully avoid the incoming wall. Points are awarded for completion of the task.

Figure 8.3 Mean active-unassisted ROM for Subject 1 and 2 during 6 weeks of training using HEXORR. For Subject 1, active ROM increased 100% (20º MCP and PIP rotation) for the fingers (**A**) and 300% (10º CMC, 45º IP) for the thumb (**B**). Subject 2 entered the trial with full active finger ROM (**C**), and thumb (**D**) active ROM increased 400% (15º CMC, 68º IP).

Figure 9.1 Design of a modular left hand finger assembly (**A**) able to replace the original right hand finger assembly design (**B**) to include participants with impaired left hands. These modular assemblies can be removed from and affixed to HEXORR's base (**C**) by using three screws (red) and by engaging the assembly's drive shaft to the shaft coupler (green).

Figure 9.2 The thumb component redesigned to accommodate left hand users. The thumb component is converted for left hand use by releasing the linear bearing's supports via the four (red) screws (**A**). A set screw is loosened and the drive shaft (blue) and vertical supports (yellow) are all rotated about the main shaft (**B**). Finally, the IP digit interface (orange) is rotated and reattached with two screws (purple) (**C**). The completed left hand modification is shown in **D**.

List of Tables

CHAPTER 1:

INTRODUCTION

After therapy intervention, the majority of stroke survivors are left with a poorly functioning hemiparetic hand. Rehabilitation robotics has shown great promise in providing patients with intensive activity-based therapy leading to functional gains. Because of its crucial role in performing activities of daily living, attention to hand therapy has recently increased. This thesis introduces a newly developed Hand Exoskeleton Rehabilitation Robot (HEXORR). A pilot study was conducted to investigate the device's ability to allow physiologically accurate hand movements throughout the full range of motion (ROM). The study also tested the efficacy of a force assistance mode with the goal of increasing stroke subjects' active ROM while still requiring active extension movements. The protocol design and preliminary results of a clinical trial providing hand therapy to stroke patients are also discussed.

Chapter 2 provides a literature background that forms the foundation of the rationale behind this research project. Cerebral Vascular Accident (CVA), or stroke, is described and demographic statistics are provided to highlight the importance of addressing the motor impairments of stroke survivors through therapy intervention. The neurologically mediated impairments of the paretic hand are discussed. A description of the contemporary, evidence-based approach to motor therapy, namely activity-based, goal-oriented training, is provided. This chapter introduces rehabilitation robotics and illustrates the potential benefits they provide to current therapy practices. Previously designed hand therapy robots and their investigative studies are detailed. This Chapter concludes with the introduction of HEXORR.

Chapter 3 describes the mechanical design of the finger and the thumb components of HEXORR. Details are provided about the 2-dimensional modeling of the linkages designed to guide the motion of the hand's digits. The force analysis of the linkages' mechanical advantage is discussed. Illustrations of the 3-dimesional computer-automated design models are shown. Finally, an explanation of how the hand and the exoskeleton interact is provided.

Chapter 4 highlights the system's hardware, electronics and software. System power supplies, sensor technology, wiring guides and signal conditioning methods are all covered. This chapter also details a compensation algorithm that increases the

backdrivability of the geared motors by calculating and counteracting the weight of the linkages and static and kinetic friction of the system.

Chapter 5 describes the material and methods of a pilot study using HEXORR with unimpaired and stroke subjects. This pilot study serves two purposes: to examine HEXORR's ability to allow physiologically accurate extension and flexion movements of the hand's five digits throughout the full ROM and to test a potential hand therapy exercise designed to promote greater hand extension by participants that have suffered a stroke. Nine unimpaired subjects performed hand extension/flexion movements under three conditions: passive stretching inside HEXORR, active-unassisted movements inside of HEXORR, and active hand movements outside of the device. Stroke subjects performed hand extension/flexion movement inside the device including passive stretching, active-unassisted movements and active force-assisted movements. The data analysis methods are also described in this chapter.

Chapter 6 explains the results of the pilot study. For many of the joints' active ROM, there were no significant differences between active movements performed inside the exoskeleton and outside of the device. For the 1^{st} and 3^{rd} digits of the hand, mean joint-pair coordination comparisons between active-unassisted extension movements inside HEXORR and those made outside of the device show no significant differences. The active forced-assistance mode increased the active ROM of the stroke subjects while still requiring active participation.

Chapter 7 discusses the interpretation of the pilot study results. It is concluded that this exoskeleton is capable of moving the hand's digits through the entire ROM with physiologically accurate trajectories. Stroke subjects received the device intervention well and were able to actively extend and flex their hand inside of HEXORR. The active force-assisted condition was successful in increasing the subjects' ROM while generally promoting active participation. It is argued that these results justify a clinical therapy trial to examine the efficacy of the exoskeleton.

Chapter 8 covers the protocol design and preliminary results of an ongoing clinical trial using HEXORR as a therapy device. The development of a more sophisticated performance-based adaptive assistance algorithm is described. The design of two therapy exercises, the Gate Game and an Isometric Squeeze-Release Game, are explained. The experimental setup and therapy protocol are also covered. Finally, the preliminary results of two stroke subjects that have complete their therapy sessions are presented.

CHAPTER 2:

BACKGROUND

2.1 Cerebral Vascular Accident (Stroke)

CVA, or stroke, is the rapidly developing loss of brain function(s) due to disturbance in the blood supply to the brain leading to permanent brain damage or death. For stroke survivors, impairments depend on the affected area of the brain. Common impairments include hemiparesis, or partial paralysis of one side of the body, inability to understand or formulate speech, and/or inability to see one side of the visual field [1]. Stroke is the leading cause of adult disability in the United States and Europe and it is the number two cause of death worldwide [2].

Stroke can be classified into two major categories: ischemic and hemorrhagic. Ischemic strokes are caused by a disruption of the blood supply to the brain, while hemorrhagic

strokes are caused by a rupture of a blood vessel or an abnormal vascular structure. Approximately, 80% of strokes are due to ischemia and the remainder is due to hemorrhages. Though stroke causes deficits in many of the neurological domains, the most commonly affected is the motor system [3]. Nearly 80% of stroke survivors suffer hemiparesis of the upper arm [4] and approximately 40% of patients claim that a non-functional hand is the most debilitating impairment [5].

2.2 Hand Joint Anatomy

This thesis will refer to a number of digits and joints of the hand and it is helpful to review the joint anatomy of the hand. The digits of the hand are referenced by number: the thumb (1^{st} digit), the index finger (2^{nd} digit), the middle finger (3^{rd} digit), the ring finger (4^{th} digit) and the small finger (5^{th} digit). The five digits of the hand have a total of fifteen joints. For the thumb, the three joints are, from proximal to the wrist to the distal joint, the carpometacarpal joint (CMC), the metacarpalphalangeal joint (MCP) and the interphalangeal joint (IP). The finger joints are called, from proximal to the wrist to the distal joint, the metacarpalphalangeal joint (MCP), the proximal interphalangeal joint (PIP), and the distal interphalangeal joint (DIP). Figure 2.1 displays the skeletal anatomy of the hand's digits.

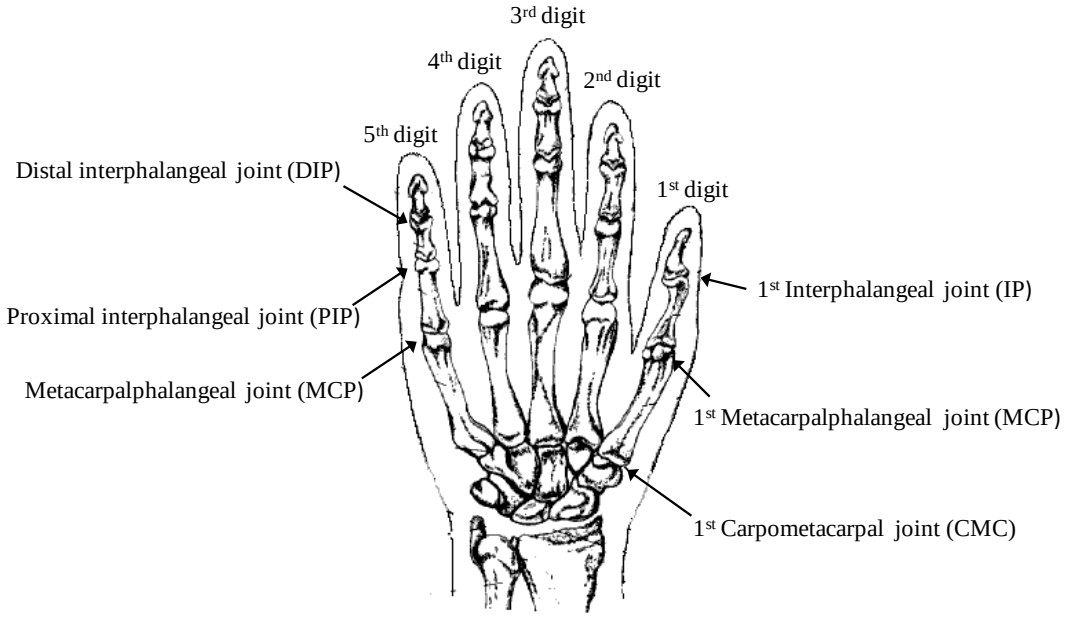

Figure 2.1 The hand's digits and their joints. The digits are referred, from medial to lateral, as the 1st -5th digits. The 1st digit joints, proximal to distal, are the CMC, the MCP and the IP. For the fingers, the joints, proximal to distal, are the MCP, the PIP and the DIP.

2.3 Neurologically Mediated Impairment of the Hand Following Stroke

In order to provide effective and efficient motor therapy for stroke survivors, it is crucial to understand the underlying mechanisms causing impairment. Accordingly, a number of neurologic factors that contribute to hand impairment have been investigated.

It was once thought that biomechanical malformations were the major contributors that impaired hand function after stroke [6]. After years of disuse, the muscles in the hand

atrophy, further contributing to hand weakness. Contractures, or the shortening of muscle tendons, can reduce the passive ROM of the hand's digits. Although these mechanical changes can hinder the active ROM of the hand, it has recently been shown that neurological mediated impairments, namely spasticity, muscle weakness, and involuntary co-activation of the extensors and flexors, are the most responsible for hand function impairment.

Following stroke, the flexor muscles of the hemiparetic hand become spastic, impeding voluntary active extension. Spasticity is a condition in which certain muscles have a heightened velocity-dependent reflex response to passive stretch [7]. This amplified basal contraction results in increased stiffness of the muscles, or tone. One study aimed to quantity the relative contributions of the flexor muscle stretch response to hand impairment. The flexor spasticity was recorded at the onset of movement and the response increased with faster extension stretches but little spasticity was seen during flexion movements. This indicates that resistance to muscle stretching following stroke is mediated primarily by neurological rather than biomechanical disturbances and that faster extension rates will increase the flexor spastic response [8].

Stroke also leads to overall weakness in both extensor and flexor finger muscles of the paretic limb [9]. The central nervous system's inability to activate agonist muscles plays a large role in hand weakness [10, 11]. However, muscle weakness is not uniform

between the extensor and flexor muscles [12]. Stroke survivors generally tend to regain functional flexion with minimal extension gains. These imbalances are related to altered muscle activation patterns where elevated levels of flexor activity occur during intended extension movements [13]. The inability to independently activate muscle groups during extension movements results in co-contraction of antagonistic pairs causing reduced active extension ROM [14]. Many studies have shown that activity-based retraining by independently activating weakened extensor muscles may help strengthen the extensors to overcome this inherent strength imbalance [15-17].

2.4 Contemporary Physical Therapy Concepts

Typically patients have not reached their full recovery potential after they have received initial rehabilitation and are discharged from the hospital [18]. Currently, the probability of regaining functional use of the impaired hand is low [19] and a follow up study showed that, four years after stroke; only 6% of stroke survivors were content with the function of their impaired arm [20]. Proper function of the hand, particularly prehension, is vital for many activities of daily living (ADL) including feeding, bathing and dressing. Accordingly, there has been much focus on developing optimized hand therapy techniques to elicit greater hand function gains.

Over the past 15 years, rehabilitation after stroke has evolved from analytical approaches and compensation strategies to a focus on task-oriented training exercises. Analytical therapy methods focus on localized joint movement function, particularly spasticity, and not on movement skills. Compensation strategies focus less on improving the function of the affected hand. Rather, the patient are taught to rely on the unimpaired hand to perform activities of daily living and/or develop strategies that use the trance levels of function in the paretic hand. Task-specific, goal-oriented therapy involves training of activities and skills aimed at increasing patient participation. Many investigators have advocated rehabilitation methods that include repetitive, meaningful movements that engage active participation to promote changes in the cerebral cortex (brain plasticity) to elicit motor recovery [21-23]. Following this rationale, sensory-motor training of the hand should be a total package that includes training of basic functions, for example muscle strength and increased active range of motion, skill training (grasping) and improvements in endurance.

Activity-based therapy approaches that have resulted in the most functional improvement include task-oriented training, constraint induced movement therapy (CIMT) and bilateral arm training [24, 25]. Task-oriented training focuses on repetitive training of skill-related tasks. This strategy promotes patient participation, cognitive processing and the development of goal-oriented movements. It has been shown that this therapy approach not only improves arm-hand functional recovery (e.g. muscle strength), but also

contributes to more efficient movement strategies for skill performance [26-28]. CIMT therapy is a specialized form of task-oriented training that immobilizes the unimpaired arm for a much as 90% of waking hours, thereby forcing the patient to use the hemiparetic limb to perform activities of daily living. Many CIMT studies have reported functional gains following therapy [17, 29, 30]. Bilateral arm training is a therapy approach that incorporates simultaneous active movement of both the impaired and unimpaired limb [31]. This approach has resulted in improved active ROM, grip strength and dexterity of the paretic limb [32-34].

2.5 Robotic-Assisted Therapy

The use of rehabilitation robotics to provide activity-based therapy has show great potential. Robotic rehabilitation systems incorporate many of the aspects that have made activity-based therapy successful. Some of the benefits of rehabilitation robotics include introducing the ability to perform precise and repeatable exercises, reduction of the physical burden of participating therapists, incorporation of interactive virtual reality systems, and collection of quantitative data that can be used to optimize therapy sessions and assess patient outcomes.

Many of these devices have been designed to promote active goal-oriented movement therapy. Depending on the impaired limb's functionality, robots can be programmed to

provide assistance, resistance, and even perturbations to movement exercises. Virtual reality systems have been shown to engage patients, thereby encouraging them to actively participate in therapy sessions [35]. Most robots are equipped with sensors able to provide information that can be used to accurately measure ROM, strength, level of subject active participation, and efficiency of movement. This information can be used to tailor therapy sessions to meet the patient's needs, track performance over the course of therapy and even as a diagnostic tool. By relieving the therapist of the physical burden of manually assisting paretic limb movement, rehabilitation robots allow therapists to focus other aspects of the therapy session.

Many investigators have focused on developing devices designed to retrain an impaired upper limb [36-40]. Robot-assisted therapy is proven to significantly improve proximal arm function [41-45]. However, regaining the ability to 'reach and grasp' allows patients to perform many ADLs, providing both functionality and increased independence. Therefore successful upper arm therapy requires focus on not only the proximal joints of the arm, but also the distal joints found at the hand.

2.6 Rehabilitation Robots for Hand Motor Therapy

Hand therapy via rehabilitation robotics has received less, but growing, attention. Lately, a number of robots have been developed to provide hand motor therapy. Although designed for the same goal, each robot has unique design features and limitations. However, many investigative studies focusing on these devices have shown therapeutic promise. The design of many of these hand robots and their therapy studies will be described below. Pictures of the described devices can be viewed in Figure 2.2.

The Rutgers Hand Master II is a force-feedback glove powered by pneumatic pistons positioned on the palm of the hand [46-47]. Positioning pistons on the palm of the hand allows for individual control of the hand's 1^{st}-4^{th} digits, but it does not allow for manipulation of real objects and it limits flexion ROM. The glove is used as a haptic device to produce contact forces when interacting with objects simulated in virtual-reality environments [48]. Therapy studies using this device has reported that chronic stroke patients enhanced performance in clinical assessments, improved ROM and increased extension speed of the paretic digits [49-51]. One such study provided four chronic stroke subjects with therapy for two hours a day, five days a week for three weeks. After therapy, subject hand ROM was increased and two subjects had significantly better scores in the Jebsen-Taylor Test of Hand Function [49]. Another study provided three stroke subjects with 3.5 hours of daily therapy for two weeks. All participants showed

increased gains in hand movement parameters and some exhibited increased clinical assessment scores [50].

A hand module, the InMotion 5.0 Hand Robot, has been designed to complement the prolific arm therapy robot, the MIT-Manus. The intent of this hand device is to focus on 2-dimensional 'reach to grasp' tasks and provide therapy for not only the shoulder and elbow, but also the hand. Subjects grasp onto a cylinder attached to the end-effector of the MIT-Manus. The outer shell of this cylinder consists of 6 panels and the radius of the cylinder linearly expands and retracts relative to the motion of the rotors' rotation. However, this device provides limited hand extension ROM [52]. To date, no clinical studies have been reported for this device.

Developed by a group at the University of California-Irvine, the Hand Wrist Assistive Rehabilitation Device (HWARD) is an exoskeleton designed for hand-wrist therapy intervention. HWARD is a 3 degrees-of-freedom robot that controls finger rotation about the metacarpophangeal joint (MCP), thumb abduction/adduction and wrist extension/flexion [53]. The PIP and DIP joints of the fingers are not directly controlled. The device allows for approximately 65^{o} of finger rotation about the MCP, 90% of thumb extension ROM and 35^{o} of wrist extension. The hand's digits are guided by a lever design and the robot is actuated by double-acting air cylinders capable of providing assistance in the extension and flexion directions. A recent clinical trial reported

significant behavioral gains, increases in task-specific cortical activation and a dosage effect where subject gains increased with increased robotic therapy duration [54].

The Hand Mentor (Kinetic Muscles Inc., Tempe, AZ) is a commercially available hand therapy device. The device is designed to encourage patients to actively extend their wrist and fingers. When maximum self extension is achieved, the device uses an artificial, pneumatic muscle to simultaneously extend and flex the fingers and wrist [55]. The fingers are controlled in bulk and the Hand Mentor does not actuate the thumb.

A recent pilot study using the Finger Trainer, Reha-Digit, a hand device specifically designed for controlled passive movements of hemiplegic fingers, showed that the intervention was well received by sub-acute stroke patients and tone did not increase during the intervention [56].

A pneumatic orthosis has been developed by a group from the Rehabilitation Institute of Chicago. Users don a glove with an air bladder and channels that run along the palmar side of all of the hand's digits. An electro-pneumatic servovalve is strapped to the back of the patient and is used to regulate air pressure to provide assistance in digit extension. Without pressure, the glove does not impede physiological ROM of the hand. A pilot study of this device resulted in modest functional gains [57].

A number of hand therapy devices have been developed and initial pilot data indicates promising therapeutic results [46-57]. They show that robotic-assisted therapy for stroke patients will lead to therapeutic and functional gains. However, although many different approaches where taken to achieve the same goal (increase active extension ROM), there are common issues with these devices. The general issues include: i) limited ROM ii) partial control of the hand iii) basic controllers designed to provide therapy. It is believed that designing an exoskeleton that maximizes the ROM and control of the hand's digits combined with sophisticated controllers developed to specifically target the neurological impairments of stroke patients will result in improved therapeutic outcomes.

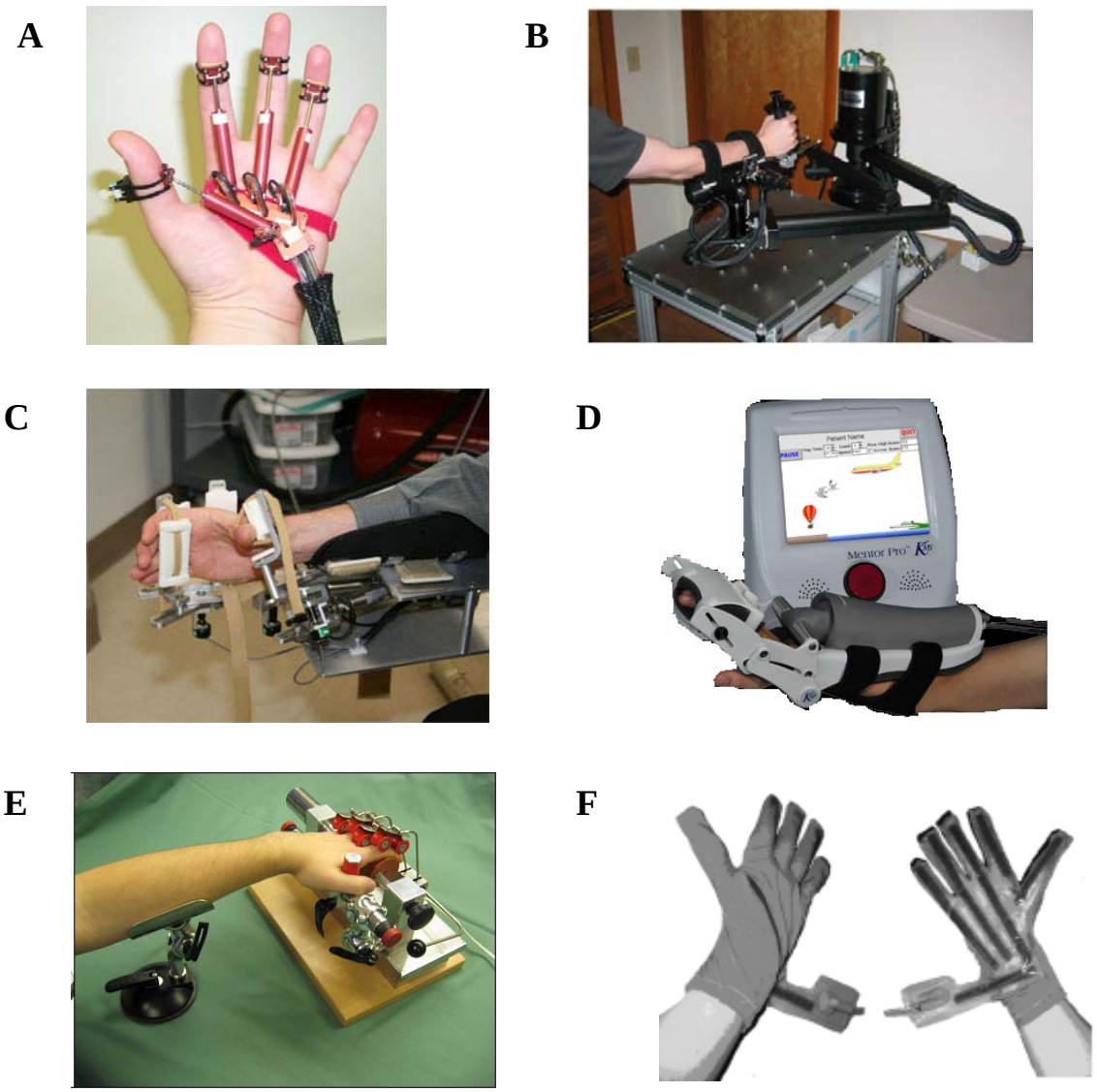

Figure 2.2 Pictures of several devices developed for robot-assisted hand motor therapy: (**A)** Rutgers Hand Master II force-feedback glove (**B)** the InMotion 5.0 Hand Robot (**C)** HWARD (**D)** the Hand Mentor (**E)** the Finger Trainer Reha-Digit (**F)** RIC pneumatic orthosis.

2.7 Hand Exoskeleton Rehabilitation Robot

This thesis introduces a recently developed rehabilitation robot for the hand, the Hand Exoskeleton Rehabilitation Robot (HEXORR). This device has been designed to provide full ROM for all of the hand's digits. The thumb actuator allows for variable thumb plane of motion to incorporate different degrees of extension/flexion and abduction/adduction. Compensation algorithms have been developed to improve the exoskeleton's backdrivability by counteracting gravity, stiction and kinetic friction. We have also designed a force assistance mode that provides extension assistance based on each individual's needs.

The mechanical design of the exoskeleton and a pilot study will be described. This pilot study serves two purposes: to examine HEXORR's ability to allow physiologically accurate extension and flexion movements of the hand's five digits throughout the full range of motion and to test a particular potential hand therapy exercise designed to promote greater hand extension by participants that have suffered a stroke. The beginning of an ongoing clinical trial using this device is also discussed.

CHAPTER 3:

MECHANICAL DESIGN OF THE HAND EXOSKELETON

HEXORR consists for two modular components that are capable of separately controlling the extension and flexion of the fingers and the thumb. The device acts as an exoskeleton so that the joints of the robot and the user are aligned throughout the allowed ROM. This approach allows for multiple points of contact between the digits and the device, which is critical for properly controlling the kinematic trajectory of the assisted hand movements. General design criteria of this exoskeleton included: i) allowing the digits full ROM ii) emulating physiologically accurate kinematic trajectories iii) providing adjustability to comfortably fit different hand sizes.

3.1 Mechanical Design of the Finger Component

The component that actuates the fingers is driven by a four-bar linkage, where the driver and coupler links guide rotation about the MCP and the PIP joints, respectively. During grasp movements, the distal phalanges of the fingers move in a spiral pathway relative to the MCP joints [58]. Therefore, kinematic synthesis of the four-bar linkage was approached as a path generation problem so that the distal end of the coupler link moved in a spiral trajectory relative to the ground joint of the driver link. Initially, the linkage was graphically modeled in Working Model 2D®, (Design Simulation Technologies, Inc., Canton, MI) a 2-dimensional modeling software package. This graphical approach led to a general solution capable of generating the desired coupler link path. The driver link guides the motion of the fingers' MCP joints and the coupler link controls the rotation of the fingers' PIP joints. The motion of the fingers' DIP joints is not directly controlled by the finger component. Figure 3.1 displays the general solution of the four-bar linkage. Figure 3.1.A illustrates flexed fingers in the device and Figure 3.1.B shows the fingers in an extended position. The endpoint of the coupler link was tracked during the extension movement. This profile highlights the four-bar linkage's ability to emulate the spiral pathway of the fingers' distal phalanges.

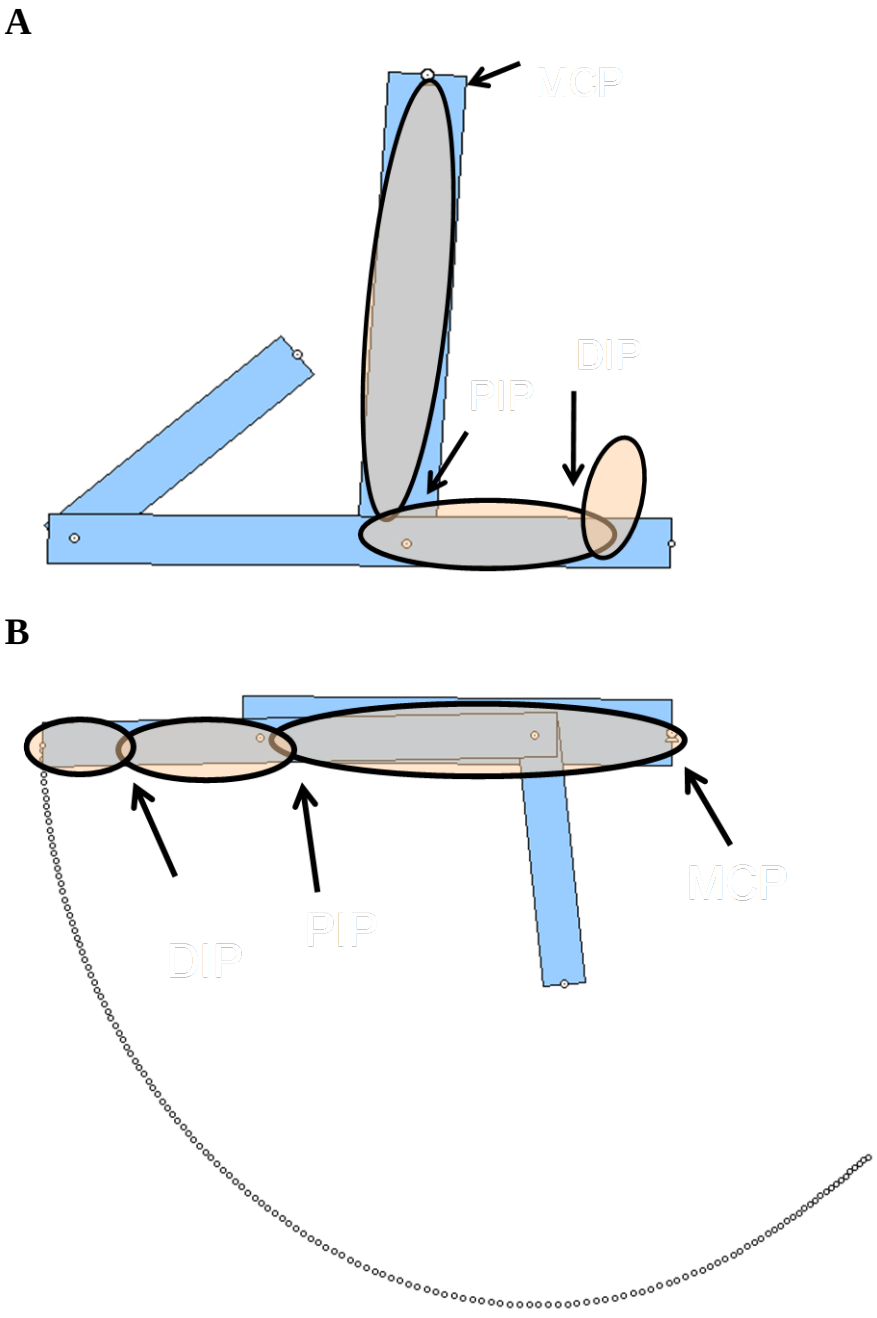

Figure 3.1 General design of the finger linkage using Working Model 2D®. Positions of the fingers' phalanges are shown and the joint locations are pointed out. (**A)** The linkage (blue) in the flexed position and (**B)** the linkage in the fully extended position.

Using MATLAB® (MathWorks™, Natick, Massachusetts), custom software programs were developed to further analyze and improve the linkage design. The goal of this analysis was to choose a four-bar linkage configuration that minimizes the required force applied by the fingertips needed to move the linkage through its ROM. The lengths of the driver link (length of 3rd digit's proximal phalanx) and the coupler link (length of 3rd digits' intermediate phalanx) are known, and their initial positions are set so that the hand is fully flexed. One hundred possible linkage configurations were tested by generating a 2" x 2" grid with a resolution of 0.2" centered about the coupler-follower joint position given by the graphical solution. For each configuration, the positions of the links were found at three different points in the linkage's trajectory, full flexion, mid-extension and full extension. Then, the position of the follower link ground point was identified by finding the intersection point of the two orthogonal bisectors of the segments connecting the three through points. With the positions of the coupler-follower joint and the follower link ground point, a linkage rotation simulation was derived. This program simulated the rotation of a linkage by rotating the driver link from full flexion to full extension (90 degrees, 5 degrees per iteration) and solved for the corresponding positions of the other dependent links to ensure that the linkage followed its intended path and that there are no singularities throughout its ROM.

Finally, 2-dimensional force analysis was performed per iteration on each of the generated linkage configurations. For this analysis, mechanical advantage was defined as

the moment arm about the drive shaft of a force located at the contact point between the tip of the coupler link and the DIP joints, assuming the force direction was maintained normal to the coupler link throughout the range. This simulates driving the linkage through the most distal point of contact between the fingers and the linkage. This point of contact was analyzed in detail because of the potential for very small moment arms when the linkage is in the flexed position.

The final linkage configuration was chosen by considering both fabrication feasibility and the provided mechanical advantage. The resulting four bar linkage design is shown in Figure 3.2.A and the final design performance can be seen in Figure 3.2.B. In the flexed position, the linkage space is approximately 2.25” x 2” and the linkage extends to a length of about 2.7 inches. The mechanical advantage of the four bar linkage is lowest at the flexed position but increases as the linkage extends.

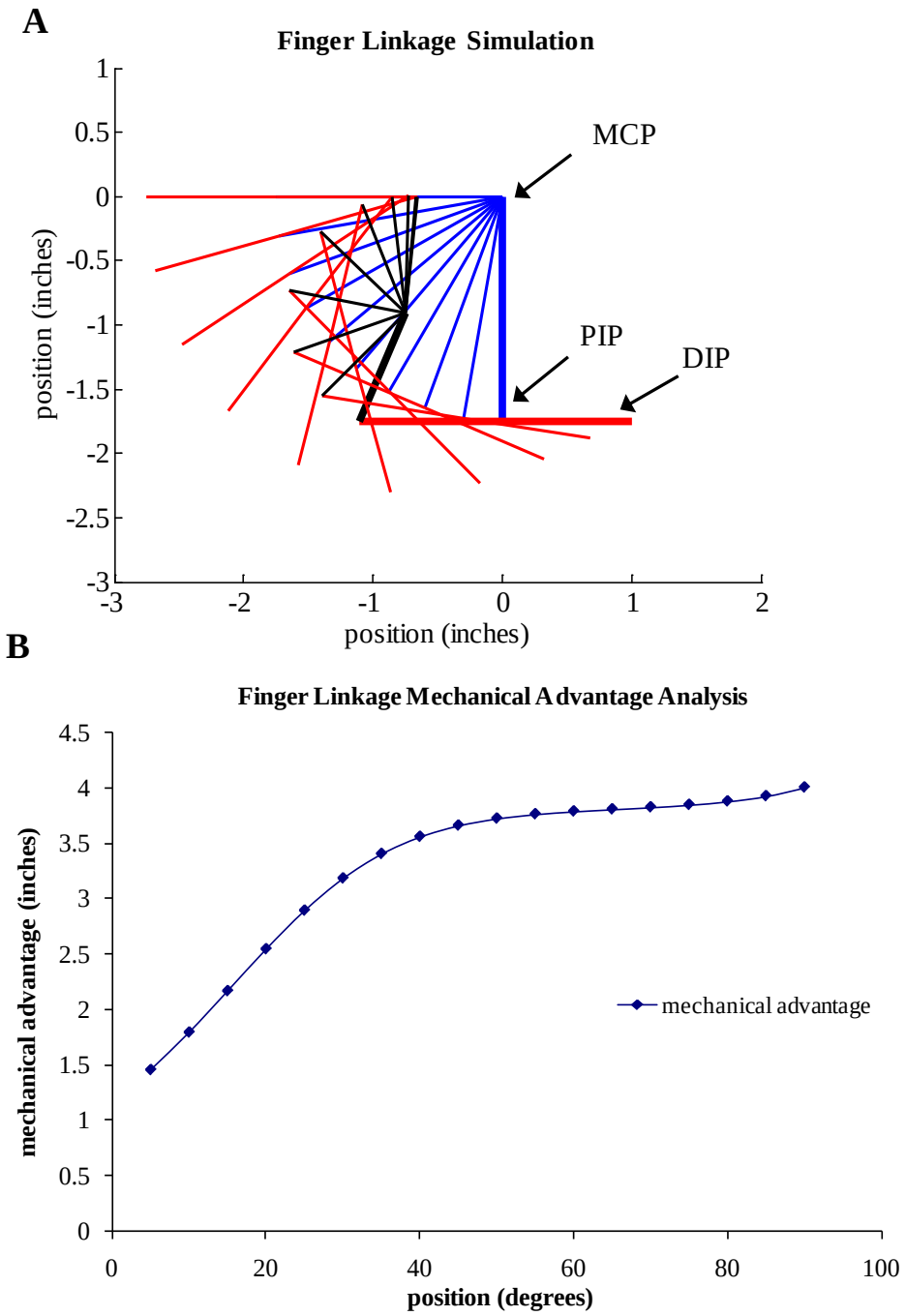

Figure 3.2 (**A**) The four-bar linkage rotation simulation (5^{o} rotation per iteration) of the chosen linkage configuration. The position of the linkage in the flexed position is bolded. (**B)** The force analysis of the chosen linkage.

Once the design of the four-bar linkage was finalized, the hand component was modeled using 3-dimensional computer automated design (CAD) software (SolidWorks, SolidWorks Corp.). Figure 3.3 illustrates the finger component model. The finger component was designed as a table-top exoskeleton. It is actuated by a geared DC motor with an encoder. A torque sensor is position between the gear head and the finger/exoskeleton interface. Detailed description of the geared DC motor and the torque sensor will be covered in following sections. The design of the finger/exoskeleton interface can be seen in detail by viewing Figure 3.4.

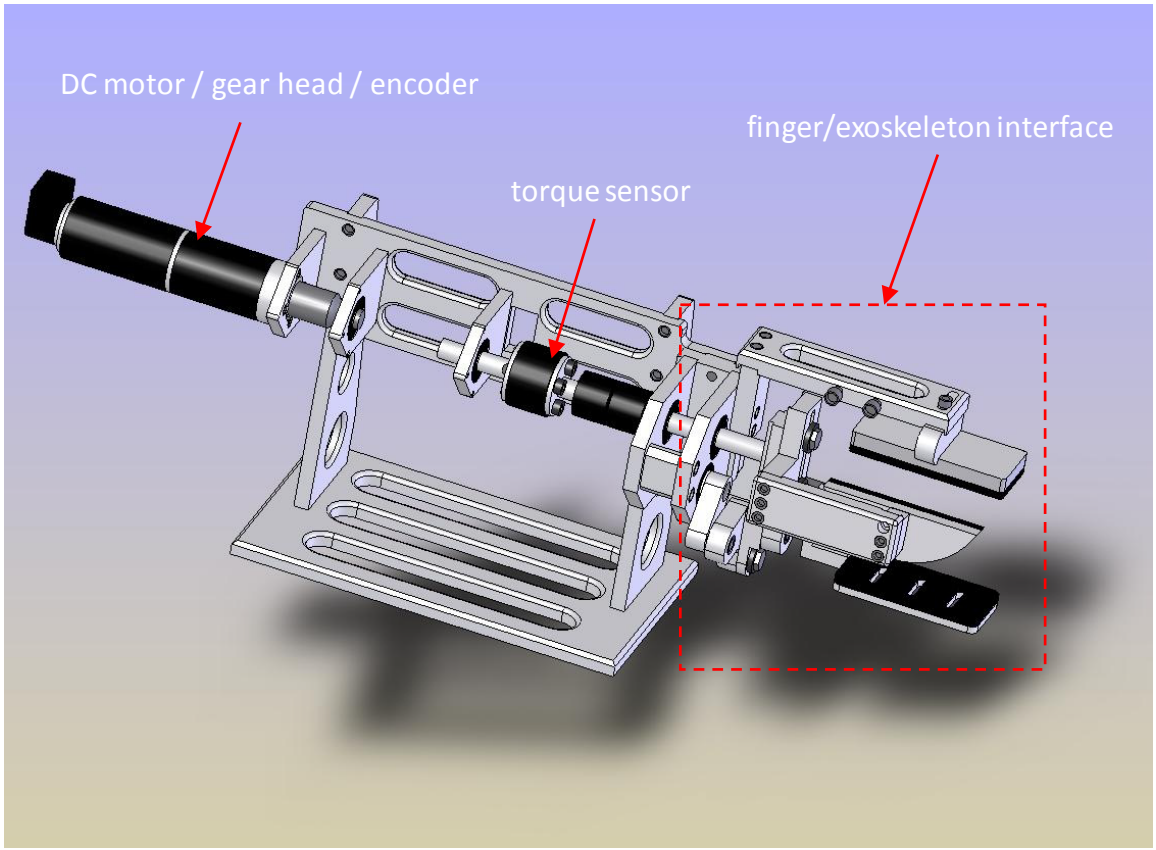

Figure 3.3 Finger component modeled by 3-dimensional computer automated design software. The system consists of a geared DC motor with an encoder and a torque sensor between the motor's gear head and the finger/exoskeleton interface.

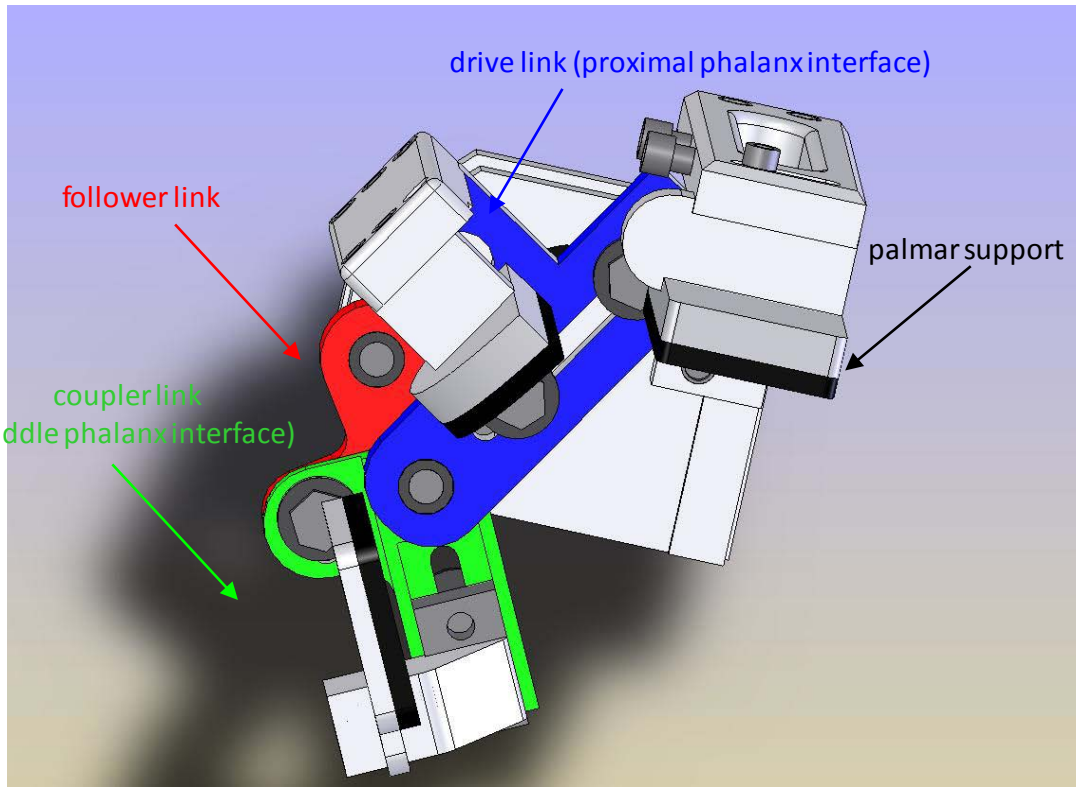

Figure 3.4 An illustration of the finger/exoskeleton interface. This consists of the driver link (blue), coupler link (green) and follower link (red). The palmar support, designed to hold the hand in position, the MCP pad and the PIP pad can also be seen.

To compensate for different hand sizes, the driver link and the coupler link are adjustable and able to fit the proximal and the intermediate phalanges, respectively. These two links can collapse and expand by sliding the links along slots and locking them into place. Examples of driver link and coupler link adjustments can be seen in Figure 3.5.A and Figure 3.5.C. Figure 3.5.A shows the linkage adjusted for a small hand and Figure 3.5.C displays the linkage sized for a large hand. Note that when the driver link is adjusted, the coupler link is no longer orthogonal to the driver link in the flexed position. This would

hyper-flex the PIP joints for small hands (Figure 3.5.A). For large hands, the PIP joints would not be able to fully flex (Figure 3.5.C). To compensate for this problem, an auxiliary joint was designed to rotate the coupler link about the driver link-coupler link joint. Figure 3.5.B and Figure 3.5.D illustrates how this mechanism allowed for link length adjustments while maintaining the desired orthogonal relationship between the driver link and coupler link when the linkage is in the flexed position.

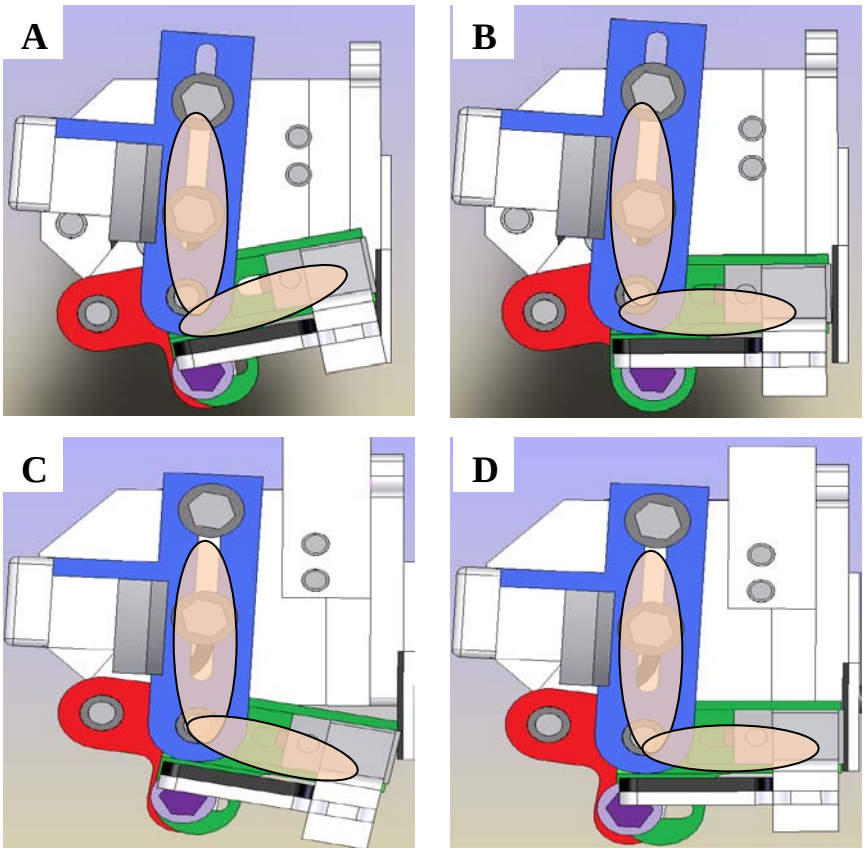

Figure 3.5 Finger linkage adjustments for small and large hands. The driver link is shifted up (**A**) to fit a small hand and down (**B**) to fit a large hand. Without further adjustment, the coupler link (green) would not position the PIP joints orthogonal to the MCP joints. (**C** and **D**) Rotation of the coupler link about an auxiliary joint (purple) positions the coupler link so that the PIP joints are orthogonal to the MCP joints.

The hand component contacts the fingers at three locations. To help stabilize the hand inside the exoskeleton, a hook and loop strap around the palm holds the hand stationary. Also, hook and loop straps are used to attach the proximal and intermediate phalanges to the respective robotic links. Once the fingers are comfortably strapped to the proper robotic links, the fingers are free to perform extension and flexion movements. Mechanical stops were implemented to ensure patients are never hyper-flexed or hyper-extended during testing sessions. Figure 3.6 shows the hand inside the manufactured hand component, illustrating how the hand fits into the device and the Velcro strap arrangement used to hold the hand in place.

A **B**

Figure 3.6 (**A**) Top down view of the hand component with a hand inside of the device. The palmar support is a rigid support designed to hold the hand in place. The MCP and PIP joint interfaces rotate with the four-bar linkage. **(B)** Displays a palmar view of the device, highlighting the Velcro strapping arrangement used to attach the fingers to the device.

3.2 Mechanical Design of the Thumb Component

The thumb component is an end-effector robot that controls planar thumb extension/flexion and abduction/adduction movements by directly controlling the rotation of the thumb's distal phalanx. Like the finger linkage, thumb linkage graphical synthesis was performed using Working Model 2D®. The focus of the design was to allow full IP rotation (nearly 90^o flexion to extension) while allowing the CMC and MCP joints to rotate up to 20^o. The model simplifies the rotation of the thumb's CMC and MCP joints by treating the metacarpal and the proximal phalanx as a single link that rotates about the CMC joint. During graphical synthesis, it was noticed that the thru-points of the coupler link-follower link joint could be accurately modeled via linear regression. Therefore, instead of using a follower link to guide the rotation of the coupler link, the follower link was replaced by a linear slider. With this design simplification, the thumb linkage was designed as a crank and slider mechanism**.** Figure 3.7 depicts the general linkage design. Figure 3.7.A illustrates a flexed thumb in the device and Figure 3.7.B shows the thumb in an extended position. The endpoint of the coupler link was tracked during the extension movement. This profile highlights the crank-slider's ability to allow full rotation of the IP joint.

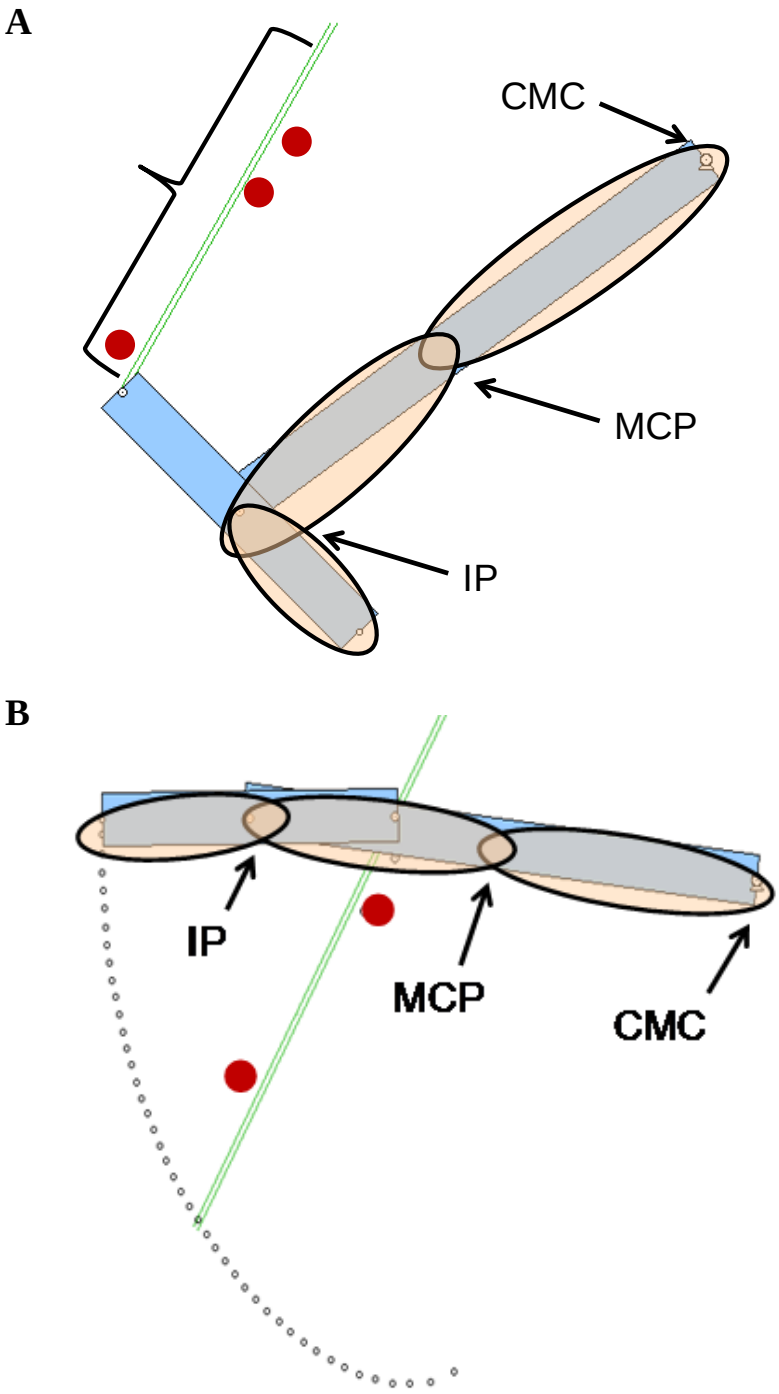

Figure 3.7 General design of the thumb linkage. Positions of the thumb's phalanges are shown and the joint locations are pointed out. (**A)** Linkage (blue) in the flexed position and (**B)** linkage in the fully extended position. The through points of the coupler-slider link are displayed (red) and the estimated linear slider is shown (green).

Custom programs were used to further analysis the general linkage design. These programs simulated the motion of the linkage from the flexed to the extended position and also performed force analysis to determine the amount of force required by the thumb to move the linkage. The ROM simulation and mechanical advantage analysis was similar to the finger component analysis that has been previously described (see Section 3.1). The thumb linkage was iteratively rotated about the driver link ground (5^{o} increments) and the moment arm was calculated as an orthogonal force was applied to the distal end of the coupler link. The translation of the coupler link-slider joint was also examined. The position of this joint was plotted per iteration and linear regression was used to further validate our decision to simplify the linkage design by using a slider. This analysis confirmed that the coupler slider joint translation was highly linear ($R^2 = 0.95$). The results of this analysis can be reviewed in Figure 3.8. Figure 3.8.A shows the linkage motion simulation and Figure 3.8.B depicts the force analysis.

A

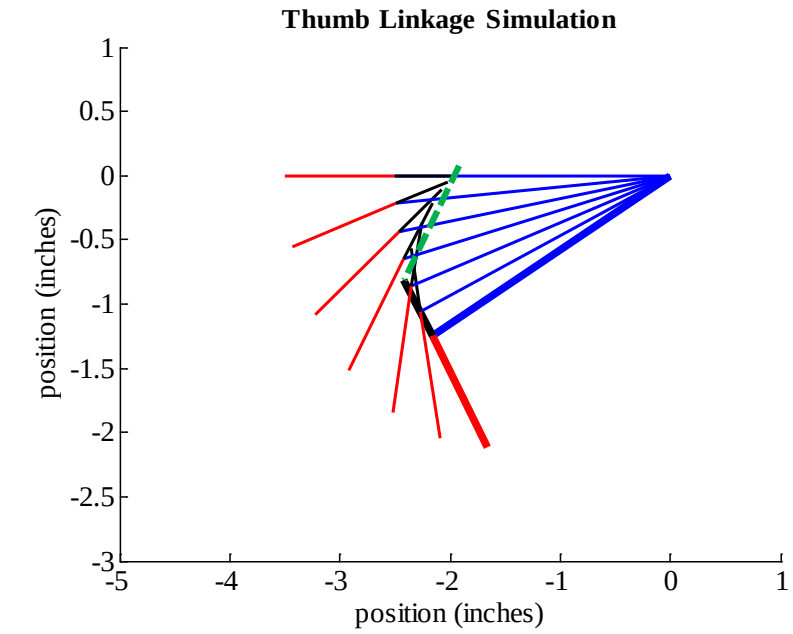

B

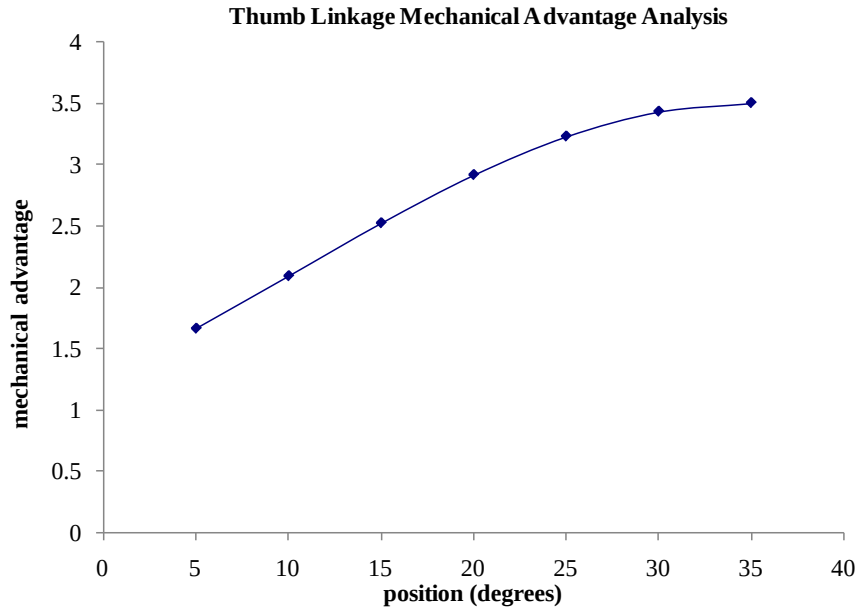

Figure 3.8 (**A**) The thumb linkage rotation simulation at 5^{o} rotation per iteration about the driver link's ground joint. The linkage's position that results in a flexed thumb is bolded. The orientation of the linear slider is highlighted as a green dashed line. (**B)** The force analysis of the thumb linkage.

Like the finger component, the thumb component was modeled using three-dimensional CAD software (SolidWorks). Figure 3.9 illustrates the thumb component model. The thumb component was designed to fit directly underneath the finger/exoskeleton interface. Because of this design constraint, the size requirement of the thumb component was particularly strict. The crank serves as the driver link that guides the motion of the coupler link. The slider was created with a linear bearing that translates along a shaft. The coupler link's motion is dependent on the rotation of the driver link and the translation of the linear bearing. The thumb's distal phalanx is attached to the coupler link with a hook and loop strap. As the CMC joint rotates about the driver ground joint, the thumb's metacarpal and proximal phalanx closely follow the motion of the crank. Concurrently, the thumb's distal phalanx follows the motion of the coupler link as the IP joint rotates about the driver link-coupler link joint. The thumb linkage is mounted on a highly adjustable base. The base can ascend and descend vertically along a slotted shaft to accommodate varied hand sizes. The base can also be adjusted (tilted and rotated) to increase or decrease the amount of thumb abduction/adduction involved in the thumb movement exercises. The crank is driven by a geared AC motor with an encoder. A torque sensor is position between the gear head and the crank. Detailed description of the geared AC motor and the torque sensor will be covered in following sections.

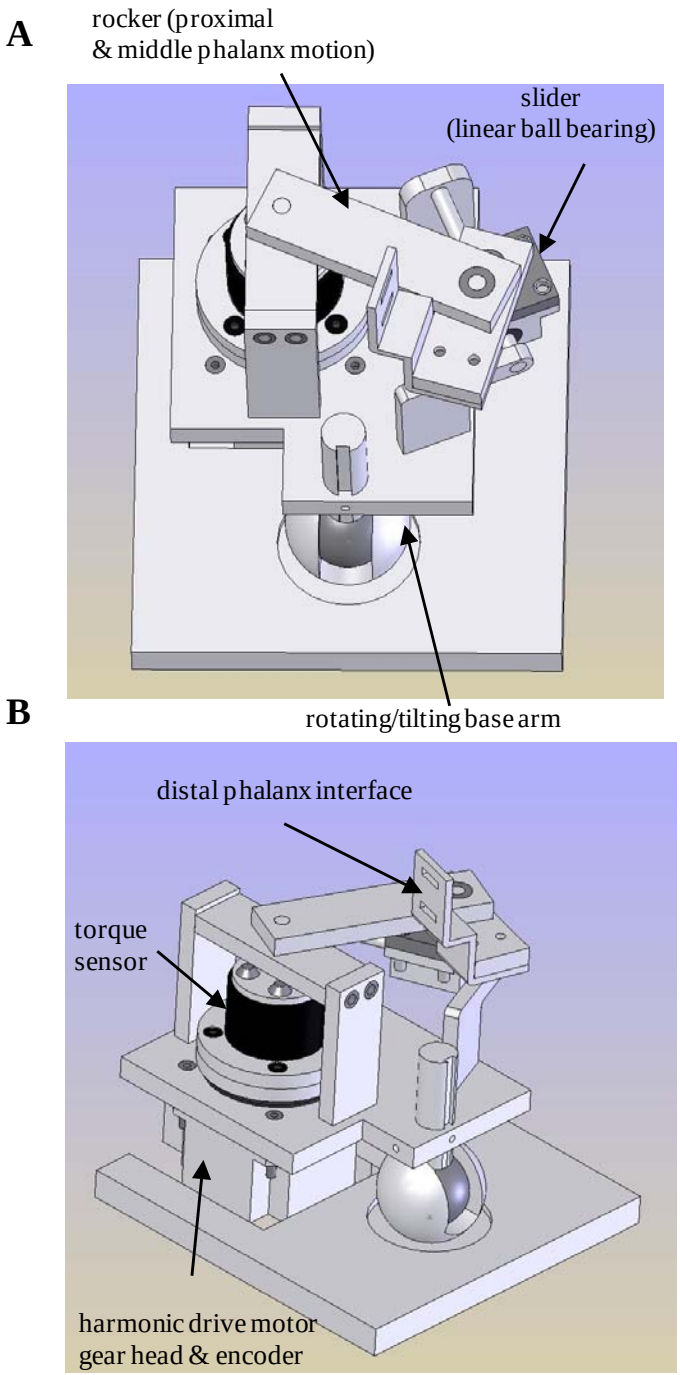

Figure 3.9 Oblique drawings of (**A)** top and (**B)** side views of the modeled thumb component. The system consists of a geared DC motor with an encoder and a torque sensor between the motor's gear head and the thumb/exoskeleton interface. A slider replaces the follower link. The linkage is mounted on a pivot and can be rotated and tilted to incorporate different amounts of thumb abduction/adduction.

3.3 Hand Exoskeleton Rehabilitation Robot

HEXORR consists of both modular components that control the motion of the fingers and the thumb. This exoskeleton is capable of separately controlling the extension and flexion of the fingers and the thumb. The device acts as an exoskeleton so that the joints of the robot and the user are aligned throughout the allowed range of motion. Figure 3.10 shows a number of pictures of how the finger and thumb components are combined to control the motion of the hand. A flexed hand within HEXORR is shown (Figure 3.10.A). A palmar view of the hand in HEXORR highlighting the Velcro strap arrangement is provided (Figure 3.10.B). And an extended hand with the thumb in pure extension (Figure 3.10.C) and the thumb in abduction (Figure 3.11.D) are displayed.

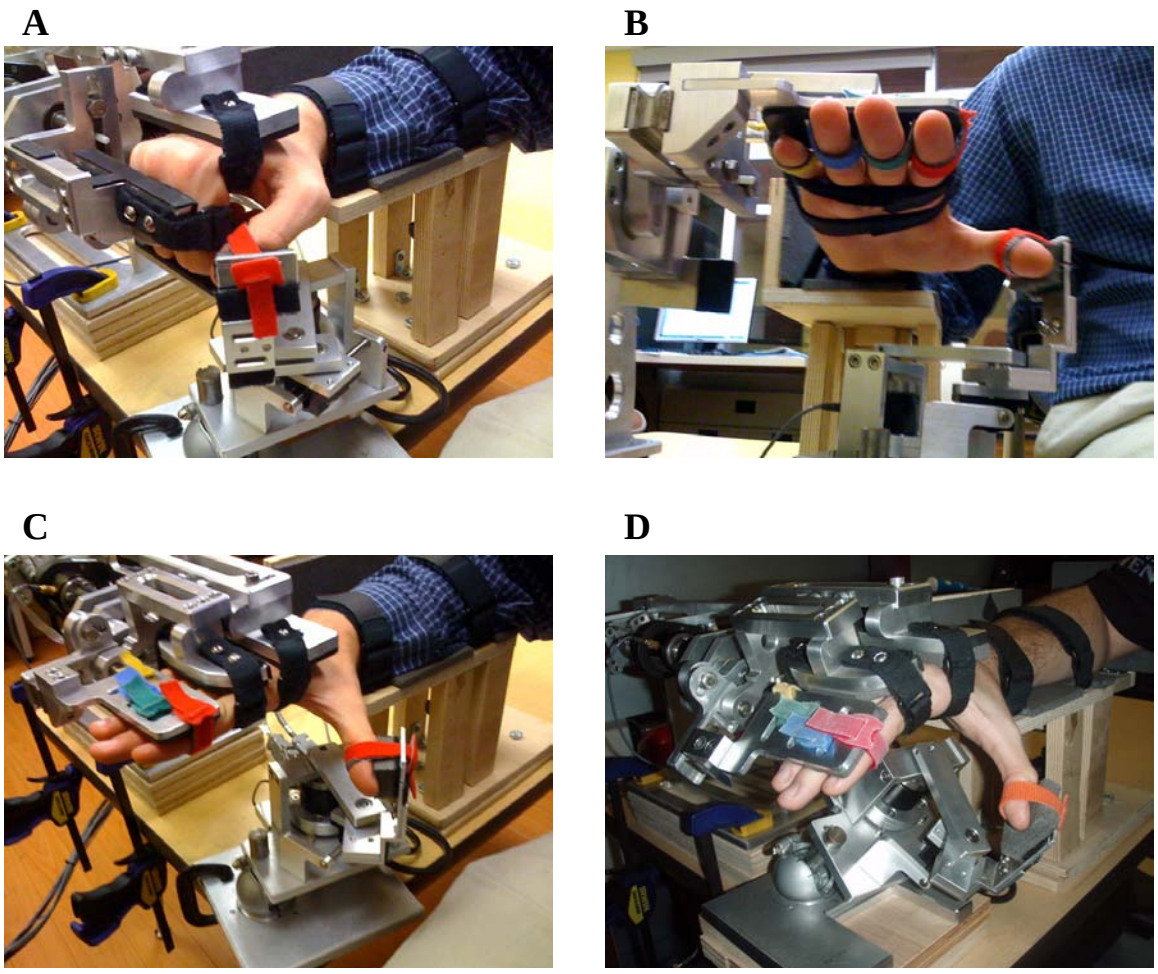

Fig. 3.10 Pictures of a hand in HEXORR at different postures. (**A**) The hand flexed (**B**) palmar view of the hand, highlighting the Velcro strap arrangement (**C**) The hand extended, with the thumb in pure extension and (**D**) the hand extended with the thumb in abduction.

CHAPTER 4

ELECTRONIC HARDWARE AND SOFTWARE

4.1 Electronics Hardware and Sensors

Figure 4.1 displays the electronics panel that houses the hardware needed to output command signals to the two motors and condition the input signals from the motors, torque sensors and encoders. The motors and torque sensors are powered by power supply units (Power One, HE Power Supply Series) capable of drawing from a standard electrical outlet (120 AC) and outputting up to 24 VDC and 12 VDC, respectively.

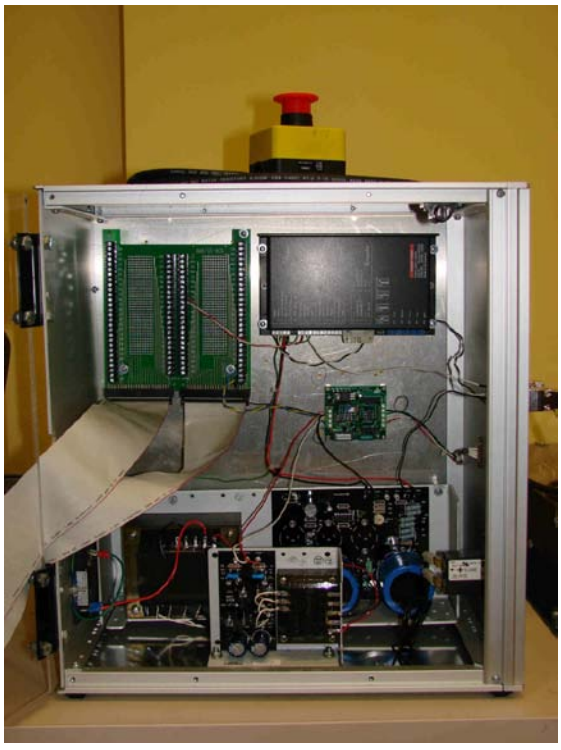

Figure 4.1 Electronics panel.

The two motors are controlled by servo drivers (Maxon Motor Control, 4-Q-DC and Accelnet, ACP-055-18). For added safety, a custom kill-switch can be used to shut down power to both motors. Custom circuit boards were designed to both amplify (gain of 665) and filter (RC filter, cut off frequency 15 Hz) the analog torque sensor input signal. These analog signals are converted to digital signals by a data acquisition board (Measurement Computing, PCI-DAS1200).

4.2 Motor Specifications and Servo Drivers

Before finalizing the specifications of the motors, we measured the resistive forces of a TBI volunteer with high tonicity (Ashworth scale of 4) during extension movements. The peak resistive force during an extension movement was approximately 5 Newton meters (Nm). Accordingly, this system requires a motor that will overcome such resistance in order to open and close a severely impaired hand. For the finger component, a DC, brushless motor (Maxon Precision Motors, RE 40) in series with a planetary gear head (Maxon Precision Motors, reduction ratio 74:1) was chosen. This geared motor is capable of outputting a continuous torque of 9.8 Nm. The thumb component's crank is driven by a FHA mini-series AC servo actuator (Harmonic Drive LLC, Peabody, MA) with a harmonic drive gear head (reduction ratio of 100:1). This actuator was chosen for two reasons. First, this geared motor has a very small housing

(60 x 59 x 56 mm). Using this motor ensures that the thumb component will easily fit underneath the finger component. Also, even though the actuator is small in size, it is capable of outputting a continuous torque of 11 Nm, an ample amount of force to extend a thumb with high tone. A wiring guide for both motors can be viewed in Figure 4.2.

4.3 Encoders

Encoders were used for position and derived velocity sensing for both the hand and thumb components. A HEDL 5540 quadrature encoder (500 count) is mounted on the finger component motor. Accounting for the 74 reduction ratio of the planetary gear head, the resolution of this encoder is 0.002º/count. Another encoder (2048 quadrature count, US Digital) is mounted between the motor and the finger/exoskeleton interface. This encoder is capable of reading subtle movements performed by the subject within the backlash range of the motor's planetary gear head with a resolution of 0.044º/count. The recordings of these slight movements are used in control algorithms that will be explained in a succeeding chapter. The Harmonic Drive servomotor was provided with a mounted quadrature encoder. Considering the 100 reduction ratio of the gear head, this encoder (2000 count) has a resolution of $4.5e^{-4}$ degrees/count.

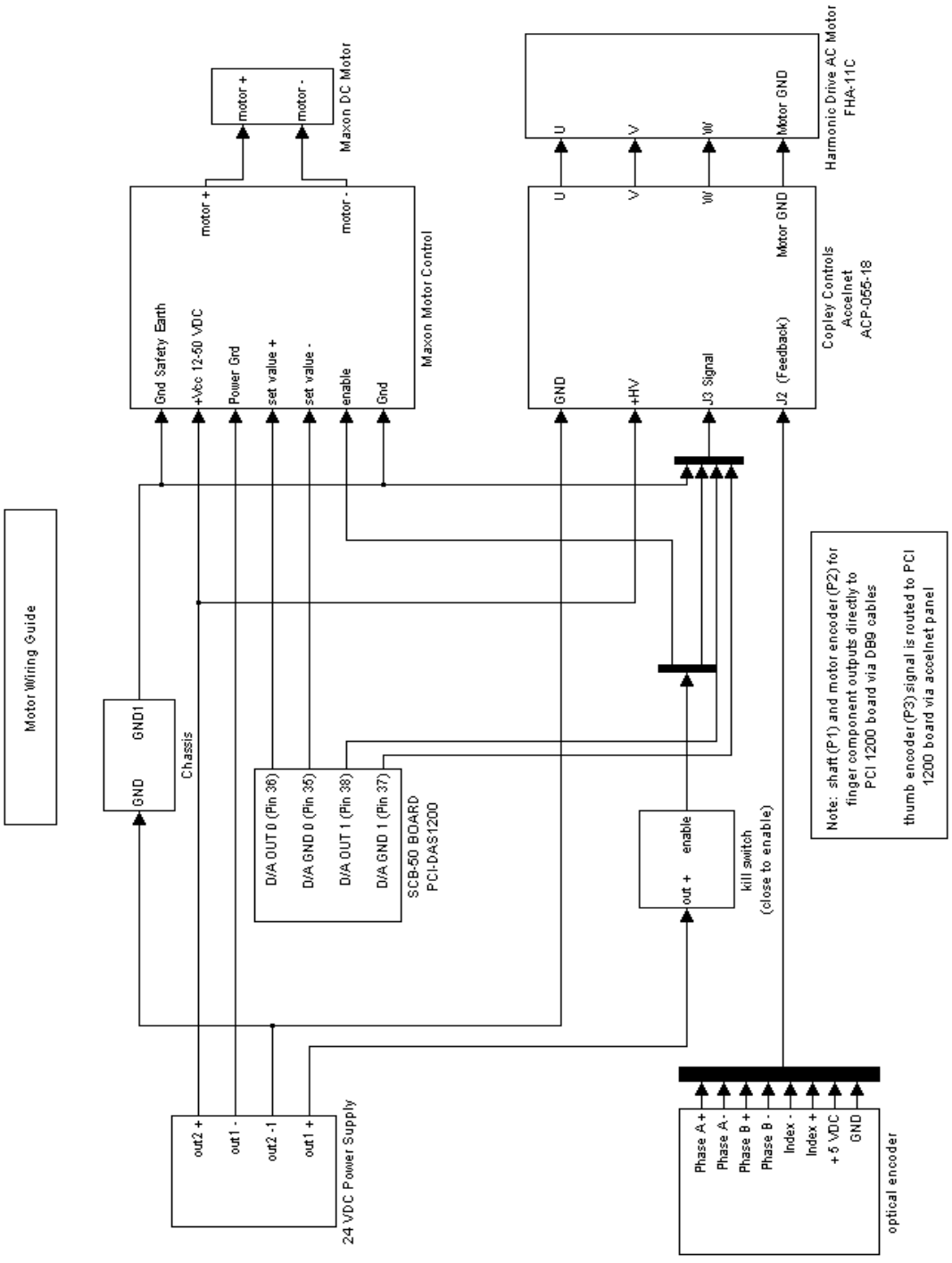

Figure 4.2 Wiring guide for both finger and thumb motors.

4.4 Torque Sensors

For both the hand and thumb components, a torque sensor (Transducer Techniques, TRT-200) is positioned between the actuators and the linkages. This torque sensor is capable of handling a maximum load of 33 Nm with an accurate resolution of 0.02 Nm. The torque sensors were calibrated to determine accurate voltage to Nm conversions. The calibration plots can be viewed in Figure 4.3. Judging from the coefficients of determination (R^2), the calibration curves were highly linear ($R^2 \geq 0.99$). For both torque sensors, the conversions were quite similar. For the finger torque sensor and the thumb torque sensor the conversions amounted to 1V = 1.42 N-m and 1V = 1.53 N-m, respectively. A wiring guide for both torque sensors can be seen in Figure 4.4.

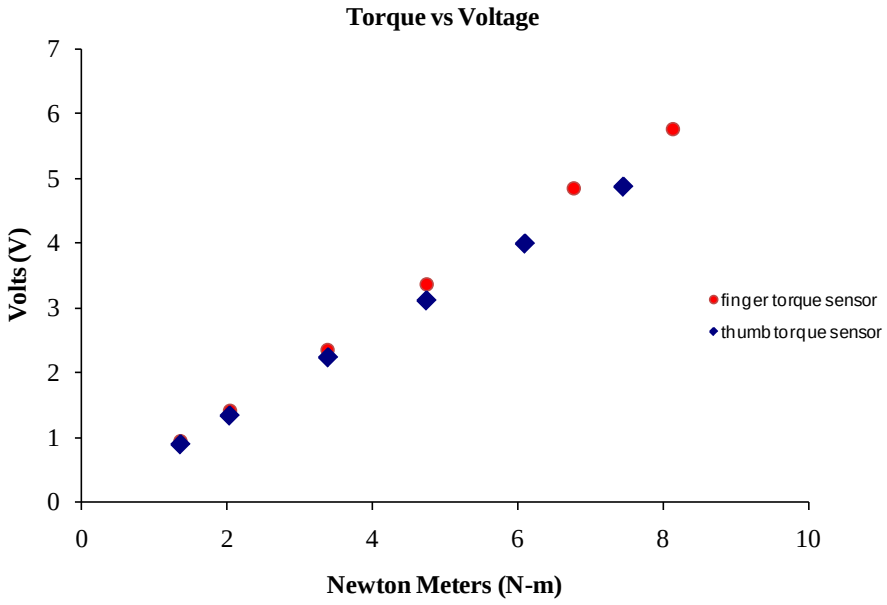

Figure 4.3 Torque sensor calibrations for both the finger and thumb torque sensors. The outputs were highly linear ($R^2 \geq 0.99$).

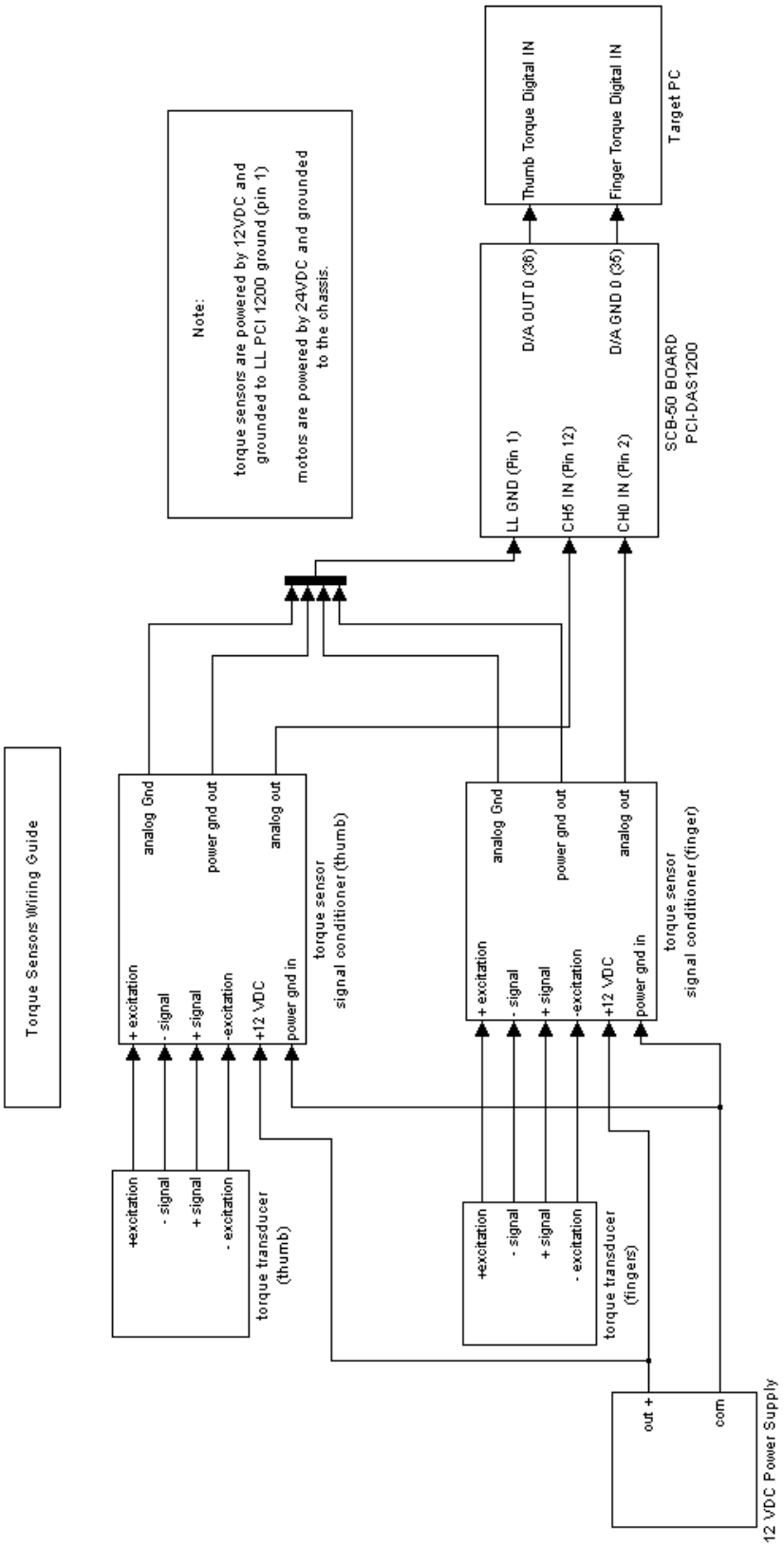

Figure 4.3 Torque sensor wiring guide.

4.5 Software and Compensation Algorithms

The exoskeleton is controlled with custom software programs developed using the Simulink®, XPC Target®, and Stateflow® toolboxes in MATLAB®. XPC Target® uses the graphical coding capabilities of the Simulink® toolbox to create a host-target environment for real time applications. The Stateflow toolbox is a graphical design and development tool for control and state machine logic. This toolbox proved particularly helpful by using state charts and flow diagrams to develop control algorithms. By designating machine states, the finger and thumb motors could easily be controlled in parallel. For example, if it was required that both the fingers and the thumb must complete an extension movement prior to beginning flexion, states could be used to identify the status of each component for proper decision making. If the finger state indicated that it has completed an extension movement, but the thumb state was still undergoing extension, the finger state would not be allowed to enter the flexion state until the thumb state has indicated that the movement has been completed.

Because stroke survivors have weakness in the paretic hand, it is critical that the torque needed open and close one's hand inside HEXORR be as low as possible. Similar to the work outlined in a recent technical note [59], we developed algorithms to model and compensate for the weight and friction (both static and kinetic) of the exoskeleton, thereby increasing the backdrivability of the geared motors.

For the finger component, gravity compensation was modeled by identifying the motor current (amps) required to move the linkages throughout the entire range of motion at a slow, constant velocity (10^{o}/second). The difference between the extension and flexion values at each position is equal to the motor current required to compensate for the weight of the exoskeleton linkage. To ensure that the motor would not move the linkage while providing weight compensation, input values were reduced by a gain of 0.9. These values were tabulated into an interpolation-extrapolation program to provide real time weight compensation. The motor current required to move the finger linkage at different, constant speeds and the calculated gravity compensation values can be viewed in Figure 4.5.

Gravity compensation was not performed for the thumb component. The linkage base is positioned along different planes, depending on the desired amount of thumb abduction/adduction for each task. Also, the high reduction ratio of the harmonic drive gear head (100) and the friction of the linear bearing dominated any effect that gravity had on the linkage.

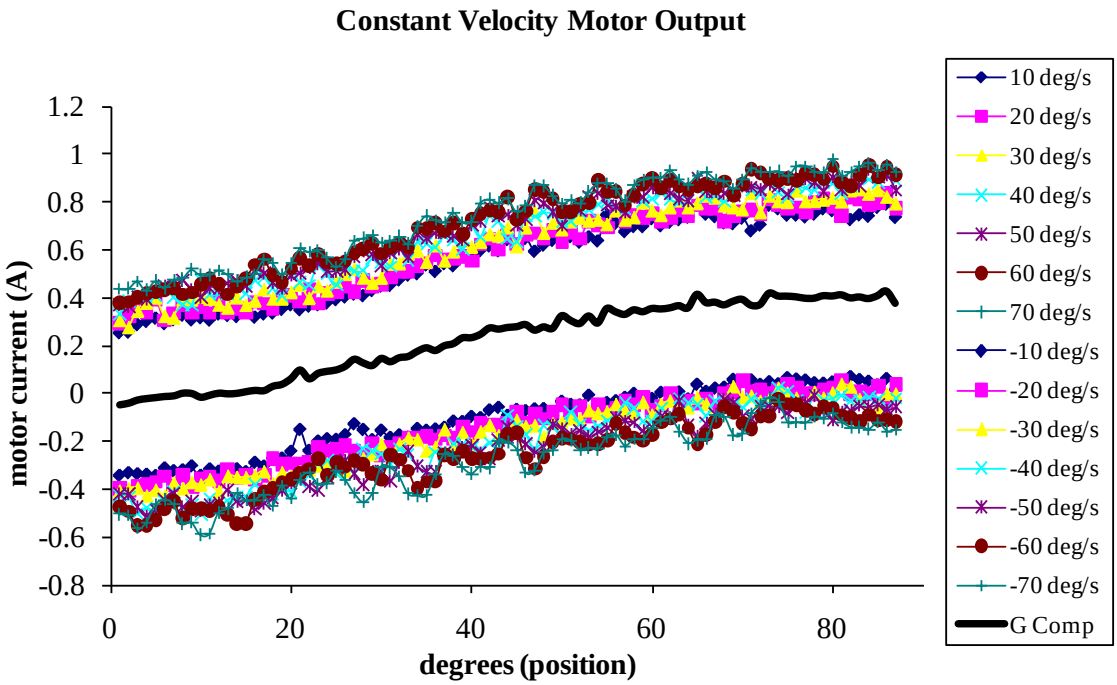

Figure 4.5 Motor current (amps) required to move the finger linkage in extension (+) and flexion (-). The gravity compensation values (black) were calculated as the difference between the extension and flexion output values.

Kinetic friction compensation was modeled through viscosity coefficients. These coefficients were calculated by moving the exoskeleton at different, constant velocities and subtracting the motor output required for gravity compensation. The required motor output increases linearly with velocity ($R^2 > 0.99$) and can be accurately modeled with linear regression equations. These linear models were used to predict and counter velocity-dependent friction. The mean velocity dependent viscosity coefficients for both extension and flexion directions can be viewed in Figure 4.6.

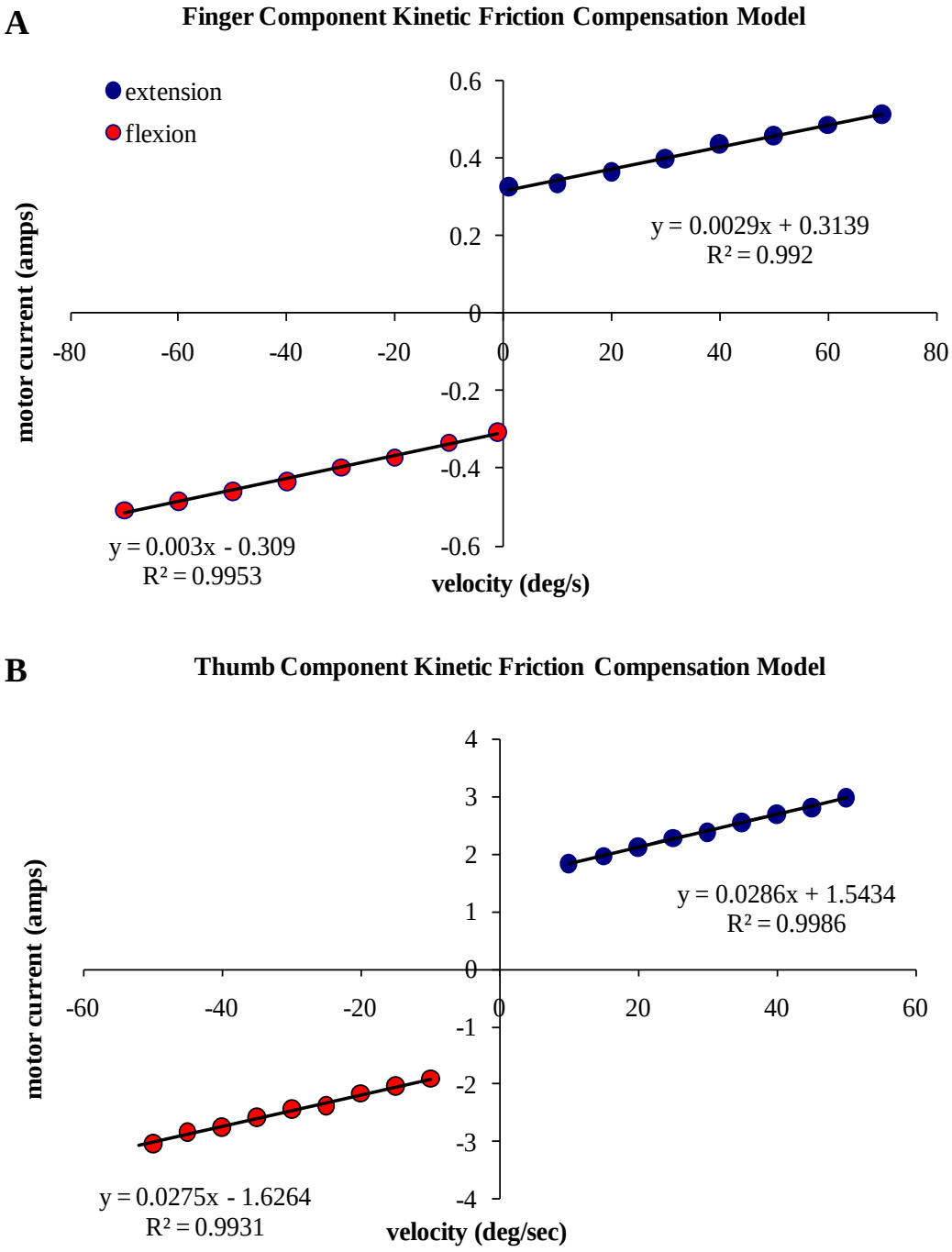

Figure 4.6 The mean viscosity coefficients for both extension (blue) and flexion (red) directions. The finger component (**A**) and thumb component (**B**) values were modeled with linear regression and the models were used to compensate for kinetic friction of the finger component.

Our compensation algorithm also accounts for static friction, or stiction. Static friction is responsible for resisting motion at zero velocity. The motors moved the exoskeleton very slowly throughout its ROM at a velocity of ±1 degrees/sec. These motor currents were reduced by a factor of 0.85 to ensure that the linkage does not move when no other forces are applied to the exoskeleton. The stiction compensation values were active only when the velocity of linkages was between ±0.1º degrees/second. Once the velocity of the linkages increased beyond this bandwidth, stiction compensation was deactivated and the kinetic friction compensation was activated.

The backdrivability of HEXORR was tested by a subject moving the exoskeleton at a constant velocity (40 degrees/sec) with and without compensation (Figure 4.7). Figure 4.7.A illustrates the torque required to move the hand component from full flexion (0°) to full extension (90°). Without any compensation, the required torque increases from 0.45 Nm to 0.8 Nm as the linkage extended. However, with gravity and friction compensation, the required torque is reduced to about 0.1 Nm and remains constant throughout the movement. Figure 4.7.B shows the torque profiles during the flexion phase for the finger component. Note that between 60° and 90°, without compensation, gravity causes the linkage to collapse. Therefore little torque is needed to flex the linkage within this range without compensation. Eventually more torque is required to finish the flexion movement and the torque increases to about 0.4 Nm. Again, the compensation algorithm reduces the required torque significantly to values no greater than ±0.1 Nm.

Figures 4.7.C and 4.7.D illustrate the extension and flexion backdrivability of the thumb motor, respectively. Without compensation, the mean torque required to move the thumb linkage is 0.6 Nm and -2.5 Nm in the extension and flexion directions, respectively. With compensation, the required torque in the extension direction (mean = 0.2 Nm) and the flexion direction (mean = -0.5 Nm) have been dramatically reduced. On average, the weight and friction compensation algorithms increase HEXORR's backdrivability by more than 66%.

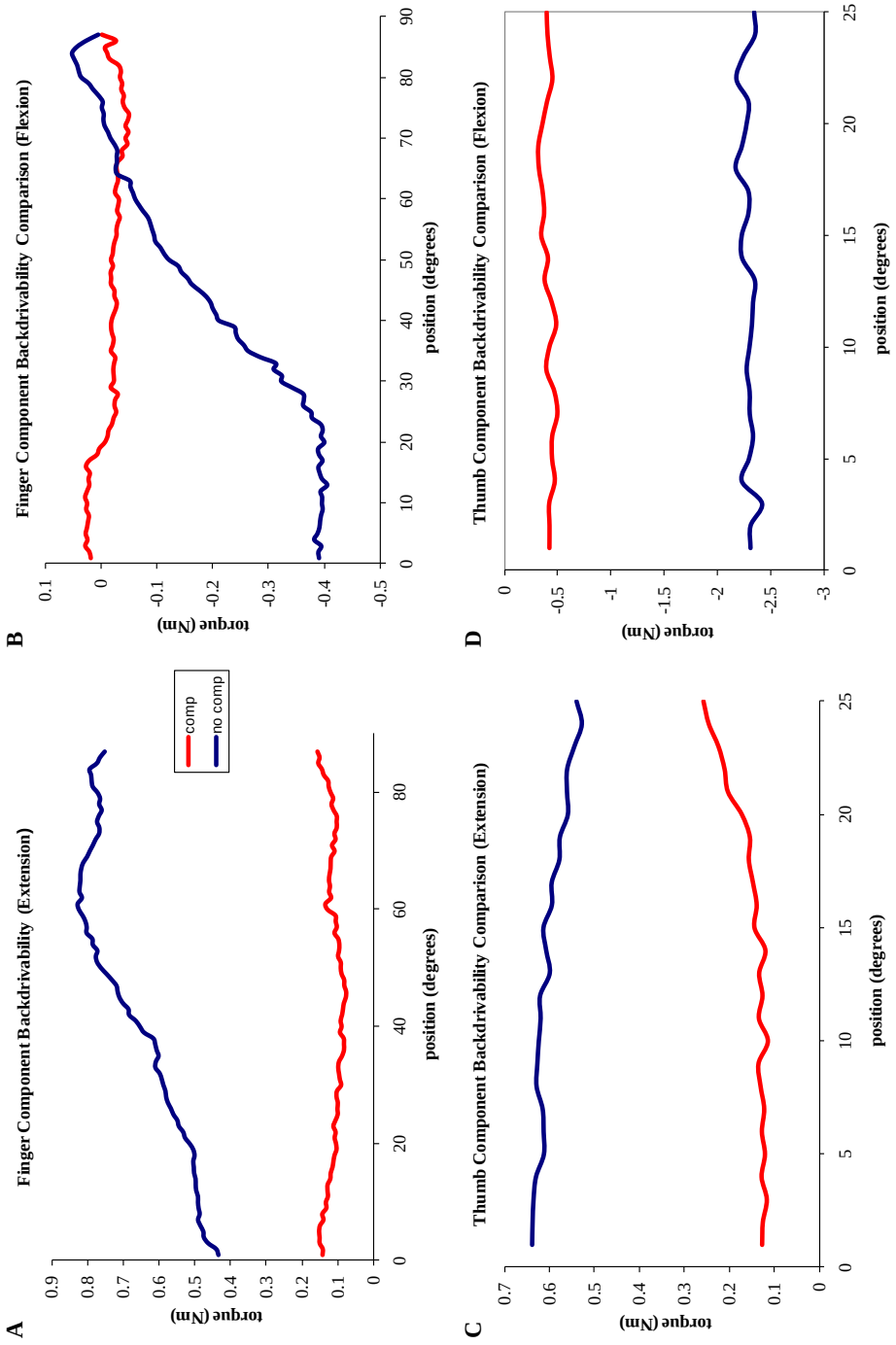

Figure 4.7 Torque required to rotate the linkages with (red) and without (blue) weight and friction compensation. Compensation was provided for the finger component in the extension (**A**) and flexion (**B**) direction and also for the thumb component in the extension (**C**) and flexion (**D**) direction. Compensation reduced the required torque by 66%.

CHAPTER 5:

MATERIALS AND METHODS

5.1 Experimental Setup

Nine right-handed, neurologically intact subjects, (aged 23-57 years, mean = 32±12), and five subjects with chronic stroke (aged 33-61 years, mean = 53±12) participated in this experiment. Handedness was assessed with the ten item Edinburgh inventory [60]. Only subjects that received a laterality quotient of 80% or greater were admitted into this study. All subjects signed an informed consent form prior to admission to the study. All protocols were approved by the National Rehabilitation Hospital's Internal Review Board for Protection of Human Subjects.

For the subjects with chronic stroke, inclusion criteria required a first ischemic or hemorrhagic stroke occurring more than 3 months prior to acceptance into the study,

some proximal upper extremity voluntary activity at the shoulder and elbow, and trace ability to control movement at the wrist, MCP and PIP joints in extension. Exclusion criteria included excessive pain in any joint of the affected extremity that could limit ability to cooperate with the protocols, serious uncontrolled medical problems as judged by the project therapist, and a full score on the hand and wrist sections of the Fugl-Meyer motor function test [61].

Before using the robot, stroke subjects were clinically evaluated (Table 1). Upper extremity movement impairments were evaluated with the Action Research Arm Test [62, 63] and the Fugl-Meyer motor function test. Muscle tone was measured at the elbow, wrist and fingers with the Modified Ashworth Scale [64]. Because this pilot study was not designed for therapy treatment, no follow up clinical assessments were performed.

Table 5.1

Measure	All subjects	Subject 1	Subject 2	Subject 3	Subject 4	Subject 5
n	5					
Age (year)		59	61	51	62	33
Gender	1F/4M					
Time post-stroke (months)		14	19	12	300	34
Right (affected) side						
Action Research Arm Test (total score = 57)	22.4±3.2	20	21	21	22	28
Grasp (total score = 18)	6.2±1.1	6	5	6	6	8
Grip (total score = 12)	5.2±1.3	4	4	5	6	7
Pinch (total score = 18)	6.2±0.45	6	6	6	6	7
Gross Movement (total score = 9)	4.8±1.1	4	6	4	4	6
Arm Motor Fugl-Meyer score (total score = 66)	33.7±7.1					
Proximal arm subportion (total score = 42)		22	19	20	9	25
Hand/wrist subportion (total score = 24)		12	13	14	13	15
Coordination/Speed (total score = 6)		1	2	1	1	3
Modified Ashworth Spasticity Scale (unimpaired = 0)	1.7± 0.3	1 +	1 +	2	1 +	2
Elbow		1 +	1 +	2	1 +	2
Wrist		1 +	1 +	2	1 +	1 +
Finger		1 +	1 +	2	1 +	1 +

Results are mean ± standard error. Subject received clinical assessment prior to using the robotic device. This pilot study was not intended to provide therapy, so no follow-up assessment was conducted.

Subjects were seated in a chair and their right hand was placed inside HEXORR to perform both passive and active hand extension/flexion movements. The forearm was placed on an arm rest in the neutral position and the table was adjusted so that the elbow was flexed at 90º and the shoulder elevated approximately 45º. An elbow support pad was placed on the posterior side of the upper arm to minimize shoulder retraction and extension. For each subject, the linkages of the exoskeleton were adjusted to comfortably fit the size of the hand. The wrist was held in the neutral position by placing the dorsal side of the hand against a rigid, padded support and using a Velcro strap around the palm of the hand. The dorsal sides of the hand's digits were positioned against the machine-hand interfaces and Velcro straps were wrapped around the palmar side to attach the digits to the exoskeleton. The subjects performed hand movements inside HEXORR for

about 30 to 60 minutes while watching a real-time display of their hand's position on an eye level computer monitor.

5.2 Experimental Tasks

Unimpaired subjects performed tasks specifically designed to evaluate HEXORR's ability to emulate comfortable hand movements throughout the five

Figure 5.1 CyberGlove II

digits' full ROM. During these tasks, the subjects wore the wireless CyberGlove II® (CyberGlove Systems, San Jose, CA) on their right hand (Figure 5.1). This glove features three extension/flexion sensors per finger, four abduction sensors, a palm-arch sensor, and sensors to measure wrist flexion and abduction. For baseline ROM measurements, subjects performed five hand extension/flexion movements outside of the device. For these movements, the arm and wrist were positioned as if the hand was inside the exoskeleton (elbow flexed at 90^{o}, wrist and forearm in neutral position). Afterward, the right hand was placed inside HEXORR and the exoskeleton's motors were used to perform five continuous passive extension/flexion movements (finger encoder rotation 0^{o} to 80^{o}, thumb encoder rotation 0^{o} to 20^{o}). Following the passive movements, the subjects performed 10 active-unassisted hand extension/flexion movements inside of

the device. During these unassisted movements, the motors provided previously described weight and friction compensation.

Stroke subjects performed hand movements within HEXORR during three different modes: continuous passive movements, active-unassisted extension/flexion and active force-assisted extension/flexion. During the five passive movements, subjects were asked to relax their hand fully as the motors moved their digits throughout a comfortable range of motion (all stroke subjects tolerated full extension of the fingers and thumb). Then, subjects were asked to perform five active-unassisted finger and thumb extension/flexion movements. During these movements, motors provided only weight and friction compensation. This mode was also designed to 'catch' involuntary flexion movements during an intended extension movement. Any unintended flexion movement was halted by the motors, and the exoskeleton was held in place. Subjects were given three attempts to further extend their digits before the experimenter prompted the motors to finish the extension movement. After finishing the five active-unassisted hand movements, subjects were given a five minute break.

The motor currents required to passively extend the subject's digits were tabulated into a position dependent assistance profile. Figure 5.2.A displays an example of the motor current required to passively stretch a stroke subject's hand. This profile was scaled by

an adjustable gain and delivered feed-forward during the movements. The gain was reduced from 1 in increments of 0.2 until the subjects indicted that they were actively opening their hand. Once a proper gain was found, subjects opened and closed their hand 5 times with assistance. Figure 5.2.B illustrates a block diagram to further describe the active-unassisted and active force-assisted conditions.

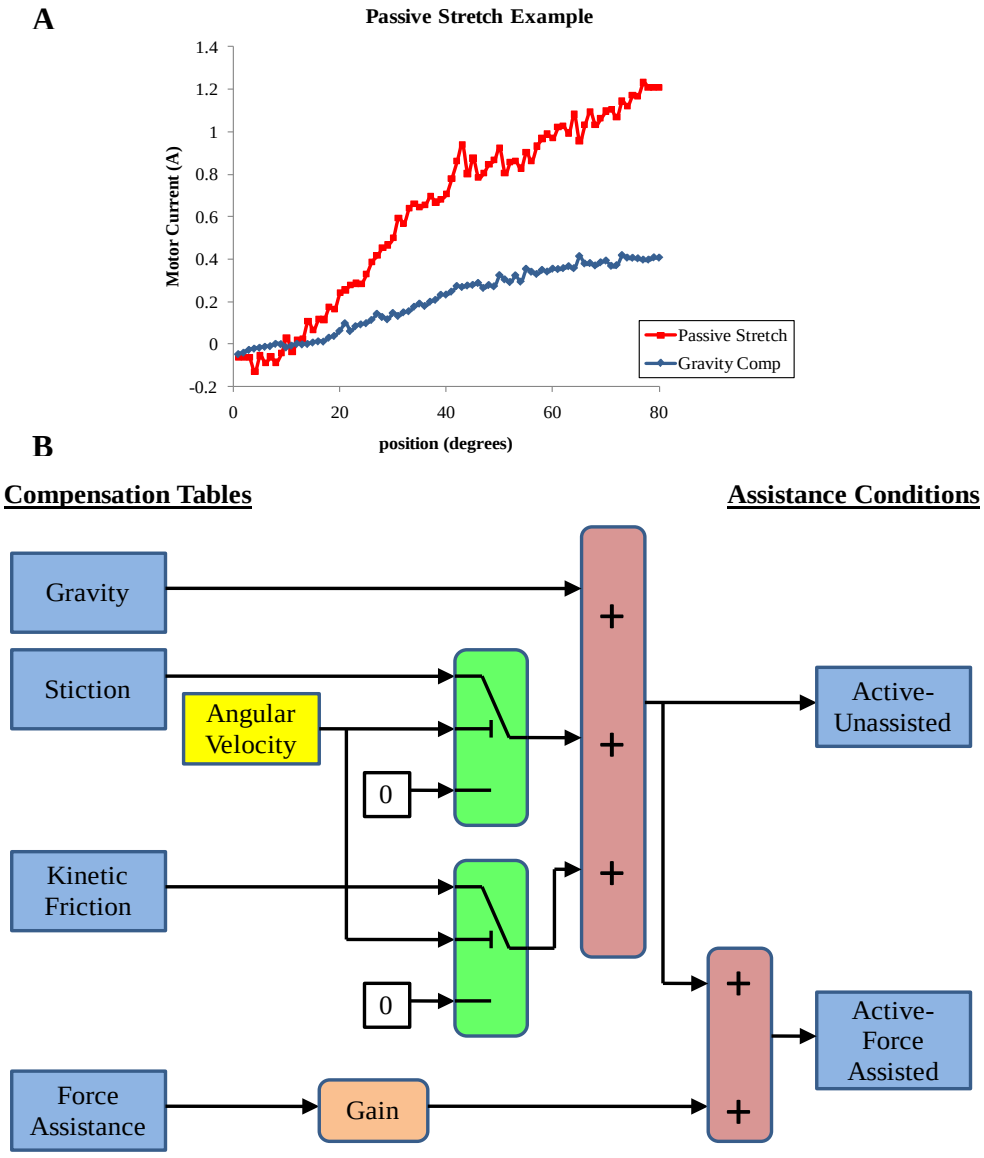

Fig 5.2 (**A)** An example of the motor current needed to passively stretch a stroke subject's fingers, compared to gravity compensation. (**B)** Block diagram of the compensation provided for the active-unassisted and active force-assisted conditions. Stiction is provided when -0.1º/sec ≤ angular velocity ≤ +0. 1º/sec. Otherwise, kinetic friction compensation is provided.

5.3 Data Analysis

Data analysis was performed using the hand robot's encoders and torque sensors and, for unimpaired subjects, the CyberGlove II®. Custom software recorded the positions and torques of the hand's digits (f_S = 1 kHz). The encoder signals were digitally differentiated and low pass Butterworth-filtered (f_C = 30 Hz) to yield angular velocity. Torque sensor signals were filtered (f_C = 15 Hz) and biases were removed prior to data analysis. Without a hand in the exoskeleton, the linkages were moved slowly (1^o/second) throughout the ranges of motion and the torque was recorded. These torque values were interpolated, averaged and used as position dependent torque sensor bias values. CyberGlove II® data was separately collected using the manufacturer's data acquisition software (f_S = 100 Hz). The initiation and cessation of hand movements were defined as 5% of the maximum angular velocity.

For the unimpaired subjects, active ROM and joint-pair coordination were investigated. Active ROM was assessed using the CyberGlove II® data under three conditions: hand movements outside of the exoskeleton, and passive stretching and active-unassisted movements inside the exoskeleton. ROM analysis consisted of calculating the mean difference between the maximum values of the digits' extension and flexion position for all subjects under each condition. Joint-pair coordination was assessed for the 1^{st} and 3^{rd} digits under two conditions: outside and inside HEXORR. For the 1^{st} and 3^{rd} digits, the angular rotations about the CMC, MCP and DIP and about the MCP, PIP and DIP were

analyzed, respectively. Joint-pairs were considered as joints joined by metacarpals or phalanges (Figure 5.3). Therefore, the 1st digit joint-pairs consisted of the CMC-MCP and MCP-DIP and the 3rd digit joint-pairs were MCP-PIP and PIP-DIP. These pairs were plotted (x axis: proximal joint, y axis: distal joint) and modeled by linear regression. Linearity was measured with the coefficient of determination (R^2).

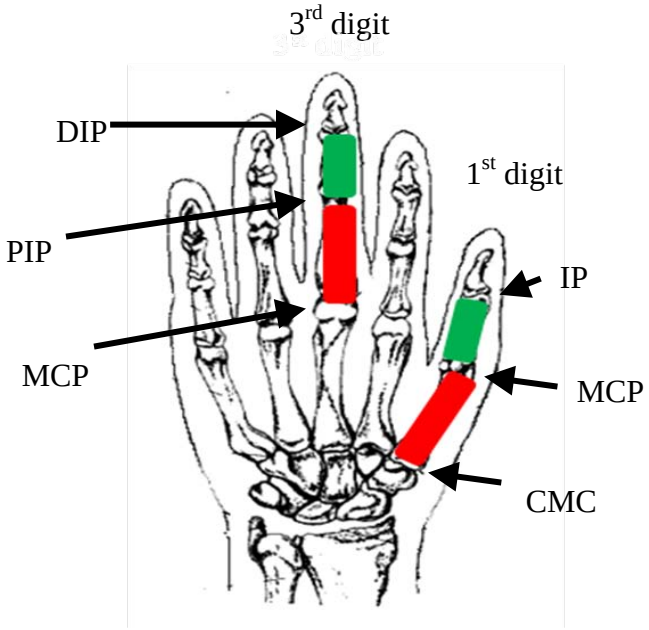

Figure 5.3 Joint Pairs. Proximal joint pairs (3rd digit: MCP-PIP 1st digit: CMC-MCP) are highlighted in red. Distal joint pairs (3rd digit: PIP-DIP 1st digit: MCP-IP) are highlighted in green.

For the stroke subjects, the ROM and torque production of the fingers and thumb were compared in the active-unassisted and active force-assisted conditions. The ROM analysis was similar to the unimpaired subject ROM calculation, but by using the

HEXORR's encoders instead of the CyberGlove II®. Average torque values were calculated to investigate the extent of the subjects' voluntary participation during extension movements. Only torque values during exoskeleton movement were considered and torques produced during a pause in motion, caused by hand flexion during a designated extension movement, were removed from the analysis. By convention, positive torque values indicate torque in the extension direction. Therefore, if the average torque during an extension movement was positive, we concluded that the subject performed an active extension movement. Accordingly, if the average torque value was negative, then the provided assistance was too high and the robot pulled the digits open.

Unimpaired subjects' finger active ROM analysis was performed by repeated measures ANOVA with two within subject factors: condition (2: inside and outside of HEXORR) and joint active ROM (12).

CHAPTER 6:

RESULTS

6.1 Unimpaired Subject Active ROM

One of the major design criteria of HEXORR was that the finger and thumb linkages allow for full active ROM. Figure 6.1 illustrates the unimpaired subjects' active ROM (mean ± standard error) under the three conditions: hand movements outside of the exoskeleton, and passive stretching and active-unassisted movements inside the exoskeleton. For many of the joints' active ROM, there were no significant differences between active movements performed inside the exoskeleton and outside of the device. Paired t-test analysis showed no significant differences in thumb active ROM. However, the condition factor was significant ($F_{(1,8)}$ = 11.6, P = 0.009) for finger active ROM. Post-hoc analysis was performed with Bonferroni corrected paired t-tests (corrected confidence level: 0.05/12). For MCP rotation (Figure 6.1.A), the 4th (difference = 19^{o}, P

= 0.017) and 5th (difference = 17º, P = 0.015) digits rotated significantly less inside of HEXORR than outside of the device. The PIP rotation (Figure 6.1.B) of the 5th digit was also significantly less inside of the exoskeleton compared to movements made outside of the device (difference = 23º, P = 0.003). The remaining 9 joints of the fingers had no significant active ROM differences between movements made inside and outside of HEXORR. Therefore the active ROM of 12 out of 15 joints of the hand's digits was not affected by the exoskeleton.

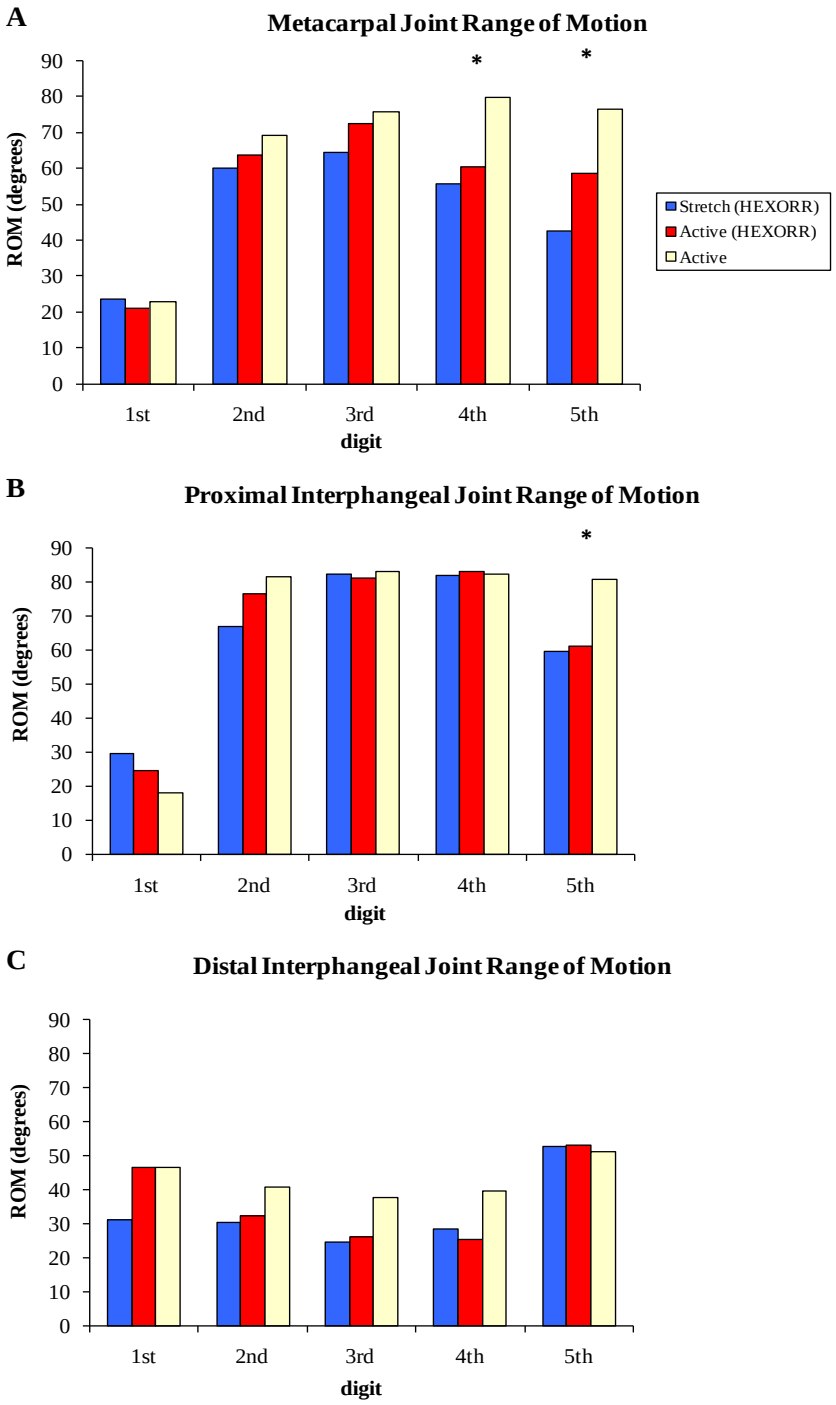

Figure 6.1 The mean values of the unimpaired subjects' (**A**) MCP, (**B**), PIP and (**C**) DIP joint ROM under 3 conditions: passive stretch, active-unassisted movements inside HEXORR and active movements outside of the exoskeleton. Twelve of the fifteen tested joints showed no significant ROM differences between active movements outside and inside HEXORR.

6.2 Joint-Pair Coordination

For the 1st and 3rd digits of the hand, mean joint-pair coordination comparisons between active-unassisted extension movements inside HEXORR and those made outside of the device can be seen in Figure 6.2. For the 1st digit, joint-pairs consisted of the CMC-MCP and MCP-DIP. For the 3rd digit, joint-pairs were MCP-PIP and PIP-DIP. For every subject, the coordination between joint pairs for both the 1st and 3rd digits was highly linear ($R^2 \geq 0.957$) both inside and outside of HEXORR. Also, paired t-tests indicated no significant differences between the slopes of the joint-pair coordination plots for the 1st ($P > 0.143$) and 3rd ($P > 0.171$) digits. This indicates that performing extension movements with the hand inside HEXORR emulates physiologically accurate extension trajectories.

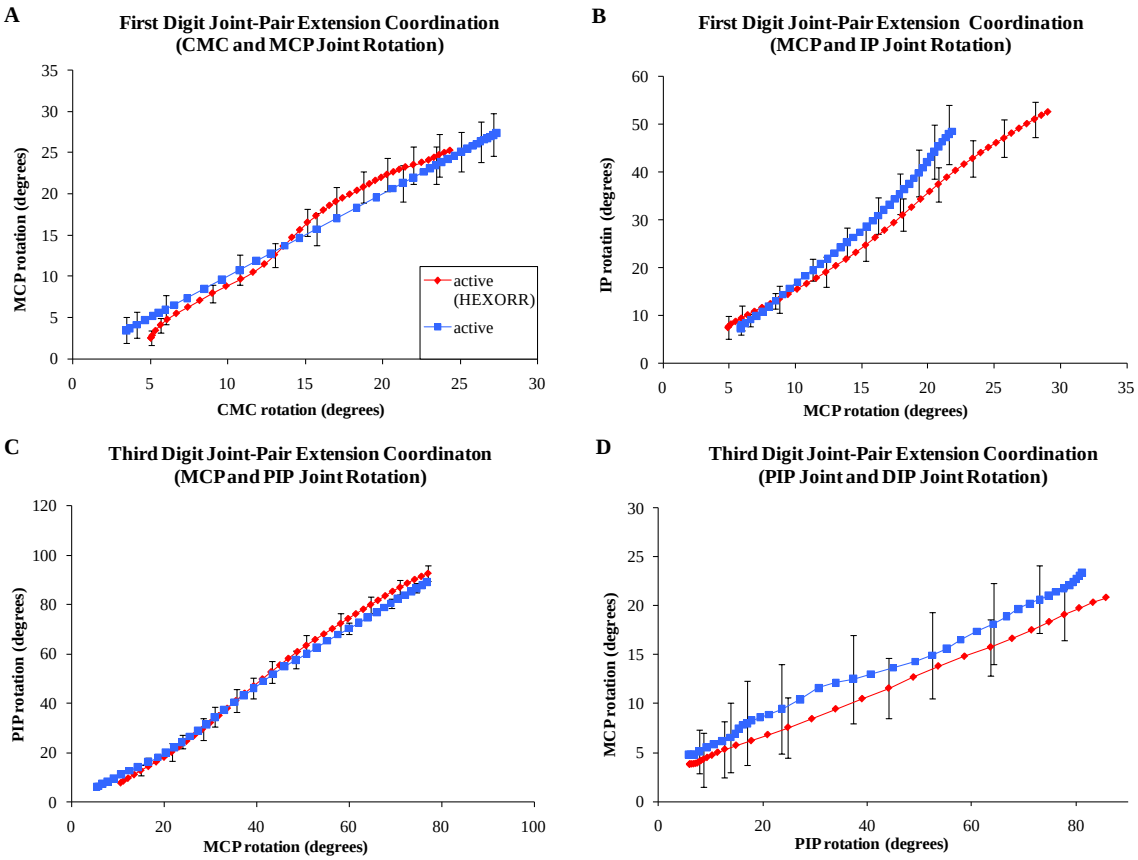

Fig 6.2 Joint-pair coordination plots for unimpaired subjects' 1st digit (**A**) CMC-MCP pair (**B**) MCP-IP pair and 3rd digit (**C**) MCP-PIP pair and (**D**) PIP-DIP pair (mean ± standard error). Paired t-tests indicate no significant differences between trajectories performed inside and outside of the exoskeleton.

6.3 Stroke Subject Performance

Figure 6.3 summarizes each stroke subject's performance during both the active-unassisted and active force-assisted conditions. ROM varied widely on an individual basis (Figures 6.3.A and 6.3.C). The finger active ROM during the active-unassisted condition ranged from 5^o to full ROM (80^o) and thumb ROM varied between approximately 1^o to 16^o and 5^o to 64^o for the CMC and IP, respectively. Average extension torque correlated positively with extension ROM (Figures 6.3.B and 6.3.D). Generally the higher the average torque, the greater the active ROM. The displayed active force-assisted condition values were generated by averaging 5 extension movements while providing assistance with a gain of 0.6. Note that mean thumb extension torques during the active force-assisted condition for Subjects 4 and 5 were negative. This indicates that the provided assistance pulled the thumb open. Accordingly the thumb data for these two subjects were not considered in the group analysis below. With assistance, the mean active extension ROM increased by $17^o \pm 0.2^o$ (excluding Subject 1) for the fingers' MCP and PIP and by $2.6^o \pm 1.2^o$ and $11.7^o \pm 3^o$ for the thumb's CMC and IP, respectively. For nearly all extension movements, the average torque remained positive. With the provided assistance the mean finger extension torque dropped from 0.37 ± 0.09 Nm to 0.29 ± 0.06 Nm and the mean thumb extension torque decreased from 0.32 ± 0.04 to 0.23 ± 0.02 Nm. The provided assistance increased finger

ROM by 43%, while reducing the required finger extension torque by 22%; thumb ROM was increased by 24%, while the required thumb extension torque was reduced by 30%.

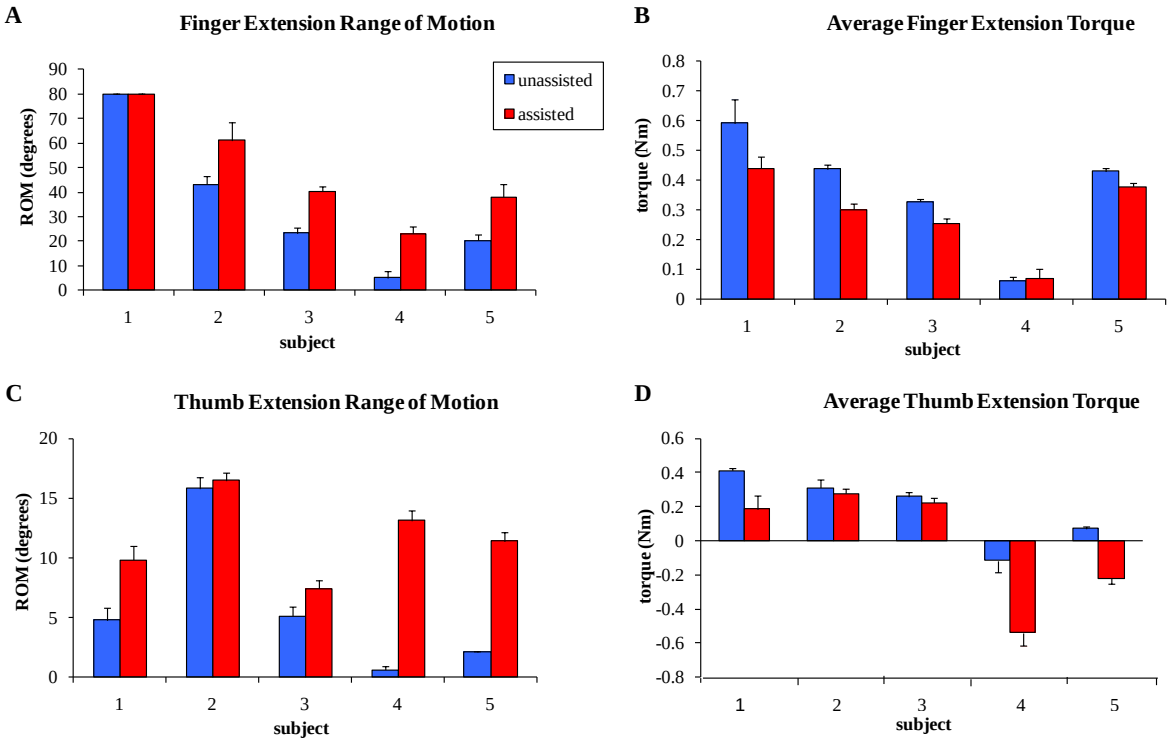

Fig. 6.3 Active-assisted (**A)** finger ROM and (**B**) mean torques and (**C)** thumb extension ROM and (**D**) mean torques are shown. The provided assistance increased finger ROM by 43% and reduced finger extension torque by 22%. For the thumb, active ROM was increased thumb ROM by 24%, reducing thumb extension torque by 30%. For the thumb, the mean torque for Subject 4 and 5 were negative. This indicates that the assistance forces were too high and extended the thumb.

6.4 Flexion Catch

During both the active-unassisted and active force-assisted conditions, any involuntary flexion movement was halted during a designated extension movement and the stroke subjects were able to try to extend their digits further from this point. Providing this 'flexion catch' greatly increased the active extension ROM for both the fingers and the thumb. On average, the flexion catch feature increased the active ROM by approximately $20^{o} \pm 5^{o}$ for the fingers' MCP and PIP and by $5^{o} \pm 3^{o}$ and $22^{o} \pm 6^{o}$ for the thumb's CMC and IP, respectively. An example of a stroke subject taking advantage of the 'flexion catch' to increase his fingers' active ROM during the active-unassisted condition can be seen in Figure 6.4.

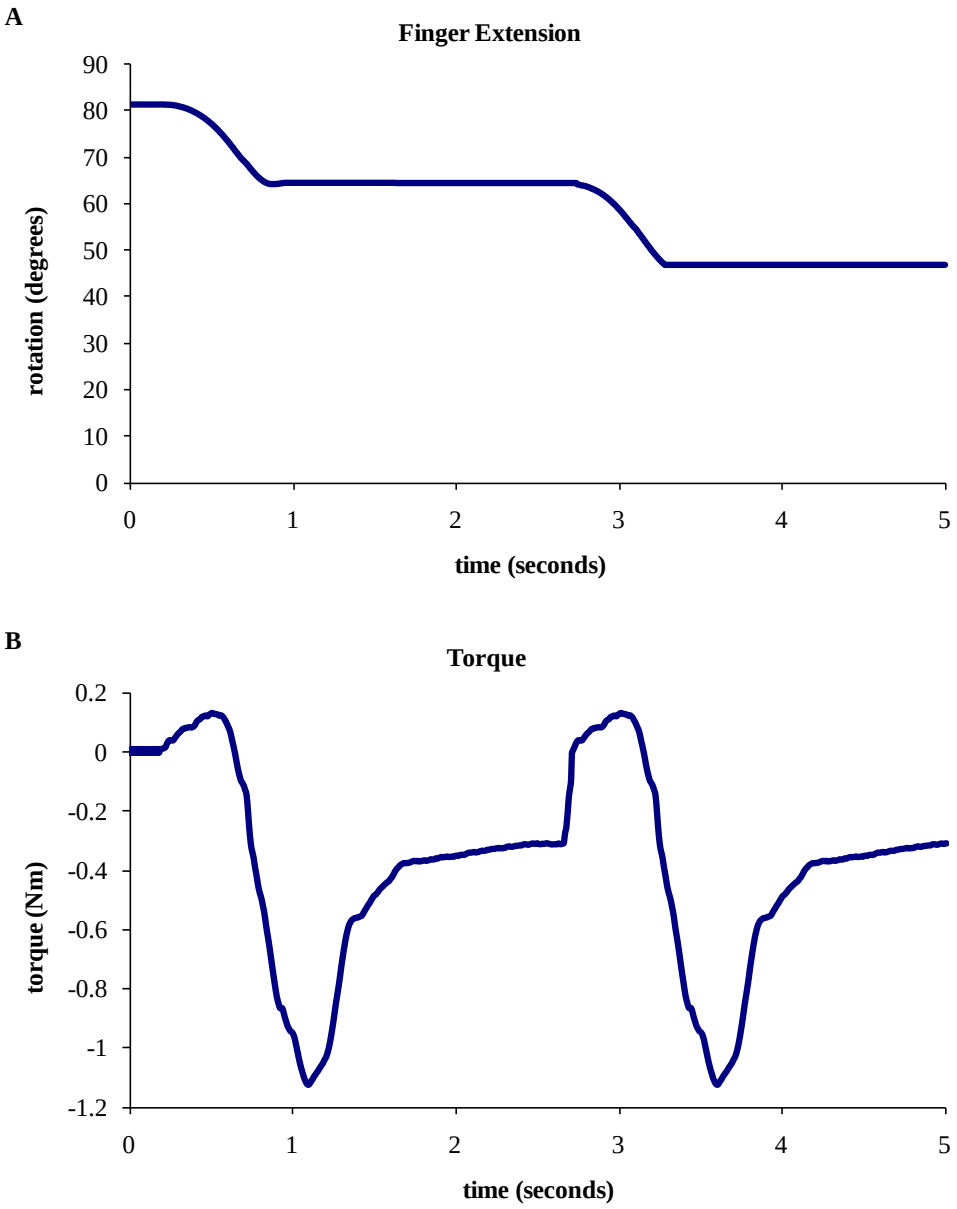

Fig. 6.4 Example of (**A**) an active finger extension movement and (**B**) torque production by Subject 2. Unintended flexor activity occurred twice during the intended finger extension. Flexion motion was halted by the motors and the subject was able to relax the flexors and then further extend the hand's digits.

CHAPTER 7:

DISCUSSION

A novel exoskeleton was developed to provide hand motor therapy to patients that have suffered a stroke and a pilot study was conducted to test the initial design goals and to determine the efficacy of a potential therapy protocol. HEXORR consists of two modular components that are capable of separately controlling the extension and flexion of the fingers and the thumb. This exoskeleton was designed to accommodate any hand size and to provide extension/flexion assistance for all five digits of the hand through their entire ROM. The compensation algorithms account for the weight and friction of the system and greatly increase the device's backdrivability. The main results of this pilot study indicate that, overall, HEXORR was successful in allowing full active ROM of the fingers and thumb. Also, the guidance of the linkages maintained physiological accurate extension trajectories, as seen by the joint-pair coordination of the hand. The stroke

subjects were capable of active extension during the active-unassisted condition and the active force-assisted condition successfully increased the stroke subject's active ROM.

7.1 Active Range of Motion

Testing with unimpaired subjects showed that for 12 of the 15 tested hand joints there were no significant active ROM differences between hand movements performed inside and outside of HEXORR. Three joints rotated significantly less inside HEXORR, the 4th and 5th digits' MCP and the 5th digit's PIP. We believe that the mechanical stop intended to avoid finger hyper-flexion caused the reduction in the two MCP joints' ROM. This stop was designed to position the 3rd digit's MCP at 90^{o} (orthogonal to the palm). Because the machine-hand interface was flat, all of the fingers' proximal phalanges were strapped into this position. However, when a hand is outside HEXORR and fully flexed, the proximal phalanges of the 4th and 5th digits are positioned more proximally. Our safety backstop slightly inhibited the MCP flexion position of these two digits, thereby reducing the total ROM. It is particularly difficult to strap the PIP of the 5th digit with the other four larger digits, resulting in a reduced ROM for the 5th digit's PIP. A simple solution calls for a slight redesign of the machine-PIP interface so that the 5th digit's phalanx can be individually strapped to the linkage thereby potentially increasing this joint's ROM. The current design of HEXORR is generally successful in producing full

ROM of the hands' digits and with a couple simple design changes this device will allow full ROM for all of the hand's digits.

7.2 Joint-Pair Coordination

The goal of the joint-pair coordination analysis was to ensure that the relative rotation of the hand's joints were physiologically accurate. Joint-pairs were categorized as joints joined by metacarpals and phalanges. These coordination plots were constructed with the proximal joint rotation along the x-axis and distal joint rotation along the y-axis. Paired T-test comparisons resulted in no significant difference between the slopes of these trajectories during extension movements performed inside and outside of HEXORR. This indicates that the exoskeleton successfully emulated physiologically accurate trajectories of the all of the hand's digits.

7.3 Stroke Subjects

The stroke subjects were capable of actively extending of the hand's digits within HEXORR during the active-unassisted condition. Stroke subjects' active ROM varied widely and correlated with their impairment level, as judged by clinical assessment. For instance, Subject 4 performed the worst in the Arm Motor Fugl-Meyer assessment and, accordingly, had the lowest active ROM within HEXORR. All subjects produced torques

in the extension direction showing that the active-unassisted condition did not provide overcompensation. Torque sensor data showed that many subjects unintentionally activated their flexors during extension movements; this typically results in flexing the hand's digits. This condition was designed to halt any unintended flexion movements during a designated extension movement. This mechanism is useful because it allows subjects to focus on individually activating their extensor muscles at positions they are normally incapable of reaching. Increasing the digits' active ROM promotes neural plasticity by creating a larger afferent signal to the brain sensorimotor areas [65].

The assistance provided during the active force-assisted condition successfully increased the stroke subjects' hand's active ROM. We designed this condition so the provided assistance was dependent on the motor current required to passively stretch the subject's digits. This approach directly counters muscle tone, one of the neural mechanisms shown to impede hand extension. Providing assistive forces in the extension direction also inherently helps to counteract the muscle weakness imbalance between the extensor and flexor muscles. Generally, torque data showed that, even with assistance, stroke subjects still actively extended their hand's digits. For Subjects 4 and 5, the average thumb torque values were negative, indicating that the assistive forces pulled the thumb open. This is not ideal because it has been shown that providing too much assistance can encourage patients to decrease their own physical effort during therapy [66, 67]. Ultimately, this can decreases motor learning [68]. Our results and previous findings call for a more

sophisticated algorithm to provide extension assistance. One potential approach is developing an adaptive controller that can adjust the gain of the provided assistance based on the subject's needs [44, 69, 70]. This approach has proven successful in prompting motor learning while reducing performance error [71].

7.4 Conclusion

We have designed a novel hand exoskeleton rehabilitation robot, HEXORR, for the purpose of providing therapy to stroke survivors. This device has been designed to provide full range of motion (ROM) for all of the hand's digits. The thumb actuator allows for variable thumb plane of motion to incorporate different degrees of extension/flexion and abduction/adduction. Compensation algorithms have been developed to improve the exoskeleton's backdrivability by counteracting gravity, stiction and kinetic friction. We have also designed a force assistance mode that provides extension assistance based on each individual's needs.

Our pilot study shows that this device is capable of moving the hand's digits through the entire ROM with physiologically accurate trajectories. Stroke subjects received the device intervention well and were able to actively extend and flex their digits inside of HEXORR. Our active force-assisted condition was successful in increasing the subjects' ROM while generally promoting active participation. We intend to develop a more

sophisticated adaptive active-assistance algorithm to provide minimal assistance that prompts motor learning while continuing to challenge the subject's abilities.

CHAPTER 8:

CLINICAL THERAPY

The pilot study shows that this device is capable of allowing the hand to move through the entire ROM with physiologically accurate trajectories. Also, stroke subject received the device intervention well and were able to actively extend and flex their digits inside of HEXORR. The active force-assisted condition was successful in increasing the subjects' active ROM while generally promoting active participation. These results justify the use of HEXORR in a clinical therapy trial to investigate the efficacy of this exoskeleton. This chapter will discuss the development of more sophisticated adaptive active-assistance algorithm, the design of therapy exercises to be used in the trial, and the initial results of the first two stroke subject participants.

8.1 Performance-Based Adaptive Active-Assistance Algorithm

Based on the results of the pilot study, it was determined that a performance-based automated adaptive active-assistance algorithm would provide a more robust therapy experience for stroke subjects in some of the therapy exercises. During the pilot study, extension assistance was modulated manually by the experimenter. The magnitude of the gain was dependent on subject performance and feedback. However, this approach was not entirely successful. For two of the subjects (Subject 4 and 5), the mean thumb torque was in flexion direction during designated extension movements. This indicates that the gain provided by the experimenter was too high and the thumb motor pulled the thumb into extension.

It is important to tune the gain so that minimal assistance is provided, yet the patient feels that it is possible to achieve the task's goal and continues to actively participate in the therapy exercises. There is a fine balance between challenging the subject, frustrating the subject (too little assistance) and encouraging slacking (too much assistance). One potential approach is developing an adaptive controller that can adjust the gain of the provided assistance based on the subject's needs.

The adaptive strategy adopted by this study is of the form:

$$G_{i+1} = G_i + g*e_i \qquad (1)$$

The gain (G_{i+1}) is tuned iteratively after each extension movement. The updated gain is a function of the previous gain (G_i) and the kinematic error between the desired active ROM and the achieved active ROM (e_i). A gain factor (g) is applied to e_i to adjust the responsiveness of the gain updates. This factor was set to 0.005 and remained constant for all patients. The advantages of using this performance-based adaptive active-assistance algorithm is that it attempts to provide the minimum extension assistance required for task completion and it does not rely on manual gain adjustment based on experimenter observation and subject feedback.

8.2 Gate Game

The first therapy exercise developed for HEXORR is based on the principles of activity-based therapy. This exercise focuses on repetitive, task-oriented (grasping) movements and the goal of the exercise is to increase the active extension ROM of the fingers and thumb. To further engage the patients, the exercise resembles an interactive video game. A virtual wall approaches a cursor on the computer screen and points are awarded when the patient successfully avoids the wall by positioning the cursor into the wall's gate.

Patients control the movement of a cursor on a computer screen by extending and flexing the hand's digits. Different versions of this game have been designed to focus on the fingers or thumb active movements and also to incorporate synchronous finger and thumb grasping. Illustrations of the Gate Game version that requires both finger and thumb active movements can be viewed in Figure 8.1.

Similar to the pilot study, stroke subjects receive additional force assistance during the extension phase. Again, this assistance is based on the mean motor current needed to passively stretch the hand's digits. However, the gain of this assistance is now tuned with the performance-based adaptive active-assistance algorithm. The first 10 extension movements of the exercise is deemed the 'auto-gain phase.' During these movements the assistance gain is automatically adjusted following each active extension movement based on equation 1. Following the auto-gain phase, subjects play additional rounds of the Gate Game (8 extension/flexion movements per round). Also, like the pilot study, any involuntary flexion movement was halted during a designated extension movement and the stroke subjects were able to try to extend their digits further from this point. However, if the subject extends past the gate position, the subject is allowed to flex and move the cursor back toward the gate.

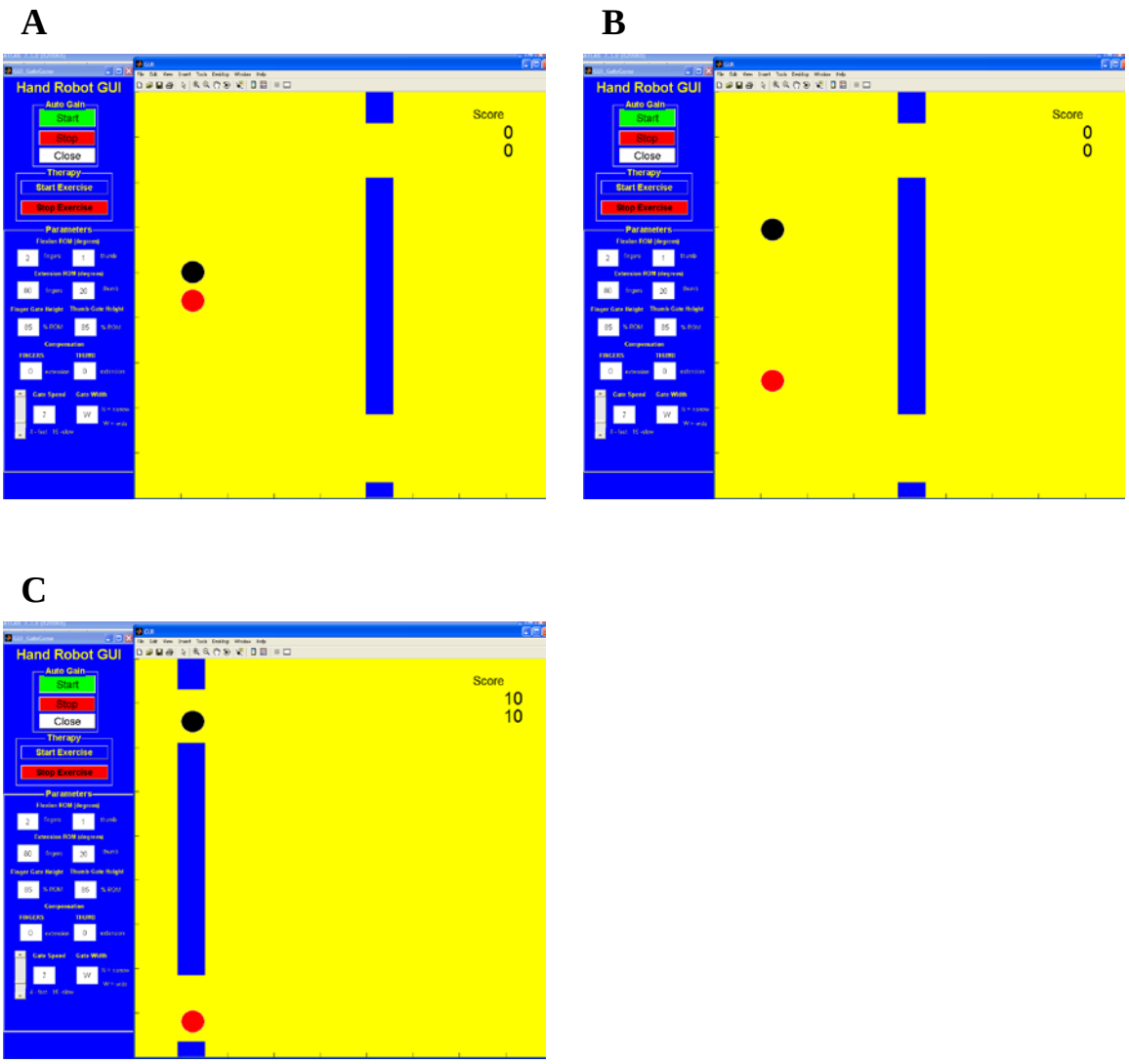

Figure 8.1 Display of different stages of the Gate Game including (**A**) finger (black) and thumb (red) cursors in the initial positions with an approaching wall, (**B**) cursor control by extending the fingers and thumb toward the wall's gates, and (**C**) successful completion of the task with points awarded.

To appropriately challenge each patient during this therapy exercise, the experimenter can change many parameters of the game after each round. These changes are based on a rubric that considers the current parameter settings and subject performance (successfully avoiding the wall). The adjustable parameters include gate position (desired active extension ROM), gate width (movement accuracy), the speed of the approaching wall, and the gain of the force assistance. Gate width can be set to either 'wide' (10º window for fingers, 5º window for thumb) or 'narrow' (5º window for fingers, 2.5º window for thumb). The speed of the incoming wall is adjusted in 1 second increments from a duration for 7 seconds to 2 seconds. Table 8.1 outlines the rubric that guides parameter changes for the Gate Game.

Table 8.1

Gate Game Rubric

---

1) Performance-based Adaptive-Assistance Algorithm

a. 8 extension/flexion movements with gate position at full extension passive ROM

b. Gain is initially set to 0.5 and is then updated based on previous gain and error between achieved ROM and desired active ROM (gate position) after each extension movement

2) Gate Game

a. Initial Settings: Gate Height set to 50% of passive ROM, Gate Width set to 'Wide,' Gate Speed set to '7 seconds,' Assistance Gain set to gain derived from automated adaptive-assistance algorithm

b. Every 8 trials: adjust gain based on subject performance
   - 70% extension movement success: decrease Gain by 0.1
   - 30% extension movement success: increase Gain by 0.05

c. Adjust other parameters if Gain reaches 1.5 or 0.2
   - If Gain $\geq$ 1.5 and extension movement success $\leq$ 30%: decrease movement length to match current extension range and return to step b
   - If Gain $\leq$ 0.2 and extension movement success $\geq$ 70%: increase movement length by 10% ROM and return to step b
   - If Gain $\leq$ 0.2 and extension movement success $\geq$ 70% and ROM = max: decrease wall speed by 1 sec (7 sec $\rightarrow$ 2 sec) and return to step b
   - If Gain $\leq$ 0.2 and extension movement success $\geq$ 70%, ROM = max and speed = 2: decrease Gate Width from 'Wide' to 'Narrow' and set speed to 7 and return to step b

---

8.3 Isometric Squeeze-Release Game

The second therapy exercise developed for HEXORR focuses on two of the major impairments of the paretic hand: the inability to activate agonist extensor muscles [10, 11] and co-contraction of antagonistic pairs during extension [14]. This exercise is designed as an interactive game that challenges a stroke patient to perform selective, isometric flexion and extension torques following cues. Having the subjects follow a flexion torque with an extension torque requires them to focus on relaxing their hyper-active flexor muscles and then selectively activating the extensor muscles.

Initially, the motors of the robot move the MCP and PIP joints at 45º of extension and the thumb CMC and IP at 10º and 45º of extension, respectively. The subject is asked to relax the paretic hand and torque readings are recorded. These readings are used to remove the torque sensor bias before starting the exercise. Afterward, the subject is asked to perform maximum voluntary contractions (MVC) in the flexion direction. These values are used to calibrate the scaling of torque production to the corresponding cursors' movement. Although the digits are held in place by the robots, the torque values control the movement of cursors on the computer screen. To play the game, the subject is tasked with flexing their hand to move and hold the cursors within a horizontal channel. Afterward, the subjects must relax their flexors and/or try and extend their digits to avoid an incoming wall. Points are awarded for successfully avoiding the incoming wall.

Subjects perform 5 flexion/extension torque repetitions per round. Illustrations of different stages of the Isometric Squeeze-Release Game can be seen in Figure 8.2.

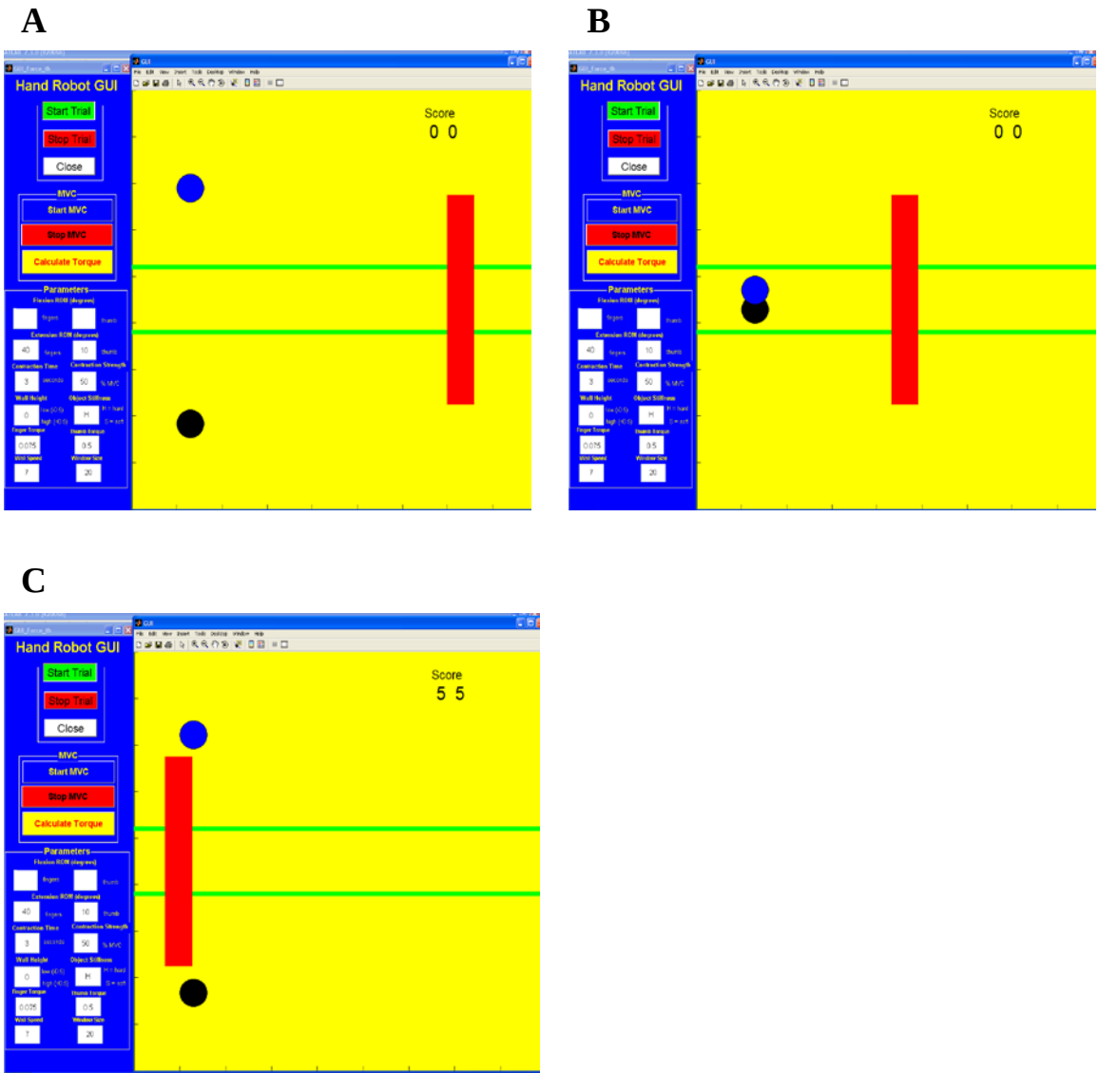

Figure 8.2 Display of different stages of the Isometric Squeeze-Release Game including (**A)** finger (blue) and thumb (black) cursors in the initial positions outside of the horizontal channel (green), (**B)** cursors moved into the channel by fingers and thumb flexion torques, and (**C)** relaxation of the flexors and extension torques to successfully avoid the incoming wall. Points are awarded for completion of the task.

Similar to the Gate Game, the experimenter can change many parameters of this game after each round to adjust the difficulty of the task based patient performance. These changes are based on a rubric that considers the current parameter settings and subject performance (successfully avoiding the wall). The adjustable parameters include the required percentage of MVC to position the cursors with the horizontal channel, the amount time the cursor must remain in the channel before the wall approaches the cursors, the speed of the incoming wall and the height of the wall. Adapting these parameters requires the subject to focus on different aspects of this task. Changing the magnitude and duration of the flexion torque requires the patient to modulate their flexor muscles. Increasing the speed of the incoming wall requires the subject to relax their flexors and/or apply extension torque at faster rate. And increasing the height of the incoming wall forces the subject to apply increasingly stronger extension torque. Ideally, this exercise will help stroke patients learn how to modulate their flexor muscle activity and quickly transition from flexion to extension. Table 8.2 outlines the rubric that guides parameter changes for the Isometric Squeeze-Release Game.

Table 8.2

Isometric Squeeze-Release Rubric

1. **Torque Calibration**

    a. Record and input torque values with relaxed fingers and thumb positioned at 45º and 10º, respectively.

2. **Maximum Voluntary Contraction**

    a. Motors position fingers and thumb at 45º and 10º, respectively.

    b. Patient performs two maximal flexion torques.

    c. Record and input mean torque values.

3. **Isometric Squeeze-Release Game**

    a. Initial Settings: Channel Position set to 25% MVC, Activation of Wall occurs when cursors are within channel for 1 second, Wall Height set to 0% MVC, Wall Speed set to 7 seconds

    b. Every 5 trials, adjust gain based on subject performance

    - If the success of the 5 attempts is ≤ 40%: decrease Wall Height to match current extension torque levels

    - If the success of the 5 attempts is ≥ 60%: increase Wall Height by 5% MVC

    - If the success of the 5 attempts is ≥ 60% and Wall Height is 50% MCV: increase Wall Activation time by 1 second, up to 3 seconds.

      If the success of the 5 attempts is ≥ 60%, Wall Height is 50% MCV and Wall Activation time is 3 seconds: increase Channel Position by 25% MVC

    - If the success of the 5 attempts is ≥ 60%,Wall Height is 50% MCV and Channel Position is 75% MVC, increase Wall Speed from 7 seconds to 2 seconds in 1 second increments

8.4 Experimental Protocol and Initial Results

The subject accrual goal for this study is 10 stroke subjects. Currently, two subjects have completed their hand therapy session using HEXORR. This section will discuss the experimental protocol of the study and report the initial active ROM results of the two subjects that have completed therapy.

Study inclusion criteria required a first ischemic or hemorrhagic stroke occurring more than 3 months prior to acceptance into the study, some proximal upper extremity voluntary activity at the shoulder and elbow, and trace ability to control movement at the wrist, MCP and PIP joints in extension. Exclusion criteria included excessive pain in any joint of the affected extremity that could limit ability to cooperate with the protocols, serious uncontrolled medical problems as judged by the project therapist, and a full score on the hand and wrist sections of the Fugl-Meyer motor function test.

Before using the robot, stroke subjects were clinically evaluated. Upper extremity movement impairments were evaluated with the Action Research Arm Test and the Fugl-Meyer motor function test. Muscle tone was measured at the elbow, wrist and fingers with the Modified Ashworth Scale. Electromyographic muscle activity of an extrinsic finger flexor muscle (flexor digitorum superficialis), two extrinsic extensor muscles (extensor digitorum communis, extensor indicis proprius) and a thumb abductor muscle

(abductor pollicis brevis) were recorded for each subject's first and last day of therapy. A 90 day clinical evaluation follow-up will also be performed.

Therapy duration lasts for 6 weeks, 2 hours a day, 3 days a week. Each daily therapy session starts with a few minutes of passive stretching. The average motor current required to stretch the hand's digits are recorded and used to provide extension assistance during the Gate Game exercise. After passive stretching, subjects interact with the Gate Game. Approximately 20 rounds of active force-assisted hand extension/flexion movements are performed each day (120-160 total movements). During this exercise, the experimenter is continually adjusting the aforementioned parameters to maintain a challenging, but not frustrating, experience for the participant. Then the subject performs around 7-10 rounds of the Isometric Squeeze-Release Game (35-50 flexion/extension torque exercises). Again, after each round, parameters are changed according to subject performance. Two subjects have completed their hand therapy using HEXORR and their progression will be summarized below.

During therapy, both subjects showed improvements in Gate Game performance. For Subject 1's first therapy session, she consistently achieved greater than 50% successful movements with the finger extension gate positioned at 40º, and an assistance gain of 0.95. And she performed greater than 50% successful movements with the thumb extension gate positioned at 7º of CMC (30º IP) rotation at an assistance gain of 0.975.

The gate speed was at its lowest setting (7 seconds). By her last therapy session, she performed over 50% successful extension movements with the finger extension gate positioned at 50º at an assistance gain of 0.6. And she achieved greater than 50% successful movements with the thumb extension gate positioned at 10º of CMC rotation (45º IP) at an assistance gain of 0.3. Also the speed of the gate was increased by one second. By the end of therapy, Subject 1 was able to extend her fingers 25% further and required approximately 60% less assistance. She was also able to extend her thumb 75% further with a 225% assistance reduction. Subject 2 entered the study with full active ROM of the fingers, but with impaired thumb active ROM. With the Gate Game, Subject 2 was able to extend his fingers fully but required an assistance gain of 1.0 to extend his CMC 14º (IP 63º) with a gate speed of 7 seconds. By the end of therapy, Subject 2 was able to extend his CMC about 17º (77º IP) with the gate speed increased to its highest setting (2 seconds) and the gate width set to 'narrow.' Subject 2's final performance showed a 21% increase in thumb active ROM without any assistance required. He also increased the speed of his movements by at least 5 seconds and showed greater endpoint accuracy.

Like the Gate Game, the subjects' performance improved while interacting with the Isometric Squeeze-Release Game. On her first day, Subject 1 was not able to fully relax her flexors. She displayed 75% flexor relaxation with a wall speed of 7 seconds. By the end of therapy, Subject 1 was able to fully relax her hand (0.01 MVC relaxation) to avoid

an incoming wall at speeds of 2 seconds. Although she wasn't able to exhibit increased extensor activity during this exercise, Subject 1 was able to fully relax her flexors at a much faster rate. Subject 2's initial performance was better than Subject 1. He was able to fully relax his hand and extend his digit to about 25% flexor MVC to avoid an incoming wall of 4 seconds. By the end of therapy, Subject 2 was able to consistently transition from full flexion to full extension torques to avoid an incoming wall with a speed of 2 seconds.

One of the preliminary assessment measures for the stroke subjects after therapy is the change in active ROM during the active-unassisted movement sessions. The mean active ROM progression for both subjects during the active-unassisted sessions can be viewed in Figure 8.3. Subject 1 began the study with approximately 20º of MCP and PIP active ROM and 3º and 13º of active CMC and IP ROM, respectively. By the end of therapy, her active ROM increase to 40º of finger MCP and PIP rotation and 10º and 45ºof thumb CMC and IP joints rotation, respectively. Subject 2 was capable of full finger active ROM at the inception of therapy, however thumb active ROM was only 5º and 25º for the thumb's CMC and IP joints, respectively. At his last therapy session, Subject 2 was able to rotate his thumb by 20º and 90º for the CMC and IP joints, respectively.

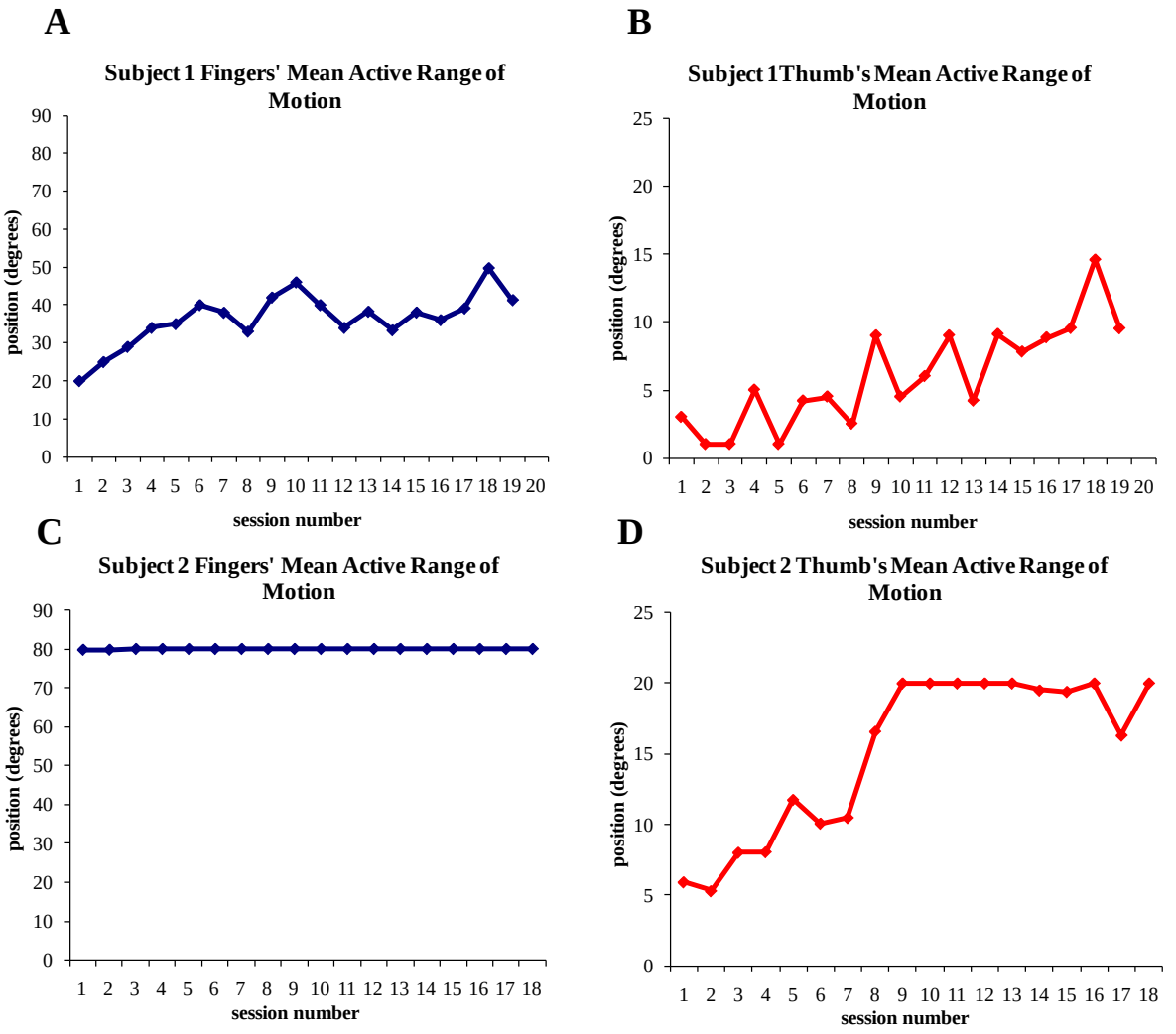

Figure 8.3 Mean active-unassisted ROM for Subject 1 and 2 during 6 weeks of training using HEXORR. For Subject 1, active ROM increased 100% (20º MCP and PIP rotation) for the fingers (**A**) and 300% (10º CMC, 45º IP) for the thumb (**B**). Subject 2 entered the trial with full active finger ROM (**C**), and thumb (**D**) active ROM increased 400% (15º CMC, 68º IP).

Although the results of this study are only preliminary, they are quite promising. Each subject showed significant progression in both the Gate Game and Isometric Squeeze-Release Game. More importantly, this progression translated into a marked increase in active ROM for their impaired digits during the active-unassisted trials. Subject 1 increased her active finger ROM by 100% (20º) and her thumb active ROM by 300% (10º CMC, 45º IP). Subject 2 increased his thumb active ROM by nearly 400% (15º CMC, 68º IP). A larger subject pool and more rigorous analysis of data are required before any conclusions can be made about the efficacy of HEXORR. However, the results of these initial subjects show that the chosen therapy exercises are successful in increasing the stroke subjects' active ROM for both the fingers and thumb.

CHAPTER 9:

CONCLUSION

9.1 Study Summary

After therapy intervention, the majority of stroke survivors are left with a poorly functioning hemiparetic hand. Rehabilitation robotics has shown great promise in providing patients with intensive activity-based therapy leading to functional gains. Because of its crucial role in performing activities of daily living, attention to hand therapy has recently increased.

We have designed a novel hand exoskeleton rehabilitation robot, HEXORR, for the purpose of providing therapy to stroke survivors. This device has been designed to provide full ROM for all of the hand's digits. The thumb actuator allows for variable thumb plane of motion to incorporate different degrees of extension/flexion and

abduction/adduction. Compensation algorithms have been developed to improve the exoskeleton's backdrivability by counteracting gravity, stiction and kinetic friction. We have also designed a force assistance mode that provides extension assistance based on each individual's needs.

Our pilot study shows that this device is capable of moving the hand's digits through the entire ROM with physiologically accurate trajectories. Stroke subjects received the device intervention well and were able to actively extend and flex their digits inside of HEXORR. Our active-assisted condition was successful in increasing the subjects' ROM while generally promoting active participation.

It is argued that the results of the pilot study justify a clinical trial to investigate the efficacy of HEXORR. A more sophisticated performance-based adaptive assistance algorithm was developed to tune the assistance gain for one of the therapy exercises. Two therapy modes were developed following contemporary physical therapy rationale. These therapy exercises were designed to specifically target the neurologically mediated impairments of the paretic hand. The Gate Game is designed to strengthen the paretic hand's weak extensor muscles through repetitive task-oriented movements. The Isometric Squeeze-Release Game focuses on involuntary co-activation of the weak extensors and stronger flexor muscles. Subjects learn how to transition from flexion by relaxing the flexors and then independently activating the extensor muscles.

Both clinical trial subjects showed substantial progression in both the Gate Game and Isometric Squeeze-Release Game. More importantly, this progression translated into a marked increase in active ROM of their paretic hand during the active-unassisted trials. The results of these initial subjects show that the chosen therapy exercises are successful in increasing the stroke subjects' active ROM for both the fingers and thumb.

9.2 Limitations and Future Considerations

Although the mechanical design of HEXORR meets the general design criteria of this project, the device can be improved. Currently, HEXORR can only interact with a subject's right hand. The right hand was chosen because it is typically the dominant hand and it is believed that impairments in the dominant limb would be more debilitating to a stroke survivor. However, redesigning HEXORR to accommodate both hands would allow the device to assist a larger stroke population.

9.2.1 Left Hand Design

Using SolidWorks® CAD software, HEXORR has been redesigned to accommodate both right and left hands. A left handed modular finger assembly has been designed and can be viewed in Figure 9.1.A. This assembly uses the same general four-bar linkage

configuration and finger-exoskeleton interfaces as the right hand assembly (Figure 9.1.B). However, the left hand assembly links are positioned so that the linkage rotates with the same trajectory as the original right hand assembly, but in the opposite direction. This design allows a participant to use HEXORR with the left hand by approaching the device on the same side of the table, but facing the opposite direction as a right hand user.

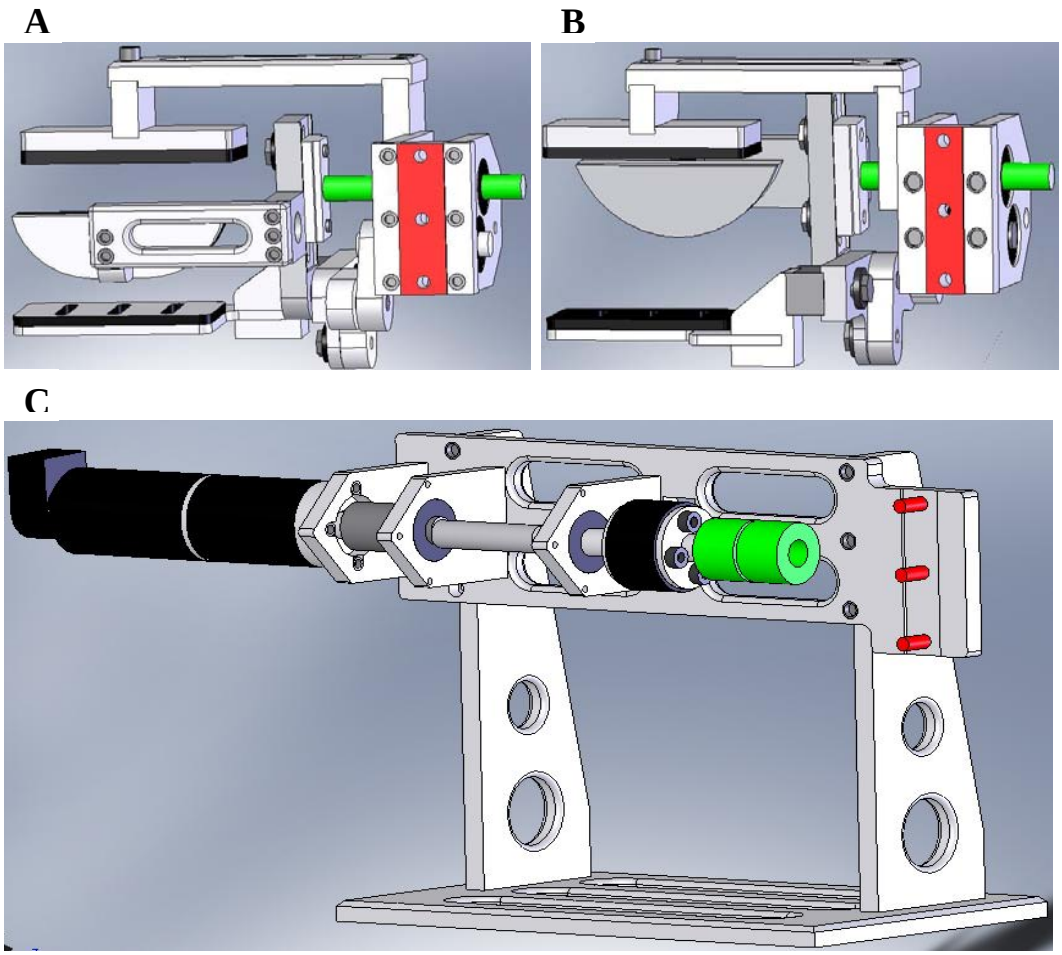

Figure 9.1 Design of a modular left hand finger assembly (**A**) able to replace the original right hand finger assembly design (**B**) to include participants with impaired left hands. These modular assemblies can be removed from and affixed to HEXORR's base (**C**) by using three screws (red) and by engaging the assembly's drive shaft to the shaft coupler (green).

The two modular finger assemblies are easily interchangeable. Both assemblies can be anchored and removed from HEXORR's base (Figure 9.1.C) with three socket head cap screws. These screws are shown on HEXORR's base and highlighted red in Figure 9.1.C. The finger assembly surface that lies flush against the table-top base is also highlighted red in Figures 9.1.A and 9.1.B. Once a chosen finger assembly is secured onto the base, the assembly's drive shaft (Figures 9.1.A and 9.1.B), highlighted in green, is engaged by sliding it into the main shaft coupler (Figure 9.1.C, green highlight) and tightening the coupler.

The thumb component has also been redesigned to accommodate left hand users. To convert the thumb component for left hand use, the entire crank-slider linkage is rotated about the main drive shaft and anchored to the intermediate base. This is achieved in three steps. First, the two vertical linear bearing supports are released from the intermediate base via the four screws highlighted in red shown in Figure 9.2.A. Then, a set screw is loosened and the drive shaft (blue) and vertical supports (yellow) are all rotated about the main motor shaft (Figure 9.2.B). Finally, the IP digit interface (orange) is rotated and reattached to the distal link with the two screws highlighted in purple (Figure 9.2.C).

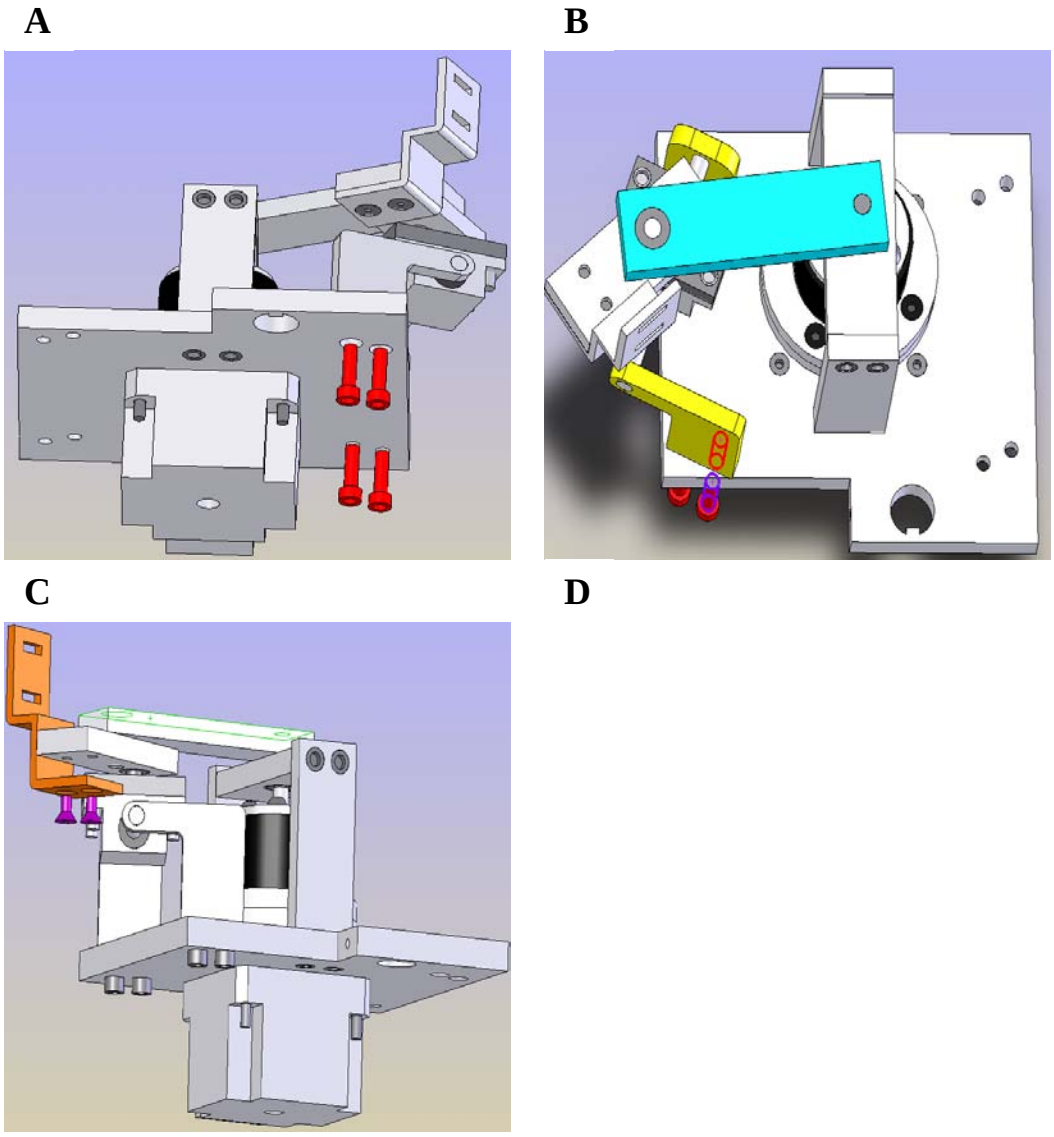

Figure 9.2 The thumb component redesigned to accommodate left hand users. The thumb component is converted for left hand use by releasing the linear bearing's supports via the four (red) screws (**A**). A set screw is loosened and the drive shaft (blue) and vertical supports (yellow) are all rotated about the main shaft (**B**). Finally, the IP digit interface (orange) is rotated and reattached with two screws (purple) (**C**). The completed left hand modification is shown in **D**.

9.2.2 HEXORR Range of Motion

Designing an exoskeleton to assist hand movements is difficult because of the many degrees of freedom. For simplicity, the design of this exoskeleton sacrifices some of the natural degrees of freedom of the hand. The finger component moves all four fingers in bulk. This allows for training of gross finger movements, such as grasping, but it does not allow the subjects to focus of moving individual digits and practice fine motor tasks. The pilot study also indicates that, for unimpaired subjects, 3 of the fingers' 12 joints had less active ROM inside of HEXORR than outside of the device. It is believed that the flexion mechanical stop prevents the 4^{th} and 5^{th} digits' MCP joints from fully flexing, thereby reducing the overall ROM (though extension range is not reduced). Also, bulk strapping the 5^{th} digit's intermediate phalanx was troublesome and this led to decreased ROM in this digit's PIP joint.

Although the thumb device allows full active planar ROM, the device reduces the degrees of freedom of the thumb's CMC spherical joint. However, for most function tasks, the thumb does move along a chosen plane. Depending on the plane of motion, different amounts of extension/flexion and abduction/adduction are required. Accordingly, the thumb device was designed to allow thumb movement along different planes.

Another design limitation is that HEXORR is a table top device. This inherently reduces the type of training a patient can receive while using the device. Training with HEXORR focuses solely on the hand's digits, while the elbow and shoulder are essentially immobile. Many ADLs require movements such as 'reach to grasp.' These functional movements require coordination of the shoulder, elbow and hand to perform a task.

9.3 Conclusion and Future Directions

A number of hand therapy devices have been developed and initial pilot data indicates promising therapeutic results [46-57]. However, although there are many different approaches to achieve the same goal (increase active extension ROM), there were common issues with these devices. The general issues include: i) limited ROM ii) partial control of the hand iii) basic controllers designed to provide therapy. HEXORR was developed to address these limitations in an attempt to increase the therapeutic potential of rehabilitation robotics for the hand. As an exoskeleton, HEXORR maximizes hand control by guiding the movements of every finger's MCP and PIP joints and the rotation of the thumb. The pilot study performed on unimpaired subjects indicates that HEXORR allows physiological hand movements throughout the digits' full ROM. The therapy modes for HEXORR were designed to specifically address the neurological impairments following stroke. The Gate Game combines a feed-forward force assistance mode with a feedback controller to help increase the active ROM of the stroke subjects' digits. The

feed-forward component includes gravity and friction compensation and a tunable, position dependent force assistance profile that is tailored to each subject's tone level. If the subject is unable to achieve full active ROM with the provided feed-forward assistance, the therapist is able to complete the motion via a PID feedback controller. The Isometric Squeeze and Release Game was designed to help subjects practice deactivating the hyperactive flexor muscles and subsequently activate the less responsive, weaker extensor muscles. It is believed that designing an exoskeleton that maximizes the ROM and control of the hand's digits combined with sophisticated controllers developed to specifically target the neurological impairments of stroke patients will result in improved therapeutic outcomes.

The presented clinical therapy data is preliminary and the work in ongoing. A larger subject pool and more rigorous analysis of data are required before any conclusions can be made about the efficacy of HEXORR. This small clinical study will include a total of 5 stroke participants and the study includes a number of assessment measures. Clinical assessment is performed by an occupational therapist at therapy initiation and cessation, with a 90-day follow-up assessment. The chosen clinical assessments include the box and block test of manual dexterity, the Fugl-Meyer Assessment, the Action Research Arm Test and the Modified Ashworth Scale. Electromyographic activity of extrinsic flexors, extensors and abductors are recorded during the first and final days of therapy. Also active ROM analysis is performed with the robot during active-unassisted trials and

outside of the device using the CyberGlove II®. It is unknown, which, if any, assessments will show significant improvement in hand function following therapy with HEXORR. However, the initial active ROM data from the first two subjects indicate increased active ROM after using HEXORR for therapy. If the results of this clinical trial show that therapy intervention with HEXORR results in positive functional gains, the results will justify a larger clinical trial designed to compare the benefits of therapy with HEXORR against dosage matched control subjects that receive contemporary therapy through an occupational therapist.

APPENDIX A:

LINKAGE SIMULATION AND FORCE ANALYSIS CODE

This Appendix contains the MATLAB® script code used to synthesize and analyze the finger and thumb linkages. The code begins with calculating an array of possible finger linkage configurations, followed by a ROM simulation and mechanical advantage calculations per iteration. HEXORR's finger linkage design was chosen by considering the general linkage configuration and its given mechanical advantage. Afterward, code is presented that simulates the rotation of the thumb linkage and a force analysis per iteration. The results of these calculations justify the use of a slider mechanism to replace the thumb linkage's follower link. A more detailed explanation of this code's rationale and the results of the calculations can be reviewed in section 3.1 Mechanical Design of the Finger Component and section 3.2 Mechanical Design of the Thumb Component.

```
%Investigate/Optimize the finger component's 4-bar linkage
%Given the positions of the drive link (ground joint as origin) and the
%the joint connecting drive link and coupler link and 3 sets of angular
%rotations investigate the optimal position of the follower ground and
%coupler/follower joint

clear all
clc

%Define initial 4 bar linkage parameters and three linkage positions
%lengths are in inches, angles in degrees

prompt={'Enter MCP length:','Enter PIP length:',...
    'Enter 1st Drive link position (angle)',...
    'Enter 2nd Drive link position (angle)'...
    'Enter 3rd Drive link position (angle)'...
    'Enter 1st Coupler link position (angle)'...
    'Enter 2nd Coupler link position (angle)'...
    'Enter 3rd Coupler link position (angle)'};
name='Parameters';
numlines=1;
defaultanswer={'1.75','1.25','0','-45','-90','0','-90','-180'};
answer=(inputdlg(prompt,name,numlines,defaultanswer));
parameter=str2double(answer);

mcp=parameter(1,1); %length of MCP (inches)
pip=parameter(2,1); %length of PIP (inches)

D_Grd=[0;0;0]; %grd pt of D link is set to origin
d_link=[0;-parameter(1,1);0]; %vector form
c_link=[parameter(2,1);0;0]; %vector form

%choose the 3 linkage positions
d_theta=[parameter(3,1),parameter(4,1),parameter(5,1)];%0 degrees = flexed,
%-90 degrees = open hand
c_theta=[parameter(6,1),parameter(7,1),parameter(8,1)];%0 degrees = flexed,
%-180 degrees = open hand
```

```
%create an array of x,y cartesian coordinates for many possible
%coupler-follower joint locations at the flexed hand position after finding a good
%general location for CF joint (via graphical analysis)
for i=1:10
   for j=1:10
     temp_grid(i,j,:)=[i*0.1,j*0.1]; %temporary grid to be manipulated
   end
end
grid(:,:,1)=-temp_grid(:,:,1)-1;%bias x components for grid to the opposite
%side of the Ftip position
grid(:,:,2)=-temp_grid(:,:,2)+.6;%shift the y origin of the grid
%proportional to the position of DC joint

total_configs=i*j;  %total number of linkage configurations to be analyzed

%Calculate the 3 thru-points of the CF joint at the 3 designated linkage
%position
a=0; b=0; c=0; %dummy variables
for i=1:3 % number of designated linkage positions
   for j=1:10
      for k=1:10
         a=a+1; %dummy counter
 cf_link(:,:,a)=[grid(k,j,1);grid(k,j,2);0]; %vectors of CF joint positions

%find the 'coupler link deflection' angle from CF joint to CD joint via dot product
c_link_theta(a,1)=acosd((cf_link(:,:,a)'*c_link)/(norm(cf_link(:,:,a))...
    *norm(c_link)));

 %find the rotation matrices for the designated linkage positions
d_rotation_matrix(:,:,i)=[cosd(d_theta(1,i)) -sind(d_theta(1,i)) 0;...
   sind(d_theta(1,i)) cosd(d_theta(1,i)) 0; 0  0 1];
c_rotation_matrix(:,:,i)=[cosd(c_theta(1,i)) -sind(c_theta(1,i)) 0;...
   sind(c_theta(1,i)) cosd(c_theta(1,i)) 0; 0  0 1];

%find the rotated vectors
rotated_d_link(:,:,i)=d_rotation_matrix(:,:,i)*d_link;
rotated_c_link(:,:,i)=c_rotation_matrix(:,:,i)*c_link;
rotated_cf_link(:,:,a)=c_rotation_matrix(:,:,i)*cf_link(:,:,a);
%organize the thru_pt data by separating the 1st, 2nd and 3rd thru pts
   if a<=100
cf_1st_thru_pt(:,:,a)=rotated_d_link(:,:,i)+rotated_cf_link(:,:,a);
   end
```

```
   if a>100 && a<=200
   b=b+1;
cf_2nd_thru_pt(:,:,b)=rotated_d_link(:,:,i)+rotated_cf_link(:,:,a);
   end
   if a>200 && a<=300
   c=c+1;
cf_3rd_thru_pt(:,:,c)=rotated_d_link(:,:,i)+rotated_cf_link(:,:,a);
   end
      end
   end
end

CF_joint=cf_1st_thru_pt; %the position of the coupler/follower joint at
                         %the flexed hand position
DC_joint=rotated_c_link+rotated_d_link; %the position of the driver/coupler
                        %joint at the 3 designated linkage positions

%Rationale: 1) Calculate the midpoints of the 2 segments created by the 3
%thru-points of joint CF.  2) Calculate the slope of these 2 segments
%and find (-m^-1), which is the slope of the perpendicular bisector.
%Using midpoint x,y coords, find y-intercept &solve for x,y of intersection
%point of the bisectors giving the follower link ground position

%Calculate midpoints of the 3 trajectory points
for i=1:total_configs
midpt1(:,:,i)=[(cf_1st_thru_pt(1,1,i)+cf_2nd_thru_pt(1,1,i))/2;...
   (cf_1st_thru_pt(2,1,i)+cf_2nd_thru_pt(2,1,i))/2];
midpt2(:,:,i)=[(cf_2nd_thru_pt(1,1,i)+cf_3rd_thru_pt(1,1,i))/2;...
   (cf_2nd_thru_pt(2,1,i)+cf_3rd_thru_pt(2,1,i))/2];

%Find the slope for the 2 segments formed by through points of CF joint
slope_thru_pts(i,1)=(cf_1st_thru_pt(2,1,i)-cf_2nd_thru_pt(2,1,i))/...
   (cf_1st_thru_pt(1,1,i)-cf_2nd_thru_pt(1,1,i));
slope_thru_pts(i,2)=(cf_2nd_thru_pt(2,1,i)-cf_3rd_thru_pt(2,1,i))/...
   (cf_2nd_thru_pt(1,1,i)-cf_3rd_thru_pt(1,1,i));

%Perpendicular slope of thru pt segments is its negative reciprocal
slope_bisector(i,:)=[-1/slope_thru_pts(i,1); -1/slope_thru_pts(i,2)];

%Given line segments' midpoint coords and slope, solve for y-intercept
right_side(i,1)=midpt1(2,1,i)-slope_bisector(i,1)*midpt1(1,1,i);
right_side(i,2)=midpt2(2,1,i)-slope_bisector(i,2)*midpt2(1,1,i);
```

```
%Solve for the point of intersection of the perpendicular bisectors
%using y-mx=b..... A =-mx+y, B = y intercept
%following [-m1 1; -m2 1]*[x;y]=[b1;b2]
  left_side(:,:,i)=[-slope_bisector(i,1) 1; -slope_bisector(i,2) 1];

 %position of the follower link ground point
 tempF=left_side(:,:,i)\right_side(i,:)';
 F_Grd(:,:,i)=[tempF(1); tempF(2); 0];
end

clear i j a b c k temp_grid answer defaultanswer numlines name prompt ...
parameter

%Finger linkage simulation and force analysis

%Calculate the moment arm about the drive shaft of a force applied normal to the coupler
link via the fingertips at each 4 bar linkage joint configuration
%see picture: joint_description.ppt for link labels

%ROTATION SIMULATION

%coordinate frame, left is +, down is +
for j=1:100
    a=-d_link;
    r=[-1;0;0]; %initial position of coupler 'extension'
    d=-F_Grd(:,:,j); % imaginary 'fourth bar' between Follower and Driver grounds
    b=-CF_joint(:,:,j)+d_link; %segment joining CF and DC joints

P=a+b; %vector addition solving for vector from Driver link ground to CF joint
c=P-d; %vector subtraction solving for follower link initial position (c)

F=[0;1;0];
H=[0;0;0];
dangle=-pi()/2;
Rn90=[cos(dangle) -sin(dangle) 0;sin(dangle) cos(dangle) 0; 0 0 1];
%3D rotation matrix (-90)
dangle= pi()/2;
Rp90=[cos(dangle) -sin(dangle) 0;sin(dangle) cos(dangle) 0; 0 0 1];
%3D rotation matrix (+90)

for i=0:1:9 %rotate linkage by steps of 5 degrees from closed to
```

```
%open hand (90 degrees total ROM)
if i==0;
   dangle=0;
else
   dangle=-10*pi()/180; %5 degrees => radians
end
R=[cos(dangle) -sin(dangle) 0;sin(dangle) cos(dangle) 0; 0 0 1];
a=R*a; %rotate a (D_link)in 5 degree increments
e=a-d; %vector from F_grd to DC_joint

%t1 and t2 are the segments created along e by the orthogonal bisector
%from the CF_joint (p) to vector e.  t3 is the vector of that bisector

%t2 was solved with pythagorean therom of 2 triangles created by 1) t1,
%t3 and C and 2) t2, t3 and B
t2=(norm(c)^2-norm(b)^2-norm(e)^2)/(-2*norm(e));
t1=norm(e)-t2; %t1 is simply e - t2 length
t3=sqrt(norm(c)^2-t1^2); %now t1,t2 are solved for: t3 = solved via
%Pythagorean theorm of triangle t1,t3,C
Pn=d + t1*e/norm(e) + t3*Rn90*e/norm(e); %Rn = negative rotation
Pp=d + t1*e/norm(e) + t3*Rp90*e/norm(e); %Rp = positive rotation
if norm(Pn-P)<norm(Pp-P)
   P=Pn;
else
   P=Pp;
end
bold=b;
b=P-a;
c=P-d;
%storing rotated linkage vectors
a_stored(i+1,:)=a'; %driver link
b_stored(i+1,:)=b'; %segment from CF joint to DC joint
c_stored(i+1,:)=c'; %follower link
P_stored(i+1,:)=P'; %segment from driver ground to CF joint

%FORCE ANALYSIS

%solving for magnitude and directionality of pheta (angle between b_old and
%b)

delta=b-bold; %delta is the vector from the head of vector bold at iteration i
%to the head of vector b at iteration i+1 (5 degree rotation of vector
```

```
    % a)
    pheta=2*asin(norm(delta)/(2*norm(bold))); %angle between bold and b by position
change
    %of delta
    temp=cross(bold,b); %if cross product of bold and b is negative pheta is negative
    if (temp(3)<0)
        pheta=-abs(pheta);
    else
        pheta=abs(pheta);
    end


    RR=[cos(pheta) -sin(pheta) 0;sin(pheta) cos(pheta) 0; 0 0 1];
    F=RR*F;
    r=RR*r;
    temp=cross(r,F);
    H(1)=-temp(3)/(b(1)*c(2)/c(1)-b(2));
    H(2)=c(2)*H(1)/c(1);
    M(i+1,:)=-cross(a,F+H);
    r_stored(i+1,:)=r';
    F_stored(i+1,:)=F';
    pheta_stored(i+1,:)=pheta;
end

Msave(:,j)=M(:,3);
%set up variables (vectors) to be graphed
TrajectoryX(:,1,j)=-a_stored(:,1)*2.54;
TrajectoryX(:,2,j)=-P_stored(:,1)*2.54;
TrajectoryX(:,3,j)=-c_stored(:,1)*2.54;
TrajectoryX(:,4,j)=-r_stored(:,1)*2.54;
TrajectoryY(:,1,j)=-a_stored(:,2)*2.54;
TrajectoryY(:,2,j)=-P_stored(:,2)*2.54;
TrajectoryY(:,3,j)=-c_stored(:,2)*2.54;
TrajectoryY(:,4,j)=-r_stored(:,2)*2.54;
% b_stored(:,1) P_stored(:,1) r_stored(:,1)];
end

k=51; %choose a linkage configuration to be graphed, configuration 51 was saved
figure();
Title('Finger Linkage Simulation');
xlabel('position (cm)'); ylabel('position (cm)');
legend('show')
```

```
legend('driver link','follower link', 'coupler link');
axis([-7.5 4 -7.5 1]);
d=F_Grd(:,:,k);
for L=1
line([0;TrajectoryX(L,1,k)],[0;TrajectoryY(L,1,k)],'LineWidth',4);
line([TrajectoryX(L,1,k);TrajectoryX(L,2,k)],[TrajectoryY(L,1,k);TrajectoryY(L,2,k)],'C
olor','r','LineWidth',4);

line([TrajectoryX(L,2,k);d(1)*2.54],[TrajectoryY(L,2,k);d(2)*2.54],'Color','black','LineW
idth',4);
line([TrajectoryX(L,1,k);TrajectoryX(L,1,k)+
TrajectoryX(L,4,k)],[TrajectoryY(L,1,k);TrajectoryY(L,1,k)+TrajectoryY(L,4,k)],'Color',
'red','LineWidth',4);
  end

 for L=2:10
line([0;TrajectoryX(L,1,k)],[0;TrajectoryY(L,1,k)],'LineWidth',2);
end

for L=2:10

line([TrajectoryX(L,1,k);TrajectoryX(L,2,k)],[TrajectoryY(L,1,k);TrajectoryY(L,2,k)],'C
olor','r','LineWidth',2);
end
d=F_Grd(:,:,k)*2.54;
for L=2:10
line([TrajectoryX(L,2,k);d(1)],[TrajectoryY(L,2,k);d(2)],'Color','black','LineWidth',2);
end
for L=2:10
line([TrajectoryX(L,1,k);TrajectoryX(L,1,k)+
TrajectoryX(L,4,k)],[TrajectoryY(L,1,k);TrajectoryY(L,1,k)+TrajectoryY(L,4,k)],'Color',
'red','LineWidth',2);
end
```

```
%Thumb linkage simulation and force analysis

a=[0;2.5;0]; %long_link
r=[1;0;0]; %distal_link
z=[-0.5;0;0]; %slider_link
F=[0;1;0];
H=[0;0;0];
grd_pos=[0;0;0];

%coordinate frame, right is +, down is +
 for i=0:1:18
    n=i+1;
    if i==0;
        angle_a=0;
        angle_r=0;
        angle_z=0;
    else
        angle_a=-5*pi()/180;
        angle_r=-20*pi()/180;
        angle_z=-20*pi()/180;
    end
    R_a=[cos(angle_a) -sin(angle_a) 0;sin(angle_a) cos(angle_a) 0; 0 0 1];
    R_r=[cos(angle_r) -sin(angle_r) 0; sin(angle_r) cos(angle_r) 0; 0 0 1];
    R_z=[cos(angle_z) -sin(angle_z) 0; sin(angle_z) cos(angle_z) 0; 0 0 1];
    a=R_a*a;
    r=R_r*r;
    zold=z;
    z=R_z*z;

     a_stored(i+1,:)=a';
     r_stored(i+1,:)=r';
     z_stored(i+1,:)=z';
     theta_a(i+1,1)=acosd(dot(a,a_stored(1,:)')/(norm(a)*norm(a_stored(1,:)')));
     theta_r(i+1,1)=acosd(dot(r,r_stored(1,:)')/(norm(r)*norm(r_stored(1,:)')));
     theta_z(i+1,1)=acosd(dot(z,z_stored(1,:)')/(norm(z)*norm(z_stored(1,:)')));

     coords(i+1,:)=[-z_stored(i+1,1)-a_stored(i+1,1), -z_stored(i+1,2)-a_stored(i+1,2)];
```

```
%Thumb linkage force analysis

   delta=z-zold; %delta is the vector from the head of vector bold at iteration i
   %to the head of vector b at iteration i+1 (5 degree rotation of vector
   % a)
   pheta=2*asin(norm(z)/(2*norm(zold))); %angle between bold and b by position
change
   %of delta
   temp=cross(zold,z); %if cross product of bold and b is negative pheta is negative
   if (temp(3)<0)
      pheta=-abs(pheta);
   else
      pheta=abs(pheta);
   end
   pheta_save(i+1,1)=pheta;

    RR=[cos(pheta) -sin(pheta) 0;sin(pheta) cos(pheta) 0; 0 0 1];
    F=RR*F;
    rr=RR*r;
    temp=cross(rr,F);
    H(1)=-temp(3)/(z(1)*coords(2)/coords(1) - z(2));
    H(2)=(coords(2)*H(1))/coords(1);
    M(i+1,:)=-cross(a,F+H);

 end
   p=polyfit(coords(13:19,1),coords(13:19,2),1);
   Regress=corrcoef(coords(13:19,1),coords(13:19,2));
   Fit_Coeff=Regress(1,2);

   est_slot_length=realsqrt((coords(13,1)-coords(19,1))^2 + (coords(13,2)-
coords(19,2))^2);
%SI conversion
    a_stored=a_stored*2.54;
    r_stored=r_stored*2.54;
    z_stored=z_stored*2.54;

  figure();
hold on
```

```
 axis([-10 1 -6 1]); %in inches
  for i=13  %13
     Title('Thumb Linkage Simulation')
     xlabel('position (cm)'); ylabel('position (cm)');
 line([0; -a_stored(i,1)],[0;-a_stored(i,2)],'Color','blue','LineWidth',4);
 line([-a_stored(i,1);-r_stored(i,1)-a_stored(i,1)],[-a_stored(i,2);-r_stored(i,2)-
a_stored(i,2)],'Color','red','LineWidth',4)
 line([-a_stored(i,1);-z_stored(i,1)-a_stored(i,1)],[-a_stored(i,2);-z_stored(i,2)-
a_stored(i,2)],'Color','black','LineWidth',4)
  end
   for i=14:19  %13
     Title('Thumb Linkage Simulation')
     xlabel('position (inches)'); ylabel('position (inches)');
 line([0; -a_stored(i,1)],[0;-a_stored(i,2)],'Color','blue','LineWidth',2);
 line([-a_stored(i,1);-r_stored(i,1)-a_stored(i,1)],[-a_stored(i,2);-r_stored(i,2)-
a_stored(i,2)],'Color','red','LineWidth',2)
 line([-a_stored(i,1);-z_stored(i,1)-a_stored(i,1)],[-a_stored(i,2);-z_stored(i,2)-
a_stored(i,2)],'Color','black','LineWidth',2)
  end
 hold off

 figure();
 hold on
 axis([-5 1 -3 1]); %in inches
  for i=13:19
 plot (coords(i,1),coords(i,2),'o','Color','black','MarkerSize',6)
  end
 hold off
```

REFERENCES

1. Donnan GA, Fisher M, Macleod M, Davis SM. Stroke. Lancet 371 (9624): May 2008 1612–23.

2. Feigin VL (2005). "Stroke epidemiology in the developing world". Lancet 365 (9478): 2160–1.

3. Rathore S, HinnA, Cooper L, Tyroler H, Posamond W. Characterization of incident stroke signs and symptoms: findings from the atherosclerosis risk in communities study. Stroke 2002; 33:2718-21.

4. Heart Disease and Stroke Statistics: 2005 Update. Dallas, Tex: American Heart Association; 2005.

5. Duncan PW, Bode RK, Min Lai S, Perera S; Rasch analysis of a new stroke-specific outcome scale: the Stroke Impact Scale. Arch Phys Med Rehabil. 2003 Jul;84(7):950-63.

6. Trombly CA. Stroke. In: Trombly AC, editor. Occupational therapy for physical dysfunction. Baltimroe: Willaims and Wilkins; 1989. 454-471.

7. Lance JW. The control of muscle tone, reflexes, and movement: Robert Wartenberg lecture. Neurology 1980;30:1303-1313.

8. Kamper DG, Rymer WZ. Quantitative features of the stretch response of extrinsic finger muscles in hemiparetic stroke. Muscle Nerve. 2000 Jun;23(6):954-61.

9. Kamper DG, Harvey RL, Suresh S, Rymer WZ. Relative contributions of neural mechanisms versus muscle mechanics in promoting finger extension deficits following stroke. Muscle Nerve. 2003 Sep;28(3):309-18.

10. Landau WM, Sahrmann SA. Preservation of directly stimulated muscle strength in hemiplegia due to stroke. Arch Neurol. 2002 Sep;59(9):1453-7.

11. Kamper DG, Fischer HC, Cruz EG, Rymer WZ. Weakness is the primary contributor to finger impairment in chronic stroke. Arch Phys Med Rehabil. 2006 Sep;87(9):1262-9.

12. Lum PS, Burgar CG, Shor PC. Evidence for strength imbalances as a significant contributor to abnormal synergies in hemiparetic subjects. Muscle Nerve. 2003 Feb;27(2):211-221.

13. Cruz EG, Waldinger HC, Kamper DG. Kinetic and kinematic workspaces of the index finger following stroke. Brain. 2005 May;128(Pt 5):1112-21.

14. Kamper DG, Rymer WZ. Impairment of voluntary control of finger motion following stroke: role of inappropriate muscle coactivation. Muscle Nerve. 2001 May;24(5):673-81.

15. Carey JR, Kimberley TJ, Lewis SM, Auerbach EJ, Dorsey L, Rundquist P, Ugurbil K. Analysis of fMRI and finger tracking training in subjects with chronic stroke. Brain. 2002 Apr;125(Pt 4):773-88.

16. Patten C, Lexell J, Brown HE. Weakness and strength training in persons with poststroke hemiplegia: rationale, method, and efficacy. J Rehabil Res Dev. 2004 May;41(3A):293-312.

17. Wolf SL, Winstein CJ, Miller JP, Taub E, Uswatte G, Morris D, Giuliani C, Light KE, Nichols-Larsen D; EXCITE Investigators. Effect of constraint-induced movement therapy on upper extremity function 3 to 9 months after stroke: the EXCITE randomized clinical trial. JAMA. 2006 Nov 1;296(17):2095-104.

18. Duncan P, Studenski S, Richards L, Gollub S, Lai SM, Reker D, Perera S, Yates J, Och V, RIgler S: Randomized clinical trial of therapeutic exercise in subacute stroke. Stroke 2003, 34(9):2173-2180.

19. Kwakkel G, Kollen BJ, an der Grond J, Prevo AJ. Probability of regaining dexterity in the flaccid upper limb. The impact of severity of paresis and time since onset in acute stroke. Stroke 2003, 34:2181-2186.

20. Broeks JG, Lankhorst GJ, Rumping K, Prevo AJ: The long-term outcome of arm function after stroke: results of a follow-up study. Disabil Rehabil 1999, 21(8):357-364.

21. Wade DT. Personal context as a focus for rehabilitation. Clin Rehabil 2000, 14(2):115-118.

22. Teasell R, Baona N, Salter K, Hellings C, Bitenskh J: Progress in clinical neurosciences: stroke recovery and rehabilitation. Can J Neurol 2006 33(4):357-364.

23. Woldag H, Hummelsheim H: Evidence-based physiotherapeutic concepts for improving arm and hand function in stroke patients: a review. J Neurol 2002, 249(5):518-528.

24. Dromerick AW, Lum PS, Hidler J. Activity-based therapies. NeuroRx. 2006 3(4):428-38.
25. Van Peppen RP, Kwakkel G, Wood-Dauphinee S, Hendriks HJ, Wees PJ Van der, Dekker J: The impact of physical therapy on functional outcomes after stroke: what's the evidence? Clin Rehabil 2004, 18(8):833-862.

26. Feys HM, De Weerdt WJ, Selz BE, Cox Steck GA, Spichiger R, Vereeck LE, Putman KD, Van Hoydonck GA: Effect of a therapeutic intervention for the hemiplegic upper limb in the acute phase after stroke: a single-blind, randomized, controleed muticenter trial. Stroke 1998, 29(4):785-792.

27. Andrews AW, Bohannon RW: Short-term recovery of limb muscle strength after acute stroke. Arch Phys Med Rehabil 2003, 84(1):125-130.

28. Sunderland A, Fletcher D, Bradley L, Tinson D, Hewer RL, Wade DT: Enhanced physical therapy afor arm function after stroke: a one year follow up study. J Neurol Neurosurg Psychiatry 1994, 57(7):856-858.

29. Lin KC, Wu CY, Liu JS, Chen YT, Hsu CJ. Constraint-induced therapy versus dose-matched control intervention to improve motor ability, basic/extended daily functions, and quality of life in stroke. Neurorehabil Neural Repair. 2009 23(2):160-5.

30. Taub E, Lum PS, Hardin P, Mark VW, USwatte G: AutoCITE: automated delivery of CI therap with reduced effort by therapists. Stroke 2005, 36(6):1301-1304.

31. Whitall J, McCombe Waller S, Silver KH, Macko RF: Repetitive bilateral arm training with rhythmic auditory cueing improves motor function in chronic hemiparetic stroke. Stroke 2000, 31(1):2390-2395.

32. Lum PS, Burgar CG, Van der Loos M, Shor PC, Majmundar M, Yap R. MIME robotic device for upper-limb neurorehabilitation in subacute stroke subjects: A follow-up study. J Rehabil Res Dev. 2006 43(5):631-42.

33. Chang JJ, Tung WL, Wu WL, Su FC: Effect of bilateral reaching on affected arm motor control in stroke-with and without loading on unaffected arm. Disabil Rehabil 2006, 28(24):1507-1516.

34. Luft AR, McCombe-Waller S, Whitall J, Forrester LW, Macko R, Sorkin JD, Schulz JB, Goldberg AP, Hankey DF: Repetitive bilateral arm training an motor cortex activation in chronic stroke: a randomized controlled trial. Jama 2004, 292(15):1853-1861.

35. Lucca LF. Virtual reality and motor rehabilitation of the upper limb after stroke: a generation of progress? J Rehabil Med. 2009 41(12):1003-100.

36. Krebs HI, Hogan N, Volpe BT, Aisen ML, Edelstein L, Diels C. Overview of clinical trials with MIT-MANUS: a robot-aided neuro-rehabilitation facility. Technol Health Care. 1999;7(6):419-23.

37. Burgar CG, Lum PS, Shor PC, Machiel Van der Loos HF. Development of robots for rehabilitation therapy: the Palo Alto VA/Stanford experience. J Rehabil Res Dev. 2000 Nov-Dec;37(6):663-73.

38. Reinkensmeyer DJ, Kahn LE, Averbuch M, McKenna-Cole A, Schmit BD, Rymer WZ. Understanding and treating arm movement impairment after chronic brain injury: progress with the ARM guide. J Rehabil Res Dev. 2000 37(6):653-62.

39. Hesse S, Schulte-Tigges G, Konrad M, Bardeleben A, Werner C. Robot-assisted arm trainer for the passive and active practice of bilateral forearm and wrist movements in hemiparetic subjects. Arch Phys Med Rehabil. 2003 Jun;84(6):915-20.

40. Nef T, Mihelj M, Riener R. ARMin: a robot for patient-cooperative arm therapy. Med Biol Eng Comput. 2007 Sep;45(9):887-900. Epub 2007 Aug 3.

41. Aisen ML, Krebs HI, Hogan N, McDowell F, Volpe BT: The effect of robot-assisted therapy and rehabilitative training on motor recovery following stroke. *Arch Neurol* 1997, 54:443–446.

42. Volpe BT, Krebs HI, Hogan N, Edelsteinn L, Diels CM, Aisen ML. Robot training enhanced motor outcome in patients with stroke maintained over 3 years. Neurology. 1999 Nov 10;53(8):1874-6.

43. Fasoli SE, Krebs HI, Stein J, Frontera WR, Hughes R, Hogan N. Robotic therapy for chronic motor impairments after stroke: Follow-up results. Arch Phys Med Rehabil. 2004 Jul;85(7):1106-11.

44. Kahn LE, Rymer WZ, Reinkensmeyer DJ. Adaptive assistance for guided force training in chronic stroke. Conf Proc IEEE Eng Med Biol Soc. 2004;4:2722-5.

45. Lum PS, Burgar CG, Shor PC. Evidence for improved muscle activation patterns after retraining of reaching movements with the MIME robotic system in subjects with post-stroke hemiparesis. IEEE Trans Neural Syst Rehabil Eng. 2004 Jun;12(2):186-94.

46. Jack D, Boian R, Merians AS, Tremaine M, Burdea GC, Adamovich SV, Recce M, Poizner H. Virtual reality-enhanced stroke rehabilitation. IEEE Trans Neural Syst Rehabil Eng. 2001 Sep;9(3):308-18.

47. Bouzit M, Burdea G, Popescu G, Boian R. The Rutgers Master II-New Design force-feedback glove. IEEE/ASME Trans Mechatronics. 2002 Aug;12(4):399-407.

48. Deutsch JE, Merians AS, Adamovich S, Poizner H, Burdea GC. Development and application of virtual reality technology to improve hand use and gait of individuals post-stroke. Restor Neurol Neurosci. 2004;22(3-5):371-86. Review.

49. Boian R, Sherman A, Han C, Merians A, Burdea G, Adamovich S, Recce M, Tremaine M, Poizner H. Virtual-reality-based post-stroke hand rehabilitation. Stud Health Technol Inform. 2002 85:64-70.

50. Merians AS, Jack D, Boian R, Tremaine M, Burdea GC, Adamovich SV, Recce M, Poizner H. Virtual reality-augmented rehabilitation for patients following stroke. Phys Ther. 2002 Sep;82(9):898-915.

51. Adamovich S, Merians A, Boian R, Recce M, Tremaine M, Poizner H. A virtual reality based exercise system for hand rehabilitation post-stroke: transfer to function. Conf Proc IEEE Eng Med Biol Soc 2004, 7:4936-4939.

52. Masia L, Krebs HI, Cappa P, Hogan N. Design and characterization of hand module for whole-arm rehabilitation following stroke. IEEE Trans Mechatronics. 2007 Aug;12(4):399-407.

53. Takahashi C, Der-Yeghiaian L, Le V, Cramer SC. A robotic device for hand motor therapy after stroke. In: Proceedings of IEEE 9th International Conference on Rehabilitation Robotics: Frontiers of the Human-Machine Interface. Chicago, Illinois; 2005. P. 17-20.

54. Takahashi CD, Der-Yeghiaian L, Le V, Motiwala RR, Cramer SC: Robot-based hand motor therapy after stroke. *Brain* 2008, 131:425:437.

55. Koeneman EJ, Schultz RS, Wolf SL, Herring DE, Koeneman JB. A pneumatic muscle hand therapy device. Conf Proc IEEE Eng Med Biol Soc. 2004;4:2711-3.

56. Hesse S, Kuhlmann H, Wilk J, Tomelleri C, Kirker S: A new electromechanical trainer for sensorimotor rehabilitation of paralysed fingers: a case series in chronic and acute stroke patients. *J Neuroeng Rehabil* 2008, 5:21.

57. Fischer HC, Stubblefield K, Kline T, Luo X, Kenyon RV, Kamper DG: Hand rehabilitation following stroke: a pilot study of assisted finger extension training in a virtual environment. *Top Stroke Rehabil* 2007, 14(1):1-12.

58. Kamper DG, Cruz EG, Siegel MP. Stereotypical fingertip trajectories during grasp. J Neurophysiol. 2003 Sept;90:3702-3710.

59. Nef T, Lum P. Improving backdrivability in geared rehabilitation robots. Med Biol Eng Comput. 2009 Apr;47(4):441-7.

60. Oldfield RC. The assessment and analysis of handedness: the Edinburgh Inventory. Neuropsychologia. 1971 1:97-113.

61. Fugl-Meyer AR, Jaasko L, Leyman (1975) The post stroke hemiplegic patient I. A method for evaluation of physical performance Scandinavian Journal of Rehabilitation Medicine 7, 1, 13 - 31.

62. Carroll D. “A quantitative test of upper extremity function.” J Chronic Diseases. 1965;18:479-491.

63. Lang CE, Wagner JM, Dromerick AW, Edwards DF. Measurement of upper-extremity function early after stroke: properties of the action research arm test. Arch Phys Med Rehabil. 2006 87(12):1605-10.

64. Gregson JM, Leathley M, Moore AP, Sharma AK, Smith TL, Watkins CL. Reliability of the Tone Assessment Scale and the modified Ashworth scale as clinical tools for assessing poststroke spasticity. Arch Phys Med Rehabil. 1999 Sep;80(9):1013-6.

65. Waldvogel D, van Gelderen P, Ishii K, Hallett M. The effect of movement amplitude on activation in functional magnetic resonance imaging studies. J Cereb Blood Flow Metab. 1999 Nov;19(11):1209-12.

66. Israel JF, Campbell DD, Kahn JH, Hornby TG. Metabolic costs and muscle activity patterns during robotic- and therapist-assisted treadmill walking in individuals with incomplete spinal cord injury. Phys Ther. 2006 Nov;86(11):1466-78.

67. Wolbrecht ET, Chan V, Le V, Cramer SC, Reinkensmeyer DJ, Bobrow JE. Real-time computer modeling of eakness following stroke optimizes robotic assistance for movement therapy. 3rd International IEEE/EMBS Conference on Neural Engineering, CNE 2007:152-158.

68. Schmidt RA, Bjork RA. New conceptualizations of practice: common principles in three paradigms suggest new concepts for training. Psychological Science. 1992 3(4):207-217.

69. Krebs HI, Palazzolo JJ, Dipietro L, Ferraro M, Krol J, Rannekleiv K, Volpe BT, Hogan N. Rehabilitation robotics: performance-based progressive robot-assisted therapy. Autonomous Robots 2003 15:7-20.
70. Reiner R, Luneburger L, Jezernik S, Anderschitz JM, Colombo G, Dietz V. Patient-cooperative strategies for robot-aided treadmill training: first experimental results. IEEE Tans Neural Syst Rehabil Eng. 2005 13(3):380-394.

71. Marchal-Crespo L, Reinkensmeyer DJ. Haptic guidance can enhance motor learning of a steering task. Journal of motor behavior 2008 40(6):545-557.